A MACHINE LEARNING COMBINED IN SILICO APPROACH FOR THE IDENTIFICATION OF FUNGICIDE COMBINATIONS TARGETING *PLASMOPARA VITICOLA* AND *BOTRYTIS CINEREA* FUNGICIDE RESISTANCE

A Thesis

by

JUNRUI ZHANG

Submitted to the Graduate and Professional School of
Texas A&M University
in partial fulfillment of the requirements for the degree of

MASTER OF SCIENCE

Chair of Committee, Sandun Fernando
Co-Chair of Committee, Maria King
Committee Member, Luc Berghman
Head of Department, Patricia Smith

May 2023

Major Subject: Biological and Agricultural Engineering

ABSTRACT

Downy mildew (caused by *Plasmopara viticola*) and Grey Mold (caused by *Botrytis cinerea*) are fungal diseases that significantly impact grape production globally. Cytochrome b plays a significant role in the mitochondrial respiratory chain of the two fungi that cause these diseases and is a key target for Quinone outside inhibitor (QoI) based fungicide development. QoI fungicides are common antifungal agents that are used to treat downy mildew or grey mold infections in fruits and vegetable crops by binding to cytochrome b and inhibiting respiratory function. Since the mode of action (MOA) of QoI fungicides is restricted to a single active site, the risk of developing resistance toward these fungicides is deemed high. Consequently, using a combination of fungicides in a rotational program is considered an effective way to reduce development of QoI resistance. In this study, a combination of *in silico* simulations that include Schrodinger Glide docking, molecular dynamics, MMGBSA and AutoQSAR modeling were used to screen the most potent QoI-based fungicide combinations to wild-type, G143A (Glycine to Alanine), F129L (Phenylalanine to Leucine) and double mutated versions that had both G143A and F129L mutations of fungal cytochrome b. The fungicides mandestrobin, fenaminstrobin and dimoxystrobin had high docking scores against multiple mutated versions of cytochrome b of *Plasmopara viticola*, which suggests their high affinity toward mutated variants of cytochrome b. Famoxadone, fenamidone, ametoctrodin and thiram also showed reasonable but relatively weaker binding affinity towards *Plasmopara viticola* cytochrome b. For the case of *Botrytis cinerea*, mandestrobin, pyribencarb and famoxadone showed strong binding affinity toward the four different variations of cytochrome b, which indicates that they are potential effective candidates against mutated cytochrome b. Four other fungicides, ametoctradin, fenamidone, metominostrobin and thiram were also effective against mutated cytochrome b.

Based on both the docking simulations and QSAR/machine learning analysis ametoctradin emerged as a potential high-affinity QoI fungicide against the G143A mutation. The QoI-based fungicide combinations that include famoxadone, mandestrobin and ametoctradin preferentially are suggested to be considered in a fungicide management program in combination with fungicides that target other MOA as a potential treatment against *Plasmopara viticola* and *Botrytis cinerea* based fungal infections.

DEDICATION

To my mother, Guiqing Wang, for showing me the importance of goodness and the value of hard work. Although she was my inspiration to pursue a degree in the foreign country, she was unable to see my graduation. Thank you so much, I will never forget you.

To my father, Muyi Zhang, and my brother, Junyou Zhang, for the constant source of support, encouragement and unconditional love during the challenges of graduate school and life.

To the rest of my family, for loving and supporting me, my success would not be possible without it.

ACKNOWLEDGEMENTS

First of all, I would like to thank my committee chair, Dr. Sandun Fernando, for all of his support, guidance and encouragement throughout the course of this research. I would also like to thank the rest of my committee, Dr. Maria King and Dr. Luc Berghman for their support and advice.

Next, thanks go to my lab group, specifically Haoqi Wang, Samavath Mallawarachchi, Nirmitee Mulgaonkar and Nalin Samarasinghe for being so patient to answer all my questions assist me unconditionally. I gratefully acknowledge the support from Texas A&M High Performance Research Computing (HPRC) and TAMU laboratory for Molecular Simulation (LMS).

CONTRIBUTORS AND FUNDING SOURCES

Contributors

This work was supervised by a thesis committee consisting of Professor Dr. Sandun Fernando and Professor Dr. Maria King of the Department of Biological and Agricultural Engineering and Professor Dr. Luc Berghman of the Department of Poultry Science.

The data in this project was completed by the student independently. The data analysis was cooperated with Dr. Sandun Fernando and Samavath Mallawarachchi.

Funding Sources

Graduate study was supported in part by Texas A&M AgriLife.

NOMENCLATURE

QoI	Quinone outside inhibitors
WT	Wild type
MM-GBSA	Molecular Mechanism-Generalized Born Surface Area
MOA	Mode of action
TIP3P	Transferable Intermolecular Potential with 3 Points
OPLS3	Optimized Potentials for Liquid Simulations 3
NPT	Normal pressure and temperature
RMSD	Root Mean Square Deviation
RMSF	Root Mean Square Fluctuation
QSAR	Quantitative structure-activity relationship
QSQE	Quaternary Structure Quality Estimate
GMQE	Global Model Quality Estimate
GLY	Glycine
ALA	Alanine
VAL	Valine
LEU	Leucine
ILE	Isoleucine
SER	Serine
THR	Threonine
CYS	Cysteine
MET	Methionine

ASP	Aspartic
ASN	Asparagine
GLU	Glutamic acid
GLN	Glutamine
LYS	Lysine
ARG	Arginine
HIS	Histidine
PHE	Phenylalanine
TYR	Tyrosine
TRY	Tryptophan
PRO	Proline

TABLE OF CONTENTS

Page

LIST OF FIGURES

LIST OF TABLES

1. INTRODUCTION

Grapes, one of the world's most valuable cash crops, play an important role in the global economy. In 2020, the global production of grapes was 78 million tonnes from 6.95 million hectares and the total production value was over $80 billion [9] with ~6 million tons of grapes being produced in the U.S. [20]. Cultivated grapes are sold as table grapes and processed grape products such as jam, wine, vinegar juice and jelly. Over 50% of grapes are used in wine production that contributes to over a billion U.S. dollars each year in the U.S. However, there is a serious impact on the growth of grapes caused by fungal diseases, which also affects the quality of wine and other products. An estimated 40% reduction in grape production occurs annually because of various fungal diseases, causing significant economic losses [27].

Downy mildew caused by *Plasmopara viticola* is one of the most serious fungal diseases that attack grapevines. Downy mildew was a native pathogen to North America and caused serious damage to European vineyards in the late 1800s [18]. *Plasmopara viticola* invades leaves, shoot and young berries under warm and moist conditions so that the pathogen can take nutrients from these parts to produce sporangia, causing larger infections [4] [18]. Yellow spots with white downy mold occur on the surfaces of infected leaves and the spots turn brown and eventually necrotic [1]. Necrotic areas on leaves caused by downy mildew largely affect the photosynthesis of the grapevine and reduce the formation of glucose provided by photosynthesis, which hinders grape growth and causes reduction of berries. Young shoots and berries are also vulnerable to downy mildew, which causes young shoots to be twisted and decreases the translocation of water and organic nutrients, slowing growth [1]. This infection also causes berries to dry out and fall causing significant losses [1]. When there is abundant rainfall in warm seasons, the pathogen easily invades grapevines and reproduces more sporangia which can be

carried by wind or rain to infect surrounding grapevines [1] [24]. Although downy mildew is devastating, QoI fungicides have thus far been able to manage the disease effectively [1] [5] [14]; however, key mutations to the target has been threatening several of these fungicides to show resistance.

Grey mold caused by *Botrytis cinerea* is another fungal disease that causes serious destruction to grapevine. Grey mold is also one of the "Top 10 fungal plant pathogens" in the survey established by Molecular Plant Pathology because this fungal disease has a wide host range, and it has the capability to invade a host plant in all stages from seedling to maturity [7]. The berries of grapevine are the most susceptible when an infection occurs under moderate temperatures and high humidity [8]. When the berries are infected, a reddish-brown and watery decay can be observed from the pedicel to the stylar end [8]. Infected regions also provide favorable conditions for a secondary inoculum which will generate more sporangia and infect other berries nearby [8]. Infected berries finally dry out, resulting in significant economic losses. *Botrytis cinerea* also invades leaves, flowers, and shoots, causing similar brown lesions on plant parts [8]. QoI fungicides are commonly used for chemical control of *Botrytis cinerea* [8]; and resistance threatens the effectiveness of several of these fungicides.

The application of fungicide is a chemical control that targets specific molecules like amino acids to block fungal metabolism, restricting fungal reproduction [11]. The binding target of QoI fungicides is cytochrome b, a protein within the cytochrome bc_1 complex in *Plasmopara viticola* and *Botrytis cinerea* which plays a significant role in respiratory function [3]. When QoI fungicides bind cytochrome b, the ubiquinol oxidase substrate is unable to transfer electrons within cytochrome b and cytochrome c_1 interrupting and inhibiting the production of ATP [3][5]. This shortage of ATP interrupts the propagation of the pathogen, meaning downy mildew treated

by QoI fungicides is not able to infect other parts of the grapevine. However, since QoI fungicides are single-site fungicides (specifically bind to cytochrome b), downy mildew and grey mold will develop fungicide resistance after continuous usage of QoI fungicides [5] [13][31]. Due to fungicide resistance development, Fungicide Resistance Action Committee (FRAC) has labeled QoI fungicides as high-risk. G143A (Glycine to Alanine) and F129L (Phenylalanine to Leucine) mutations are two main known mutations that reduce the efficacy of QoI fungicides toward grape downy mildew because the mutations of these two target sites weaken the binding affinity between protein and fungicides [5] [14] [30]. While developing new types of fungicides can resolve this issue, it takes a significant amount of time and resources to identify alternative active sites and go through rigorous approval processes. In the meantime, an effective, economic and viable management strategy may include using combinations of fungicides. A fungicide combination combines one or more high-risk fungicides with one or more low-risk fungicides from currently used fungicides [14]. By using this strategy, QoI fungicides can be combined with another low-risk fungicide so that the mixture has multiple binding targets, thus increasing the effectiveness against mutation(s) [14].

According to existing literature, no studies have addressed the selection of fungicide combinations for QoIs based on molecular structures and their affinity to the cytochrome b active site. In this study, we aim to provide a thermodynamic-based quantitative strategy to identify and select antifungal agents from QoIs (high-risk group) to be combined with low-risk fungicides to form fungicide combination(s) that can mitigate fungicide resistance. This approach is based on docking selected fungicides from QoIs and low-risk fungicides with a homology model of cytochrome b to identify the fungicides with the highest affinity, and further evaluation of the

screened fungicides using molecular dynamic simulations, MM-GBSA energy calculations and QSAR models with machine learning statistical methods.

2. MATERIALS AND METHODS

2.1 Protein structure and ligand structure preparation

A homology model in PDB format of *Plasmopara viticola* (GenBank: DQ209286.1) was created by using cytochrome b from plant mitochondrial complex III2 from *Viga radiata* (PDB: 7JRG. 1 .C) as a template on the SWISS-MODEL server [2][12] [23] [32]. The quality of this homology model was evaluated by using the program ERRAT and PROVE on the SAVES v6.0 server (https://saves.mbi.ucla.edu accessed on 8 January 2023) [6][28]. The homology model contained G143 and F129, which was a WT cytochrome b. This model was mutated into three other versions on Maestro Schrödinger: G143A, F129L and a mutation containing both G143 and F129L mutations. The 3D structures of ligands were obtained from ZINC15 or PubChem (all ligands are provided in supplementary materials) and generated in PDB format using online SMILES translator [15] [19]. All the protein and ligand structures were prepared for docking using the Protein Preparation Wizard which added missing hydrogens, corrected bond orders, fixed missing segments and minimized the structure under Optimized Potentials for Liquid Simulations 3 (OPLS3) force field [16].

A homology model was built and validated for *Botrytis cinerea* using analogous methods developed for *Plasmopara viticola.*

2.2 Molecular docking

Schrodinger Glide was used for the docking of the ligands on the protein. The grid box was centered around original active sites (G143 and F129; coordinates X - 195.53, Y – 213.29, Z – 176.3) or mutated active sites (G143A; coordinates X -192.6, Y – 212.54, Z – 171.55; F129L; coordinates X – 196.55, Y – 213.55, Z – 177.96; or F129L with G143A; coordinates X – 195.53,

Y – 213.29, Z – 176.3) and the size of the grid box was 44 × 46 × 56 Å. Glide docking scores between cytochrome b and 26 ligands were generated using Schrödinger Glide XP mode with default settings in three replicates and the highest binding scores were used for binding affinity analysis. The ligand-protein interactions were analyzed using a Ligand Interaction diagram.

2.3 Molecular dynamic simulations

Molecular dynamic simulations were conducted for select fungicides using Schrodinger Desmond for further verification. The protein-ligand structures were created by merging the protein with a selective ligand. An orthorhombic box (distance 10 × 10 × 10Å) in a Transferable Intermolecular Potential with 3 Points (TIP3P) solvent model was generated using the System Builder of Schrödinger Desmond under an OPLS3 force field. The charge of this system was kept in a neutral state by adding NaCl in 0.15 M concentration [16] [26]. The NPT (normal pressure and temperature) ensemble was applied for the molecular dynamics simulations using temperature at 300K and pressure at 1.01325 bar [17]. Each protein-ligand structure within the orthorhombic box contained around 33161 atoms with 9798 water molecules (data from the structure of cytochrome b with ubiquinol). The molecular dynamic simulation for each system was run for 500 nanoseconds (ns) and generated 1000 frames and a 500-picosecond (ps) trajectory. Root Mean Square Deviation (RMSD), Root Mean Square Fluctuation (RMSF), and Protein-Ligand contacts for each simulation were analyzed using Schrödinger Simulation Interaction Diagrams.

2.4 Binding free energy analysis

Molecular Mechanism-Generalized Born Surface Area (MMGBSA) calculation showed the binding affinity between protein and ligands was based on the free binding energy [21]. By

using the *thermal_MMGBSA.py* script from Schrödinger Prime for molecular dynamic simulation with 1000 frames, the free binding energy of each frame or each segment, depending on command -*step_size* on the script, was calculated for analysis of binding affinity [21].

2.5 AutoQSAR model analysis

In order to evaluate if the predictions made by the docking followed by molecular dynamic simulations could be replicated, the Schrodinger automated quantitative structure-activity relationship (AutoQSAR) model that uses a machine-learning approach which a subset of Artificial Intelligence (AI) was used. The AutoQSAR model is a machine-learning approach that builds numerical models with minimal inputs to interpret the relationship and make predictions between the bioactivity and chemical properties of ligands [29]. In this case, the binding affinity was used as the input variable. Numerical models were developed by using multiple linear regression (MLR), partial least-squares regression (PLS), kernel-based partial least-squares regression (KPLS) and principal components regression (PCR) based on the given ligands' fingerprints including linear, radial, dendritic and milprint2D or descriptors [29]. The AutoQSAR split the selected ligands into a 75% training set and a 25% test set for *Plasmopara viticola* and *Botrytis cinerea* [29]. This model generated a scatter plot that showed the correlation between observed and predicted binding affinity. The accuracy of this model was evaluated by an external validation data set.

3. RESULTS AND DISCUSSION

3.1 Building of the homology models for *Plasmopara viticola* Cytochrome b

The homology model of *Plasmopara viticola* cytochrome b included the regions between residues 79 to 295 found by BLAST. The sequence identity was 69.59% and sequence similarity was 0.53 [32]. The Quaternary Structure Quality Estimate (QSQE) was 0.81 (with 0.7 to be acceptable), indicating a high level of reliability of quaternary structure. The Global Model Quality Estimate (GMQE) is 0.89, meaning the homology model had over half of the target sequence coverage [32]. The ERRAT value for the homology model was 93.5 which meant that the homology model had acceptable nonbonded atomic interactions [6]. Based on the PROCHECK report, 92.9% of residues (171 out of 217) were located in the most favored regions, 6.5% (12 out of 217) were located in the additional allowed regions, 0% were located in the generously allowed regions and 0.5% (1 out of 217) were located in the disallowed regions [22]. The residue score provided by PROCHECK was 99.5%, which indicated the conformation of homology model of *Plasmopara viticola* cytochrome b was stable [34]. Based on favorable scores, this homology model was used for in-silico studies.

3.2 Identification of the Active Site for *Plasmopara viticola*

During the initial docking, the homology model was divided into top (covering residues: ARG79-TRY94, MET124-PHE180 and PHE245-MET295) and bottom sections (covering residues: ILE95-PHE121 and SER181-ILE244). To identify the docking site in cytochrome b, two conserved regions around the center of protein were picked from the top and bottom parts based on existing literature [12]. Initial docking results and Site Map shown on Figure 1 revealed strong binding of probe molecules to the top region (covering residues: ARG79-TRY94, ILE122-PHE180 and PHE245-MET295) of cytochrome b. Since the top region showed stronger binding and

included the two key residues where antifungal-resistant mutations occur, this region was used for docking analyses in all subsequent steps. Glide docking scores of selected fungicides on the top binding site of cytochrome b are given in Table 1, and the key interactions of ubiquinol at the binding site are given in Figure 1.

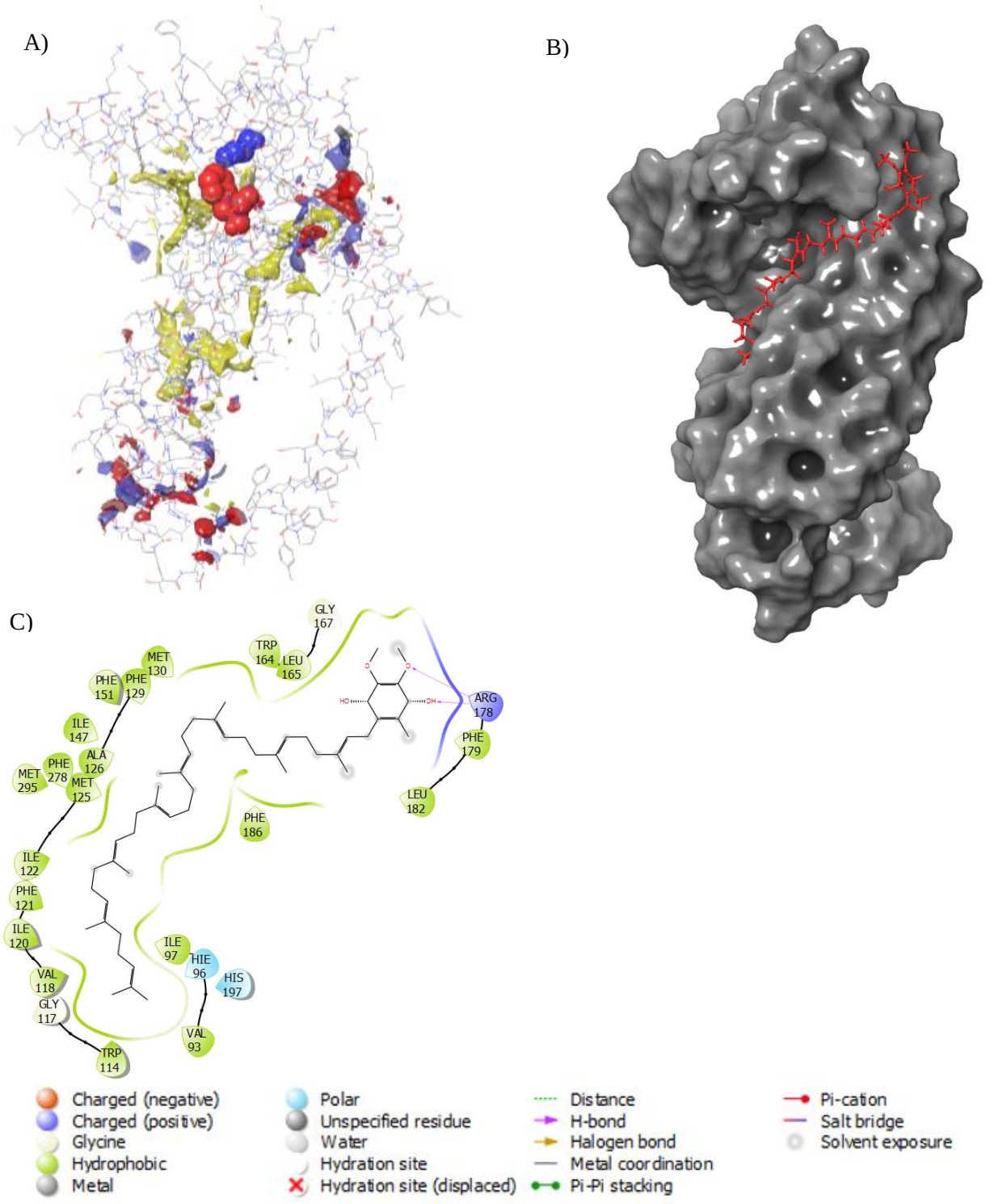

Figure 1: A) Site map output depicting possible binding sites of *Plasmopara viticola* cytochrome b (G143 - Blue residue; F129 - Red residue; hydrophobic - Yellow areas; Hydrogen bonding acceptor - Red areas; Hydrogen bonding donor - Blue areas); B) the top orientation of ubiquinol on cytochrome b; and C) key interactions of ubiquinol with cytochrome b amino acid residues.

3.3 Fungicide binding behavior on *Plasmopara viticola* Cytochrome b

3.3.1 General Observations

Since the focus of this study was to identify fungicides that were effective against multiple mutations of the cytochrome b, a set of known antifungal agents were docked onto four variations of *Plasmopara viticola* cytochrome b: the WT, G143A mutated, F129L mutated, and double mutated, which included both G143A and F129L mutations. Here, G143A and F129L mutations were specifically selected since those mutations are reported to be most significant for antifungal resistance [12]. Glide docking scores of the fungicides on each cytochrome b variation are given in Table 1.

Table 1: Average Glide docking scores (binding affinity) for fungicides on four variations of *Plasmopara viticola* cytochrome b targeting at different versions of G143 and F129 (average of the top three binding poses).

Fungicide	Wild type average docking score (G143 and F129 as binding center)	G143A average docking score	F129L average docking score	Double mutation average docking score	Resistance[1]	Fungicide Type[2]
Ubiqunol	-8.598	-7.638	-7.025	-5.343	NA	NA
Famoxadone	-6.447	-5.882	-5.565	-6.288	HR	QoI
Azoxystrobin	DNB[3]	DNB	DNB	DNB	HR/R	QoI
Fenamidone	-6.470	-6.254	-5.584	-5.276	HR	QoI
Coumoxystrobin	DNB	-6.177	DNB	DNB	HR	QoI
Flufenoxystrobin	DNB	-6.279	-3.761	DNB	HR	QoI
Enoxastrobin	-3.398	DNB	-4.570	-0.391	HR	QoI
Pyraoxystrobin	DNB	DNB	DNB	DNB	HR	QoI
Picoxystrobin	DNB	DNB	-3.774	DNB	HR	QoI
Metyltetraprole	DNB	DNB	DNB	DNB	HR	QoI
Fenaminstrobin	-7.179	-7.466	-6.570	-5.187	HR	QoI
Pyribencarb	-3.766	-5.844	-3.384	-2.790	HR	QoI
Dimoxystrobin	-7.076	-7.548	-6.095	-5.606	HR	QoI
Triclopyricarb	DNB	DNB	DNB	DNB	HR	QoI
Metominostrobin	-5.353	-5.067	-3.215	-4.896	HR	QoI
Pyrametostrobin	DNB	DNB	DNB	DNB	HR	QoI
Mandestrobin	-7.337	-7.393	-5.568	-6.193	HR	QoI
Fluoxastrobin	DNB	DNB	DNB	DNB	HR	QoI
Pyraclostrobin	DNB	DNB	DNB	DNB	HR	QoI
Orysastrobin	DNB	DNB	DNB	DNB	HR	QoI
Folpet	DNB	-5.891	-4.925	-2.942	LR	PHT
Ferbam	-1.1809	-3.0380	-1.1489	-0.1295	LR	DTC
Captan	DNB	DNB	DNB	-2.994	LR	PHT
Mancozeb	-2.368	-1.878	-1.701	-1.932	LR	DTC
Ametoctradin	-6.059	-6.299	-3.529	-5.342	HR/R	QoI
Thiram	-4.367	-4.285	-4.070	-4.358	LR	DTC
Zineb	-2.766	-2.408	-0.7244	-2.809	LR	DTC

[1] Resistance: NA native, HR high risk, LR low risk for the resistance of fungicides.

[2] Fungicide type: QoI quinone outside inhibitor, DTC dithiocarbamate, PHT phthalimides.

[3] DNB: the ligand donot bind to the Cytochrome b. HR-High Risk; LR-Low Risk; R-resistant.

Native substrate ubiquinol had the strongest binding affinity to WT, F129L mutated and G143A mutated types of cytochrome b protein (Table 1). Cytochrome b had strong hydrophobic interactions with ubiquinol, which was also predominant between cytochrome b and the fungicides tested (Figure 1). The interactions between ubiquinol and cytochrome b were strongly hydrophobic in general. Hydrogen bonding was also observed with ARG178 for WT, F129L and double mutated cytochrome b. Ubiquinol formed strong hydrogen bonding with MET295 of G143A mutated type.

Among the tested fungicides, fenamidone, famoxadone, mandestrobin, dimoxystrobin and fenaminstrobin showed strong affinity towards WT, F129 mutated G143A mutated and double mutated versions of cytochrome b, suggesting that they are the most promising candidates against these mutations. Ametoctradin had a lower binding affinity toward F129L mutated cytochrome b but it had a relatively higher affinity towards WT, G143A mutated, and double mutated versions of cytochrome, meaning it was also a potential mutation adaptive candidate against cytochrome b. Although all six fungicides are categorized as high-risk based on the MOA pertaining to only one target site, they bind strongly to cytochrome b with both known mutations suggesting their robustness against mutations.

While metominostrobin showed high affinity towards WT, its binding affinity is poor toward some of the mutated versions, suggesting its susceptibility to potential resistance. Azoxystrobin and ametoctradin were two fungicides known to be resistant for *Plasmopara viticola* [25][35]. Ametoctradin showed a somewhat strong affinity towards both G143A and double mutated versions, although the docking scores towards G143A mutated cytochrome b were lower than fenamidone, famoxadone and mandestrobin. Azoxystrobin had a poor docking score, indicating that it may not be effective against cytochrome b inhibition. Among low-risk fungicides,

i.e., the fungicide having more than one MOA, thiram showed a strong affinity toward all versions of cytochrome b. Folpet only showed a strong affinity toward G143A and F129L mutated versions of cytochrome b and not the WT or the double-mutated versions suggesting it was a weaker choice against susceptibility to resistance.

In order to capture the effectiveness of fungicides on different forms of *Plasmopara viticola* cytochrome b, a general statistical analysis was performed (Figure 2). Here, ubiquinol, as a native substrate, had the highest binding affinity toward WT, G143A, F129L and G143A- F129L double mutated types of cytochrome b of *Plasmopara viticola*. From high-risk fungicides, mandestrobin, fenaminstrobin, dimoxystrobin, famoxadone, fenamidone, and ametoctradin emerged as those with the strongest affinity toward *Plasmopara viticola* cytochrome b.

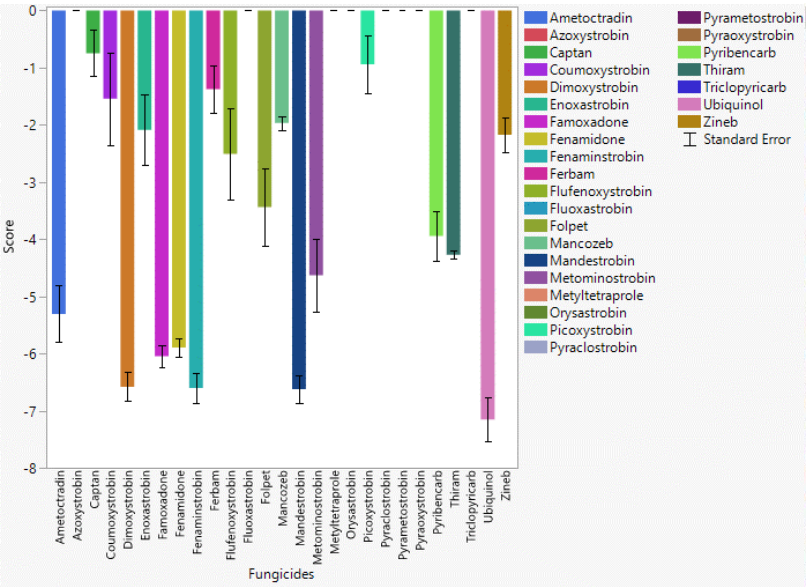

Level										Mean
Azoxystrobin	A									0.000000
Fluoxastrobin	A									0.000000
Metyltetraprole	A									0.000000
Orysastrobin	A									0.000000
Pyraclostrobin	A									0.000000
Pyrametostrobin	A									0.000000
Pyraoxystrobin	A									0.000000
Triclopyricarb	A									0.000000
Captan	A	B								-0.748557
Picoxystrobin	A	B								-0.943434
Ferbam	A	B								-1.374301
Coumoxystrobin	A	B	C							-1.544278
Mancozeb	A	B	C	D						-1.969633
Enoxastrobin		B	C	D						-2.089866
Zineb		B	C	D						-2.176801
Flufenoxystrobin		B	C	D	E					-2.509918
Folpet			C	D	E	F				-3.439438
Pyribencarb				D	E	F	G			-3.945898
Thiram					E	F	G	H		-4.269756
Metominostrobin						F	G	H	I	-4.632741
Ametoctradin						F	G	H	I	J	-5.307273
Fenamidone							G	H	I	J	-5.896093
Famoxadone								H	I	J	-6.045381
Dimoxystrobin									I	J	-6.581178
Fenaminstrobin									I	J	-6.600660
Mandestrobin									I	J	-6.622675
Ubiquinol										J	-7.150995

Figure 2: The performance of select QoI fungicides on WT, G143A, F129L, and double mutated cytochrome b of *Plasmopara viticola* in general.

Pyraoxystrobin, pyrametostrobin, pyraclostrobin, triclopyricarb, orysastrobin, fluoxastrobin and metyltetraprole did not bind (i.e., had the lowest affinity) to any type of cytochrome b indicating high susceptibility to possible resistance. Azoxystrobin, already identified to be a resistant fungicide to *Plasmopara viticola* cytochrome b in certain regions, did not bind to any version of cytochrome b – corroborating field observations. Thiram showed a stronger binding affinity than the other low-risk fungicides, indicating its potentially superior efficacy against cytochrome b among low-risk category. Fungicides folpet, zineb, mancozeb, ferbam and captan showed weaker affinity or did not bind to the protein, meaning these low-risk fungicides were not appropriate options for cytochrome b inhibition.

A common recommendation is to use fungicide combinations that consist of different MOA, i.e., to combine one MOA with others, in a fungicide rotation program. Due to the ability to tackle multiple mutations, fenamidone, famoxadone, mandestrobin, dimoxystrobin, fenaminstrobin, ametoctradin and thiram are identified as suitable candidates to be considered in a rotational program targeting *Plasmopara viticola*.

3.3.2 Mutation-specific Observations

In order to reveal any specific interactions of fungicides to particular mutations, the statistical analysis was directed to focus on each of the individual versions of *Plasmopara viticola* cytochrome b. This type of analysis will be helpful in identifying the best possible fungicide(s) if the mutation is known.

3.3.2.1 Fungicide recommendations for WT

For the case of WT, ubiquinol showed a strong binding affinity to WT cytochrome b (Figure 3) as expected. Mandestrobin, fenaminstrobin, dimoxystrobin, fenamidone, famoxadone

and ametoctradin had stronger affinity than other high-risk fungicides, meaning they were effective agents for WT cytochrome b. Metominostrobin and thiram had higher affinities than the other fungicides, indicating that they were also effective against cytochrome b. Pyraoxystrobin, pyrametostrobin, pyraclostrobin, flufenoxystrobin, coumoxystrobin, picoxystrobin, triclopyricarb, orysastrobin, fluoxastrobin and metyltetraprole did not bind to WT cytochrome b, and thus extensive usage of these fungicides have a high propensity to develop resistance. The resistant fungicide, azoxystrobin, did not bind to WT cytochrome b. Low-risk fungicides captan, folpet, ferbam and zineb did not bind tightly to WT cytochrome b, which meant that these low-risk fungicides are not recommended.

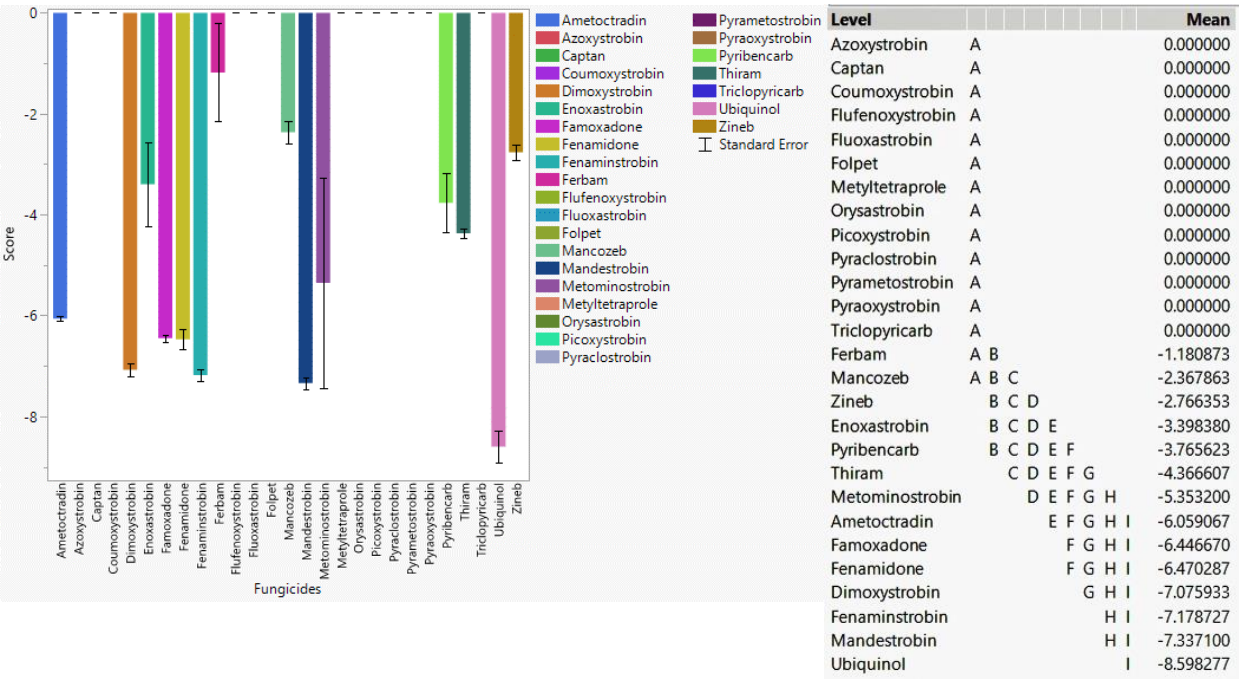

Level									Mean
Azoxystrobin	A								0.000000
Captan	A								0.000000
Coumoxystrobin	A								0.000000
Flufenoxystrobin	A								0.000000
Fluoxastrobin	A								0.000000
Folpet	A								0.000000
Metyltetraprole	A								0.000000
Orysastrobin	A								0.000000
Picoxystrobin	A								0.000000
Pyraclostrobin	A								0.000000
Pyrametostrobin	A								0.000000
Pyraoxystrobin	A								0.000000
Triclopyricarb	A								0.000000
Ferbam	A	B							-1.180873
Mancozeb	A	B	C						-2.367863
Zineb		B	C	D					-2.766353
Enoxastrobin		B	C	D	E				-3.398380
Pyribencarb		B	C	D	E	F			-3.765623
Thiram			C	D	E	F	G		-4.366607
Metominostrobin				D	E	F	G	H	-5.353200
Ametoctradin					E	F	G	H	I -6.059067
Famoxadone						F	G	H	I -6.446670
Fenamidone						F	G	H	I -6.470287
Dimoxystrobin							G	H	I -7.075933
Fenaminstrobin								H	I -7.178727
Mandestrobin								H	I -7.337100
Ubiquinol									I -8.598277

Figure 3: The performance of select QoI fungicides on WT cytochrome b of *Plasmopara viticola* in specific grid box.

3.3.2.2 Fungicide recommendations for G143A mutation

Ubiquinol as a native substrate also showed strong affinity to the G143A mutation of cytochrome b (Figure 4). Mandestrobin, fenaminstrobin, dimoxystrobin, fenamidone, famoxadone and ametoctradin, which showed strong affinity toward WT cytochrome b, also were effective agents against G143A mutated cytochrome b. Coumoxystrobin, Flufenoxystrobin, Pyribencarb and Metominostrobin did not show a high binding affinity to WT cytochrome b, but they were effective fungicides when the G143A mutation occurred, meaning the interaction between G143A mutated version and those ligands was stronger than the WT cytochrome b. Pyraoxystrobin, pyrametostrobin, pyraclostrobin, flufenoxystrobin, enoxastrobin, picoxystrobin, triclopyricarb, orysastrobin, fluoxastrobin and metyltetraprole did not bind to the G143A mutated cytochrome b indicating that these high-risk fungicides are not preferred with the G143A mutated cytochrome b. Low-risk fungicides folpet and thiram showed higher binding affinities than ferbam, zineb, mancozeb and captan, which meant folpet and thiram would be more effective fungicides for the G143A mutated cytochrome b. As a resistant fungicide, azoxystrobin did not bind to both WT and G143A mutated cytochrome b as expected.

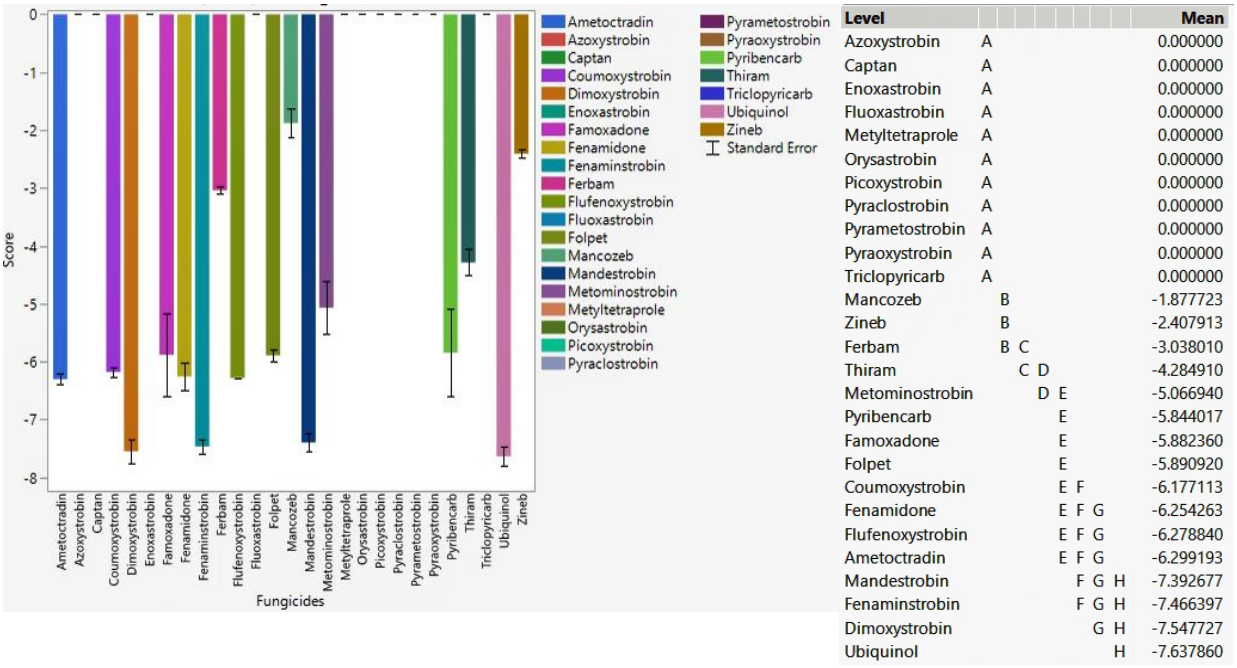

Level		Mean
Azoxystrobin	A	0.000000
Captan	A	0.000000
Enoxastrobin	A	0.000000
Fluoxastrobin	A	0.000000
Metyltetraprole	A	0.000000
Orysastrobin	A	0.000000
Picoxystrobin	A	0.000000
Pyraclostrobin	A	0.000000
Pyrametostrobin	A	0.000000
Pyraoxystrobin	A	0.000000
Triclopyricarb	A	0.000000
Mancozeb	B	-1.877723
Zineb	B	-2.407913
Ferbam	B C	-3.038010
Thiram	C D	-4.284910
Metominostrobin	D E	-5.066940
Pyribencarb	E	-5.844017
Famoxadone	E	-5.882360
Folpet	E	-5.890920
Coumoxystrobin	E F	-6.177113
Fenamidone	E F G	-6.254263
Flufenoxystrobin	E F G	-6.278840
Ametoctradin	E F G	-6.299193
Mandestrobin	F G H	-7.392677
Fenaminstrobin	F G H	-7.466397
Dimoxystrobin	G H	-7.547727
Ubiquinol	H	-7.637860

Figure 4: The performance of select QoI fungicides on G143A mutated cytochrome b of *Plasmopara viticola* in specific grid box.

3.3.2.3 Fungicide recommendations for F129L mutation and G143A-F129L double mutation

In the case of F129L cytochrome b, ubiquinol still showed a strong binding affinity (Figure 5), which followed an analogous pattern to WT and G143A mutated cytochrome b. Among high-risk fungicides, mandestrobin, fenaminstrobin, dimoxystrobin, fenamidone and famoxadone still showed strong affinity toward F129L mutated cytochrome b. Although ametoctradin had high affinity toward WT and G143A mutated cytochrome b, ametoctradin did not bind strongly to F129L mutated version. Coumoxystrobin, flufenoxystrobin, pyribencarb and metominostrobin were effective against G143A mutated cytochrome b but were not effective against F129L mutated version. Pyraoxystrobin, pyrametostrobin, pyraclostrobin, triclopyricarb, orysastrobin, fluoxastrobin and metyltetraprole did not bind to F129L mutated cytochrome b. Enoxastrobin had a weaker affinity toward WT and G143A mutated cytochrome b but it showed a better affinity for F129L mutated version. Folpet and thiram also showed a higher affinity

toward F129L mutated version than ferbam, zineb, mancozeb and captan. As a resistant fungicide, azoxystrobin did not bind to WT, G143A and F129L mutated cytochrome b as expected.

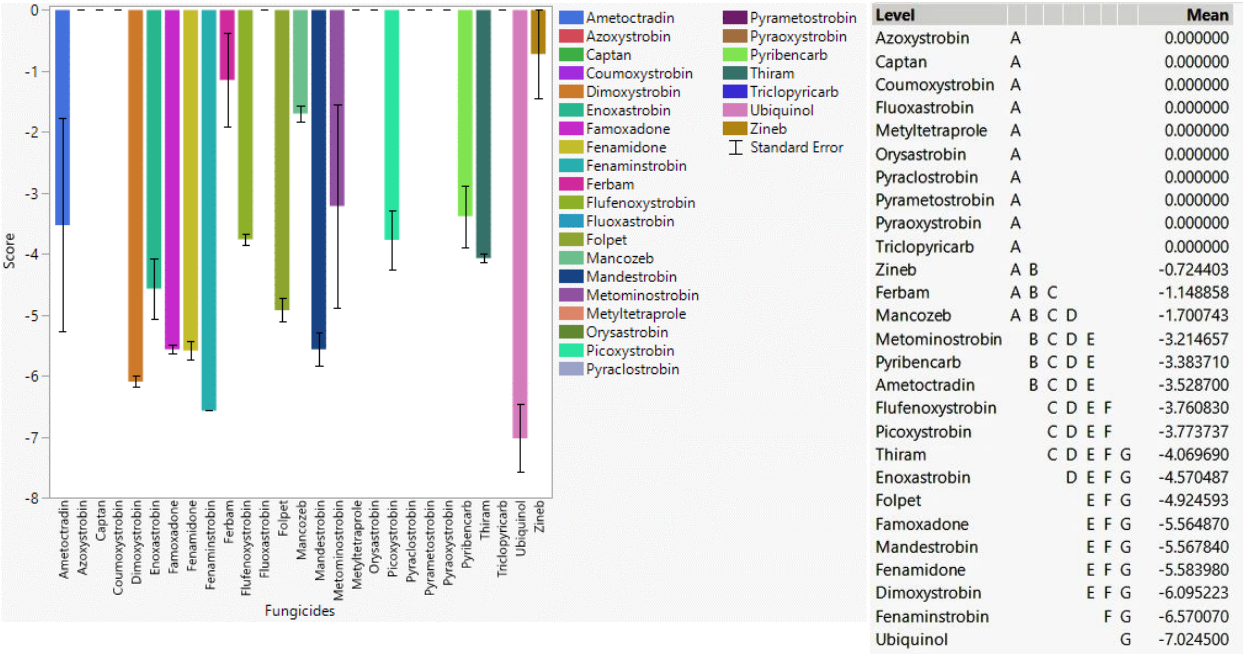

Level		Mean
Azoxystrobin	A	0.000000
Captan	A	0.000000
Coumoxystrobin	A	0.000000
Fluoxastrobin	A	0.000000
Metyltetraprole	A	0.000000
Orysastrobin	A	0.000000
Pyraclostrobin	A	0.000000
Pyrametostrobin	A	0.000000
Pyraoxystrobin	A	0.000000
Triclopyricarb	A	0.000000
Zineb	A B	-0.724403
Ferbam	A B C	-1.148858
Mancozeb	A B C D	-1.700743
Metominostrobin	B C D E	-3.214657
Pyribencarb	B C D E	-3.383710
Ametoctradin	B C D E	-3.528700
Flufenoxystrobin	C D E F	-3.760830
Picoxystrobin	C D E F	-3.773737
Thiram	C D E F G	-4.069690
Enoxastrobin	D E F G	-4.570487
Folpet	E F G	-4.924593
Famoxadone	E F G	-5.564870
Mandestrobin	E F G	-5.567840
Fenamidone	E F G	-5.583980
Dimoxystrobin	E F G	-6.095223
Fenaminstrobin	F G	-6.570070
Ubiquinol	G	-7.024500

Figure 5: The performance of select QoI fungicides on F129L mutated cytochrome b of *Plasmopara viticola* in specific grid box.

Unlike the interaction with WT, F129L and G143A mutated cytochrome b, ubiquinol did not show the highest binding affinity toward cytochrome b when F129L-G143A double mutation occurred (Figure 6). Famoxadone, mandestrobin and dimoxystrobin showed a higher affinity to double-mutated cytochrome b, indicating their potential superiority against the double-mutated cytochrome b. Ametoctradin, fenamidone, fenamindtrobin and metominostrobin also had a higher affinity than the other fungicides, meaning they were also effective against the double-mutated version. Pyraoxystrobin, pyrametostrobin, pyraclostrobin, coumoxystrobin, picoxystrobin, flufenoxystrobin and metyltetraprole did not bind to the double-mutated cytochrome b. Pyraoxystrobin, pyrametostrobin, pyraclostrobin, triclopyricarb, orysastrobin,

fluoxastrobin and metyltetraprole did not bind to any type of cytochrome b, which meant they had a high propensity to become resistant. Also, binding affinity from WT, G143A, F129L and G143A-F129L mutated versions verified the tendency of azoxystrobin to be resistant. Only thiram showed higher affinity for the G143A- F129L double-mutated cytochrome b as compared to the other low-risk fungicides analyzed (folpet, ferbam, zineb, mancozeb and captan).

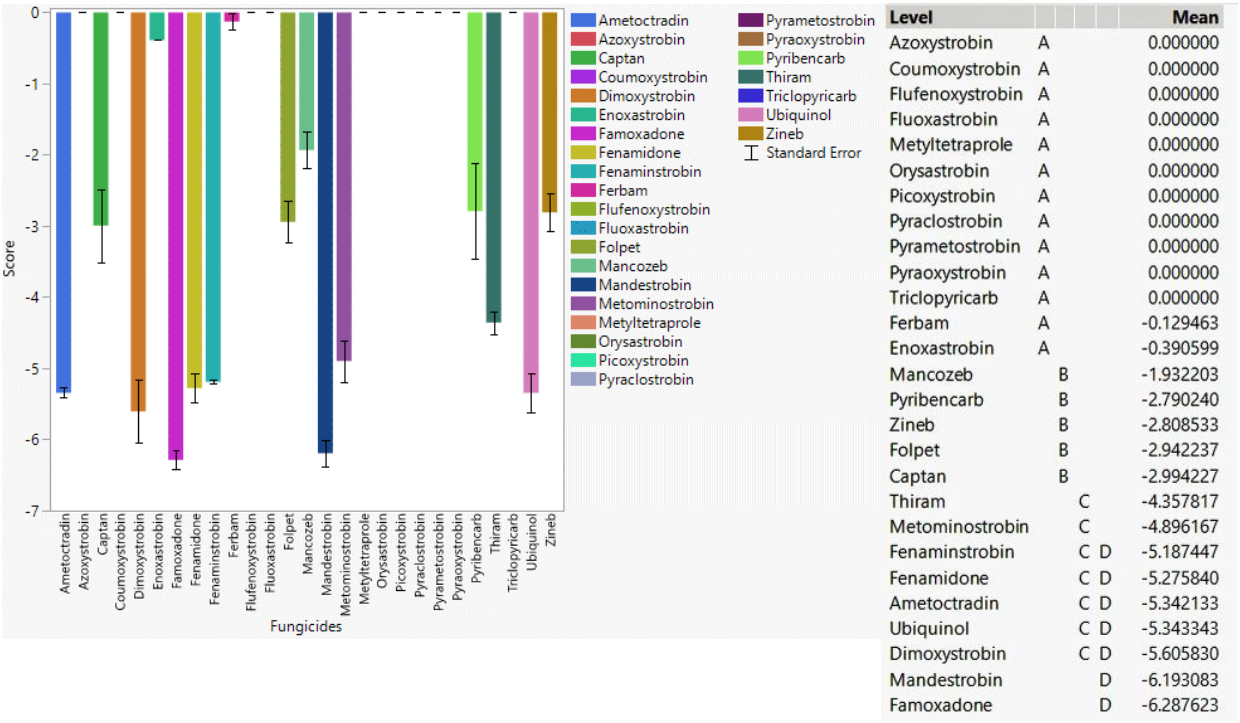

Level				Mean
Azoxystrobin	A			0.000000
Coumoxystrobin	A			0.000000
Flufenoxystrobin	A			0.000000
Fluoxastrobin	A			0.000000
Metyltetraprole	A			0.000000
Orysastrobin	A			0.000000
Picoxystrobin	A			0.000000
Pyraclostrobin	A			0.000000
Pyrametostrobin	A			0.000000
Pyraoxystrobin	A			0.000000
Triclopyricarb	A			0.000000
Ferbam	A			-0.129463
Enoxastrobin	A			-0.390599
Mancozeb		B		-1.932203
Pyribencarb		B		-2.790240
Zineb		B		-2.808533
Folpet		B		-2.942237
Captan		B		-2.994227
Thiram			C	-4.357817
Metominostrobin			C	-4.896167
Fenaminstrobin			C	D -5.187447
Fenamidone			C	D -5.275840
Ametoctradin			C	D -5.342133
Ubiquinol			C	D -5.343343
Dimoxystrobin			C	D -5.605830
Mandestrobin				D -6.193083
Famoxadone				D -6.287623

Figure 6: The performance of select QoI fungicides on F129L-G143A Double mutated cytochrome b of *Plasmopara viticola* in specific grid box.

The interactions of top conformation of the highest affinity fungicides with G143A, F129L mutated and double-mutated versions are given in Figure 7. Dimoxystrobin, famoxadone and ametoctradin showed strong hydrophobic and hydrogen bonding interactions with MET125 of all three mutated versions of cytochrome b. It was evident that the primary interactions between fungicides and cytochrome b were hydrophobic, which agreed with the predominantly hydrophobic nature of cytochrome b proteins [10][33]. Figure 7 shows three fungicides forming

strong hydrophobic interactions with 122-147 and 275-295 regions in G143A, F129L, and double-mutated versions. For the low-risk fungicide, thiram showed strong hydrophobic interactions with cytochrome b.

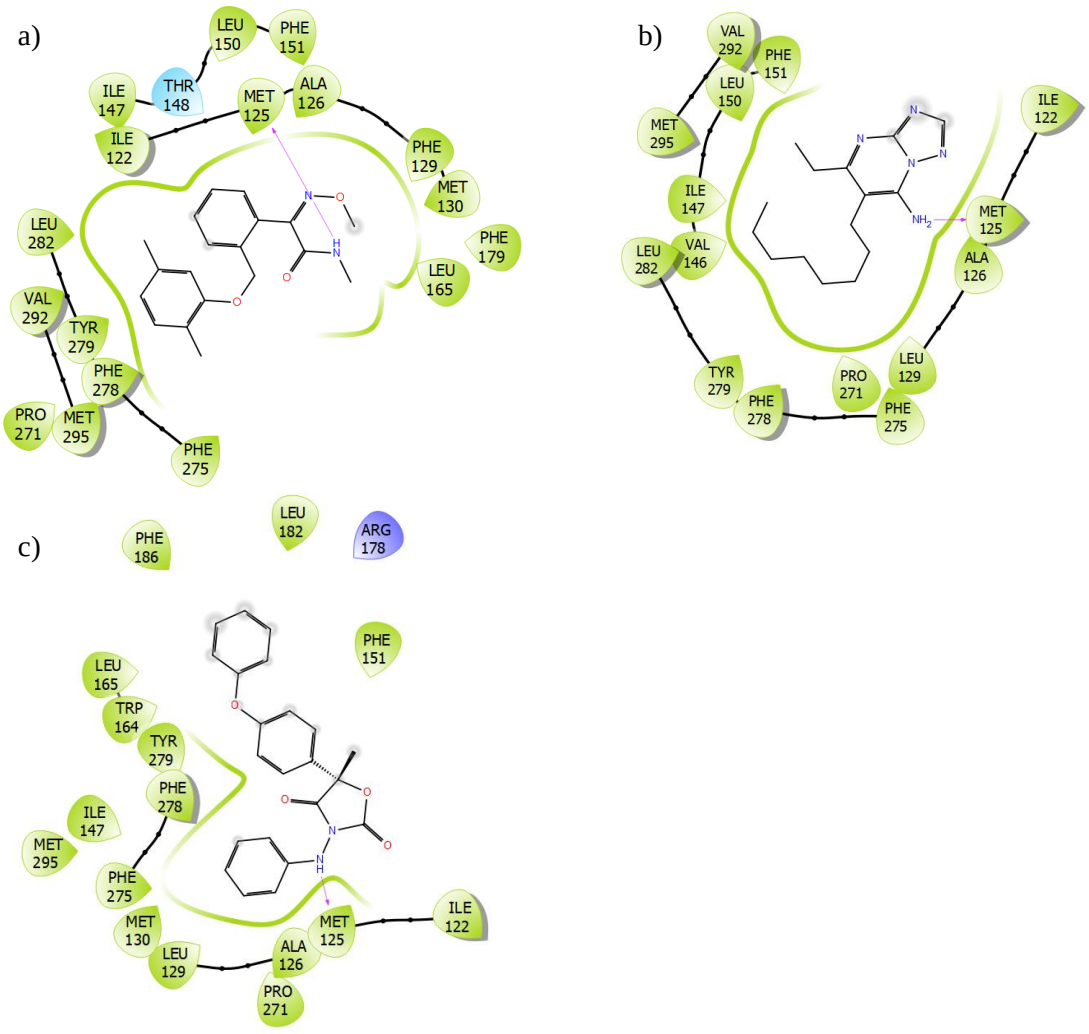

Figure 7: Binding interaction of a) Dimoxystrobin with G143A b) Ametoctradin with F129L mutated and c) Famoxadoone with double mutated type of cytochrome b.

Based on the binding analysis (Figure 8), the pocket located on the top region of cytochrome b that contains residues F129 and G143 seemed to be an important binding position when targeting *Plasmopara viticola* inhibition. Ametoctradin, famoxadone, fenamidone,

fenaminstrobin, mandestrobin, dimoxystrobin, metominostrobin and Thiram tended to bind to this pocket including the native substate ubiquinol.

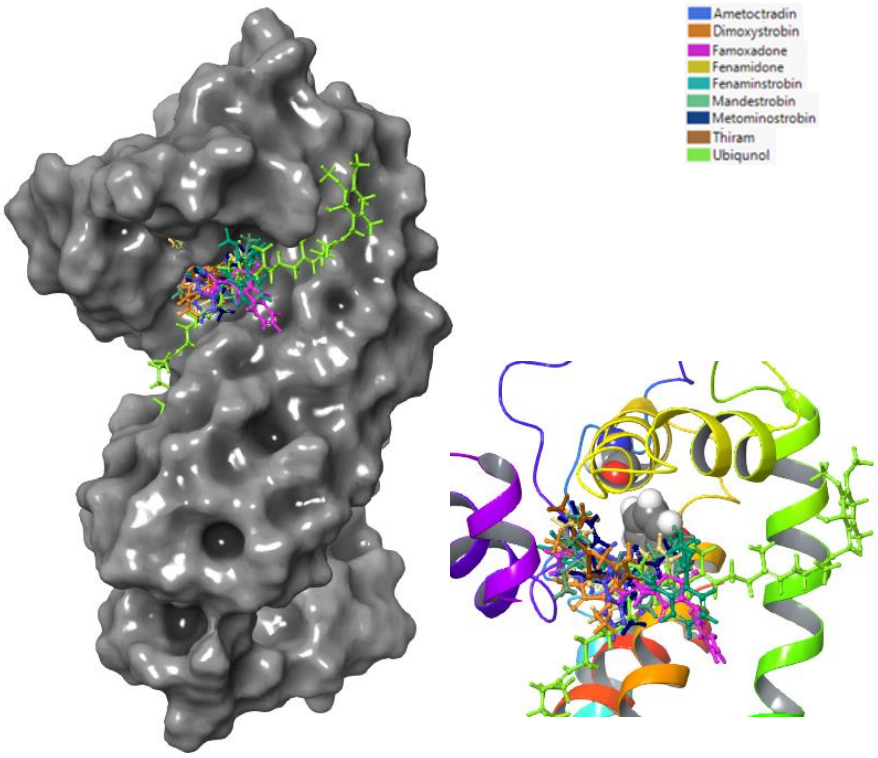

Figure 8: Ametoctradin, Famoxadone, Fenamidone, Fenaminstrobin, Mandestrobin, Dimoxystrobin, Metominostrobin, Thiram, and Ubiquinol with WT cytochrome b of *Plasmopara viticola*.

3.3.3 Molecular Dynamic Simulations with *Plasmopara viticola* Cytochrome b

To further evaluate the binding behavior of these fungicides to cytochrome b, molecular dynamic (MD) simulations were done for select antifungal agents on multiple mutated versions of cytochrome b. Emodel and MM-GBSA energies for selected antifungal agents based on MD simulations are given in Table 2. The energy values were calculated for various combinations of mutations.

Table 2: Emodel and MMGBSA Energies of the binding of antifungal agents on cytochrome b based on molecular dynamic simulations (based on two starting locations)

L123_G137	**Binding Energy (kcal/mol)**	**Emodel_MD**	**F129_G143**	**Binding Energy (kcal/mol)**	**Emodel_MD**
Ubiquinol	-112.872	-73.747	Ubiquinol	-126.815	-45.868
Fenamidone	-80.994	-43.187	Fenamidone	-76.720	-36.630
Famoxadone	-76.531	-59.682	Famoxadone	-54.023	-48.809
Mandestrobin	-61.791	-41.374	Mandestrobin	-60.710	-39.923
Azoxystrobin	-68.634	-57.910	Ametoctradin	-64.640	-38.293
Captan	-36.357	-25.133	Thiram	-52.433	-31.147
Thiram	-25.115	-32.646	Azoxytrobin	DNB	DNB
L123F_G137			**F129L_G143**		
Ubiquinol	-146.167	-78.895	Ubiquinol	-139.022	-53.130
Fenamidone	-74.073	-45.443	Fenamidone	-72.140	-43.909
Famoxadone	-92.628	-58.078	Famoxadone	-96.813	-48.809
Mandestrobin	-60.794	-38.257	Mandestrobin	-63.548	-36.662
Azoxystrobin	-60.789	-57.400	Ametoctradin	-36.603	-23.568
Captan	-51.978	-21.199	Folpet	-59.962	-32.186
Thiram	-35.643	-28.846	Thiram	-34.603	-37.411
			Azoxystrobin	DNB	DNB
L123_G137A			**F129_G143A**		
Ubiquinol	-137.872	-67.460	Ubiquinol	-92.641	-61.849
Fenamidone	-77.810	-45.726	Fenamidone	-56.688	-37.063
Famoxadone	-64.570	-57.756	Famoxadone	-62.046	-38.265
Mandestrobin	-63.381	-42.106	Mandestrobin	-52.780	-30.869
Azoxystrobin	-58.050	-55.299	Ametoctradin	-21.478	-26.039
Captan	-49.964	-28.915	Azoxystrobin	-41.085	-18.536
Thiram	-48.837	-24.120	Folpet	-47.835	-26.049
			Thiram	-51.838	-26.899
L123F_G137A			**F129L_G143A**		
Ubiquinol	-158.153	-73.468	Ubiquinol	-116.358	-57.339
Fenamidone	-60.840	-41.674	Fenamidone	-54.340	-42.041
Famoxadone	-68.740	-60.499	Famoxadone	-74.989	-46.843
Mandestrobin	-62.485	-42.106	Mandestrobin	-41.318	-41.520
Azoxystrobin	-43.013	-55.299	Ametoctradin	-35.546	-29.086
Captan	-48.054	-24.120	Thiram	-36.393	-32.139
Thiram	-42.518	-28.915	Azoxystrobin	DNB	DNB

According to the average binding free energy and Emodel values, ubiquinol, the native substrate, showed a strong affinity toward all versions of cytochrome b. When the target site was randomly confined to residues L123 and G137 or their mutated version(s) (L123F and G137A), the high-risk fungicides, including fenamidone, famoxadone and mandestrobin showed more negative binding free energy and Emodel values as compared to the low-risk fungicides (thiram and captan), indicating that the high-risk fungicides had stronger affinities as compared to low-risk ones. Similar behavior was observed when the active site was confined to F129 and G143 or their mutated version(s), with high-risk fungicides showing tighter binding with cytochrome b. Based on binding free energies and Emodel values, fenamidone and famoxadone were identified as promising antifungal agents which showed high affinity to all mutated versions of cytochrome b, while mandestrobin, ametoctradin and thiram showed strong binding to some of the variations.

In order to get an in-depth understanding of how each ligand bound to the target domain, dominant interactions of ligands with cytochrome b during MD simulations were analyzed. Interactions of fenamidone with WT and F129L mutated cytochrome b is given in Figure 9, and the interaction diagrams for all other ligands are included in Supplementary data. Similar to the docking results, hydrophobic interactions were dominant between *Plasmopara viticola* cytochrome b and the ligands. For native substrate ubiquinol, strong hydrophobic bonding could be observed for both WT and F129L mutated versions, while there was a significant change in ubiquinol interactions for G143A mutated and double mutated versions. For G143A mutated version, ubiquinol formed strong hydrophobic interactions at PHE141, and hydrogen bonding at ALA260; while for double mutated versions, TYR94 and TRP273 were the main points of hydrophobic interactions.

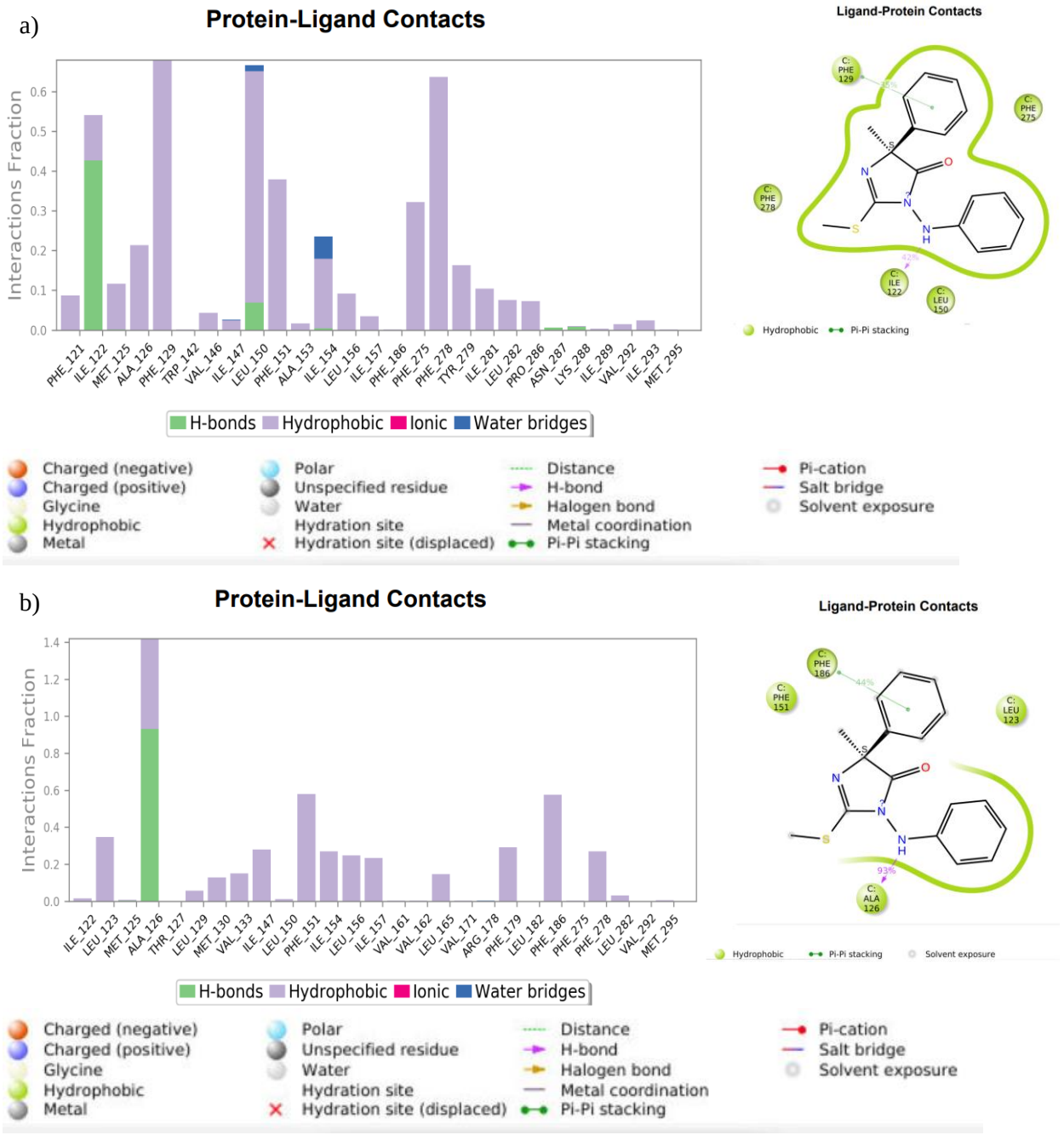

Figure 9: Interactions of Fenamidone with a) wild type and b) F129L mutated versions at F129 and G143 binding site of *Plasmopara viticola*.

Other ligands also showed significant changes in interactions as a result of the mutation. Fenamidone showed high robustness against mutations, forming strong hydrophobic interactions and hydrogen bonding in the regions of ILE122-PHE129 and PHE151-TRP164 in all mutated versions of cytochrome b. Famoxadone also showed strong interactions at these regions for all variations except for the G143A mutation, while it formed strong hydrogen bonding at ILE269 and TRY279 with the G143A mutated version. This observation agrees with the high binding energies shown by fenamidone and famoxadone against all variations of cytochrome b. Mandestrobin formed strong hydrophobic interactions in the vicinity of TYR279 for all versions except the double-mutated version, while for the double-mutated version, the ILE119 was the major site forming hydrophobic interactions. This agrees with the binding energies of mandestrobin and suggests that mandestrobin has lower affinity towards the double mutated version of cytochrome b compared to the other three versions.

Among low-risk fungicides, thiram showed strong hydrophobic interactions at the vicinity of PHE129 for both WT and G143A mutated versions, and at PHE121 and PHE278 for F129L and double mutated versions. However, the interactions of thiram were much weaker than the high-risk fungicides, which agrees with the less negative binding energies. While ametoctradin had strong hydrophobic binding at ILE147 and PHE151 with the WT protein, it had only weak hydrophobic interactions against the mutated versions, suggesting that it may not be effective against the mutations, which also agrees with the published literature [25].

When the docking site was centered on L123 and G137, a randomly selected location, interactions of native substrate ubiquinol changed significantly with mutated versions. However, both fenamidone and famoxadone showed strong hydrophobic interactions or hydrogen bonding at the region ILE121-TYR132 of all variations, suggesting that these two compounds are robust

against these mutations also. Similar to the F129 and G143 centered simulations, interactions of famoxadone changed significantly under G137A and double-mutated versions. Thiram, captan and azoxystrobin bound weakly against most of the mutated versions. Thus, based on the interactions during molecular simulations, fenamidone and famoxadone were identified as the most robust fungicides against all tested mutations.

Stability of the binding interactions during the (MD) simulations were evaluated using RMSD diagrams. Simulations of ubiquinol, fenamidone, famoxadone, mandestrobin and ametoctradin equilibrated against all versions of cytochrome b, which shows stable binding with all mutated versions. However, thiram showed significant fluctuations against F129L and F129L-G143A mutated versions, suggesting its potential susceptibility to resistance due to low affinity. Azoxystrobin also did not show stable binding with multiple mutations, which is expected since it has been shown to be resistant and ineffective against some mutations of cytochrome b. RMSD diagrams for the ligands against different variations of cytochrome b is given in Supplementary data. Overall, the MD simulations further reinforced the findings from the docking analysis.

3.4 Fungicide binding behavior on *Botrytis cinerea* Cytochrome b

To further verify binding affinities, an additional set of docking simulations were performed, this time using a grid box covering the ubiquinol binding site and the specific residues G143 and F129 on cytochrome b of *Botrytis cinerea*. For this analysis, the same 26 fungicides covering resistant, high-risk and low-risk, were selected (Table 3). *Botrytis cinerea* was used because *Plasmopara viticola* was an obligate parasite and experimental validations could only be done under field conditions, whereas *Botrytis cinerea* validations could easily be done in a laboratory setting.

3.4.1 General Observations

Table 3. Glide docking scores for fungicides on four variations of *Botrytis cinerea* Cytochrome b covering G143 and F129 site (average of the top three binding poses).

Fungicide	Wild type average docking score (G143 and F129 as binding center)	G143A average docking score	F129L average docking score	Double mutation average docking score	Risk	Fungicide Type
Ubiqunol	-9.338	-4.680	-7.805	-2.408	NA	NA
Famoxadone	-8.091	-8.765	-6.697	-4.021	HR	QoI
Azoxystrobin	DNB	DNB	DNB	DNB	HR/R	QoI
Fenamidone	-6.246	-5.950	-5.784	-5.058	HR	QoI
Coumoxystrobin	DNB	DNB	DNB	DNB	HR	QoI
Flufenoxystrobin	-7.509	DNB	-6.108	-0.0784	HR	QoI
Enoxastrobin	-10.162	DNB	DNB	DNB	HR	QoI
Pyraoxystrobin	-11.518	-4.717	DNB	-4.121	HR	QoI
Picoxystrobin	-7.473	-8.200	DNB	DNB	HR	QoI
Metyltetraprole	DNB	DNB	-4.142	-3.305	HR	QoI
Fenaminstrobin	-9.330	DNB	-2.3223	-0.6988	HR	QoI
Pyribencarb	-9.534	-8.446	-9.761	-4.671	HR	QoI
Dimoxystrobin	-8.957	-4.234	-4.469	-1.650	HR	QoI
Triclopyricarb	-5.445	DNB	DNB	DNB	HR	QoI
Metominostrobin	-7.891	-7.417	-3.576	-4.032	HR	QoI
Pyrametostrobin	DNB	DNB	DNB	DNB	HR	QoI
Mandestrobin	-10.876	-8.690	-7.911	-5.913	HR	QoI
Fluoxastrobin	DNB	DNB	DNB	DNB	HR	QoI
Pyraclostrobin	-9.060	-3.442	DNB	-3.117	HR	QoI
Orysastrobin	DNB	DNB	DNB	DNB	HR	QoI
Folpet	-7.406	DNB	DNB	DNB	LR	PHT
Ferbam	-3.034	-3.136	-0.549	-1.123	LR	DTC
Captan	-5.513	DNB	-3.705	-3.899	LR	PHT
Mancozeb	DNB	DNB	DNB	DNB	LR	DTC
Ametoctradin	-6.970	-6.954	-6.156	-5.767	HR	QoI
Thiram	-4.714	-4.935	-3.700	-4.749	LR	DTC
Zineb	-2.635	-2.452	-2.413	-2.287	LR	DTC

Based on an initial analysis, praoxystrobin, mandestrobin, pyribencarb and enoxastrobin showed stronger affinity towards WT cytochrome b. When G143A or F129L mutations occurred, pyribencarb, famoxadone and mandestrobin showed strong affinity to cytochrome b. If the G143A-F129L double mutation occurred, fenamidone, ametoctradin, mandestrobin, thiram and pyraoxystrobin showed a strong affinity to mutated cytochrome b. Ubiquinol had a strong affinity to WT, G143A or F129L cytochrome b but the binding affinity to G143A-F129L double-mutated cytochrome b was low. Praoxystrobin bound tightly to the WT cytochrome b but its affinity decreased as mutations occurred on cytochrome b. High-risk fungicides had less affinity for double mutated cytochrome b. Among high-risk fungicides, mansestrobin, pyribencarb, fenamidone, famoxadone and ametoctradin were effective fungicides against all versions of cytochrome b. Thiram showed a strong affinity to all four types of cytochrome b among all the low-risk fungicides. Azoxystrobin did not show stable binding with multiple mutations, which is expected since it was resistant against cytochrome b. Then we did a replicated study to find out the behavior of fungicides in more detail.

Comparison of binding affinities against WT, F129L, G143A and double mutated cytochrome b of *Botrytis cinerea* revealed that mandestrobin, pyribencarb, famoxadone and ametoctradin had a higher binding affinity than ubiquinol, meaning these fungicides may be effective against inhibiting cytochrome b of *Botrytis cinerea* (Figure 10). Fenamidone, metominostrobin, pyraoxystrobin, dimoxystrobin, and thiram had higher affinities than the others indicating their broad-spectrum ability to bind to the active site regardless of the occurrence of the two common mutations. It should also be noted that was azoxystrobin which was identified as a resistant fungicide did not bind to wild type nor any of the mutated versions. Also, since coumuxystrobin, fluoxastobin, and orysastrobin did not bind to WT or any of the mutated

versions, these fungicides are considered to show the highest propensity to develop resistance. Also, fungicides folpet, ferbam, zineb, and captan that were categorized as low risk did not bind with appreciable affinity to the active site indicating that these were probably not best considering their propensity to avert resistance.

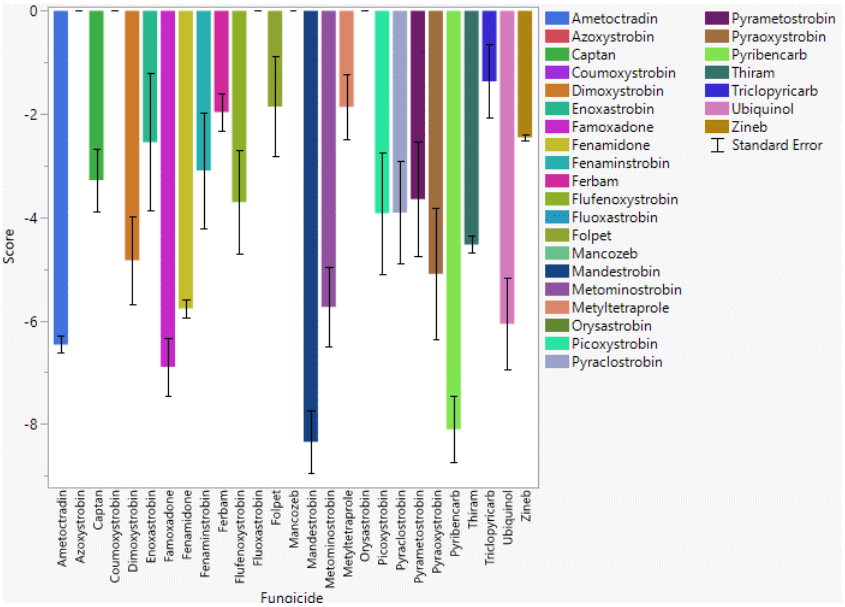

Level								Mean
Azoxystrobin	A							0.000000
Coumoxystrobin	A							0.000000
Fluoxastrobin	A							0.000000
Mancozeb	A							0.000000
Orysastrobin	A							0.000000
Triclopyricarb	A	B						-1.361281
Folpet	A	B	C					-1.851495
Metyltetraprole	A	B	C					-1.861790
Ferbam	A	B	C					-1.960295
Zineb	A	B	C	D				-2.446868
Enoxastrobin	A	B	C	D	E			-2.540386
Fenaminstrobin	A	B	C	D	E	F		-3.087881
Captan	A	B	C	D	E	F		-3.279134
Pyrametostrobin	A	B	C	D	E	F		-3.642075
Flufenoxystrobin	A	B	C	D	E	F		-3.704778
Pyraclostrobin	A	B	C	D	E	F		-3.904766
Picoxystrobin	A	B	C	D	E	F		-3.918415
Thiram		B	C	D	E	F	G	-4.524612
Dimoxystrobin		B	C	D	E	F	G	-4.827498
Pyraoxystrobin		B	C	D	E	F	G	-5.088951
Metominostrobin			C	D	E	F	G	-5.729165
Fenamidone			C	D	E	F	G	-5.759592
Ubiquinol				D	E	F	G	-6.057838
Ametoctradin					E	F	G	-6.461639
Famoxadone						F	G	-6.893328
Pyribencarb							G	-8.102745
Mandestrobin							G	-8.347541

Figure 10: The performance of select QoI fungicides on WT, G143A, F129L, and G143A-F129L double mutated cytochrome b of *Botrytis cinerea* in general.

3.4.2 Mutation-specific Observations

3.4.2.1 Fungicide recommendations for WT

It was observed that pyraoxystrobin, mandestrobin, enoxastrobin and pyribencarb had higher binding affinity than ubiquinol to WT cytochrome b indicating their potential superiority as effective fungicides via inhibition of cytochrome b of *Botrytis cinerea* (Figure 11). Fenaminstrobin, pyraclostrobin, dimoxystrobin, famoxadone, metominstrobin, pyrametostrobin, flufenoxystrobin, picoxystrobin, folpet, ametoctradin, fenamidone, captan and triclopyricarb had

higher affinities to WT cytochrome b than the other fungicides. Azoxystrobin as an identified resistant fungicide did not bind to the WT cytochrome b. Coumoxystrobin, fluoxastrobin, metyltertrapole and orysastrobin did not bind to the WT cytochrome b, indicating their high possibility to succumb to resistance. Also, zineb and ferbam were low-risk fungicides that showed weaker binding affinity than captan, thiram and folpet, which meant zineb and ferbam were likely not effective fungicides against inhibiting cytochrome b of *Botrytis cinerea*.

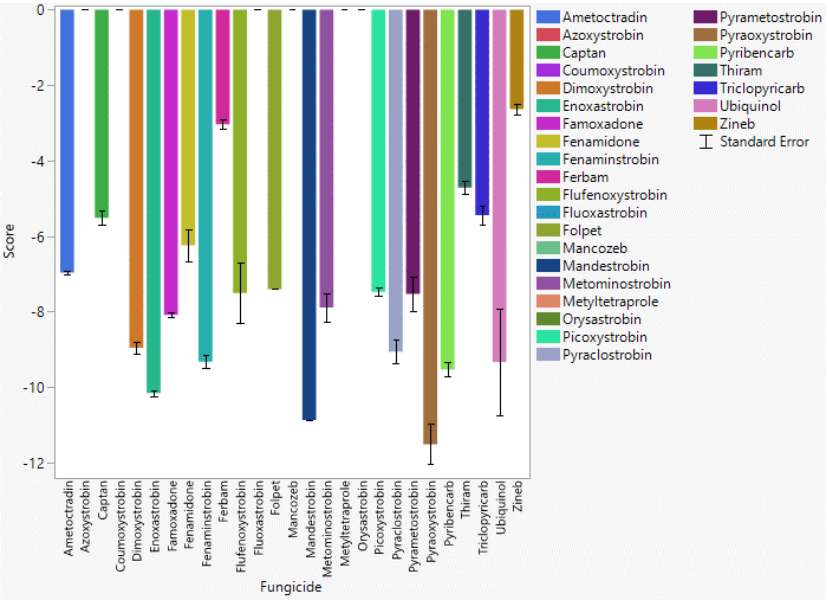

Level												Mean
Azoxystrobin	A											0.00000
Coumoxystrobin	A											0.00000
Fluoxastrobin	A											0.00000
Mancozeb	A											0.00000
Metyltetraprole	A											0.00000
Orysastrobin	A											0.00000
Zineb		B										-2.63499
Ferbam		B	C									-3.03435
Thiram			C	D								-4.71424
Triclopyricarb				D	E							-5.44512
Captan				D	E	F						-5.51340
Fenamidone				D	E	F	G					-6.24583
Ametoctradin					E	F	G	H				-6.96978
Folpet					E	F	G	H	I			-7.40598
Picoxystrobin					E	F	G	H	I	J		-7.47345
Flufenoxystrobin					E	F	G	H	I	J		-7.50890
Pyrametostrobin						F	G	H	I	J		-7.52901
Metominostrobin							G	H	I	J		-7.89130
Famoxadone							G	H	I	J		-8.09115
Dimoxystrobin								H	I	J	K	-8.95739
Pyraclostrobin									I	J	K	-9.05979
Fenaminstrobin									I	J	K	-9.33043
Ubiquinol									I	J	K	-9.33795
Pyribencarb										J	K	L -9.53408
Enoxastrobin											K	L -10.16154
Mandestrobin											K	L -10.87630
Pyraoxystrobin												L -11.51793

Figure 11: The performance of select QoI fungicides on WT cytochrome b of *Botrytis cinerea* in specific grid box.

3.4.2.2 Fungicide recommendations for G143A mutation

Fungicides famoxadone, mandestrobin, pyribencarb, picoxystrobin, metominostrobin, fenamidone, pyraoxystrobin and thiram showed strong affinity to G143A mutated cytochrome b of *Botrytis cinerea* than ubiquinol indicating their superior ability to withstand resistance caused by the G143A mutation of cytochrome b of *Botrytis cinerea* (Figure 12). Enoxastrobin, fenaminstrobin, flufenoxystrobin, pyrametostrobin also showed a strong affinity toward WT

cytochrome b but did not bind or bind weakly toward G143A mutated cytochrome b, meaning these fungicides may not be effective if G143A mutation occurred. Coumoxystrobin, fluoxastrobin, metyltertrapole and orysastrobin did not bind to the G143A cytochrome b. Azoxystrobin as identified resistant fungicide did not bind to the G143A cytochrome b. Ferbam and zineb had weaker binding affinity while captan and foplet did not bind to the G143A cytochrome b, indicating that these four low-risk fungicides were not likely effective against G143A mutated cytochrome b of *Botrytis cinerea*.

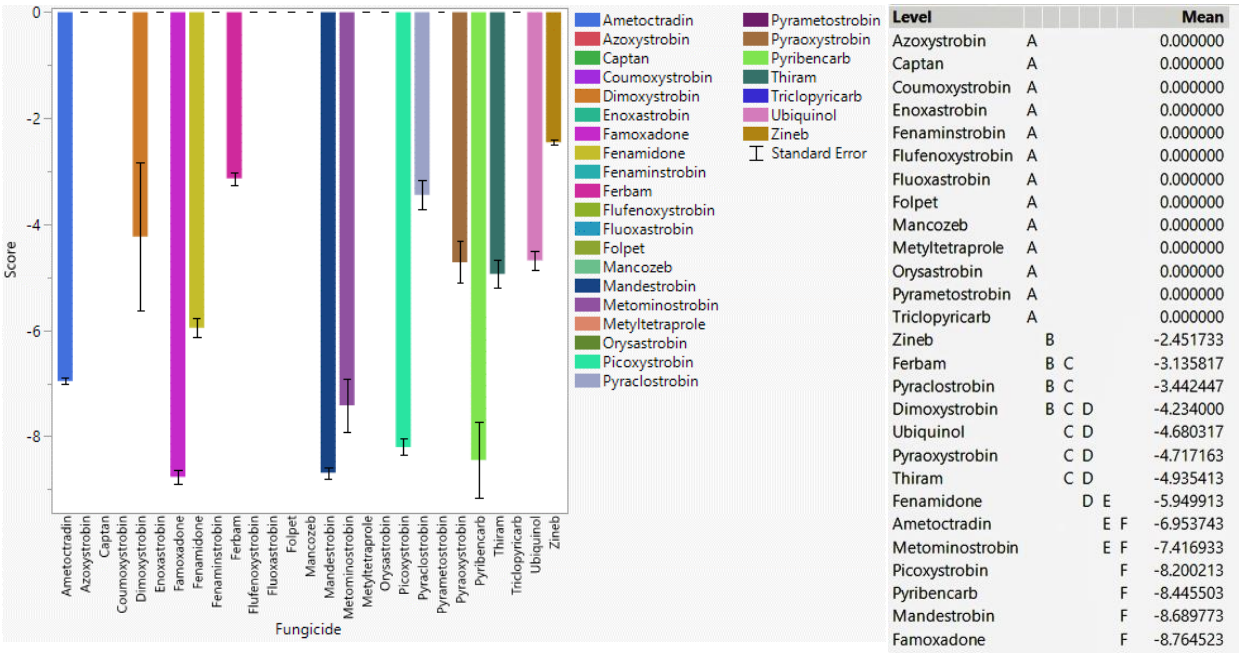

Level							Mean
Azoxystrobin	A						0.000000
Captan	A						0.000000
Coumoxystrobin	A						0.000000
Enoxastrobin	A						0.000000
Fenaminstrobin	A						0.000000
Flufenoxystrobin	A						0.000000
Fluoxastrobin	A						0.000000
Folpet	A						0.000000
Mancozeb	A						0.000000
Metyltetraprole	A						0.000000
Orysastrobin	A						0.000000
Pyrametostrobin	A						0.000000
Triclopyricarb	A						0.000000
Zineb		B					-2.451733
Ferbam		B	C				-3.135817
Pyraclostrobin		B	C				-3.442447
Dimoxystrobin		B	C	D			-4.234000
Ubiquinol			C	D			-4.680317
Pyraoxystrobin			C	D			-4.717163
Thiram			C	D			-4.935413
Fenamidone				D	E		-5.949913
Ametoctradin					E	F	-6.953743
Metominostrobin					E	F	-7.416933
Picoxystrobin						F	-8.200213
Pyribencarb						F	-8.445503
Mandestrobin						F	-8.689773
Famoxadone						F	-8.764523

Figure 12: The performance of select QoI fungicides on G143A cytochrome b of *Botrytis cinerea* in specific grid box.

3.4.2.3 Fungicide recommendations for F129L mutation and G143A-F129L double mutation

Mandestrobin and pyribencarb showed a stronger binding affinity to F129L mutated cytochrome b of *Botrytis cinerea* than ubiquinol, meaning these fungicides may be effective against the F129L mutation (Figure 13). Pyrametostrobin, famoxadone, ametoctradin, flufenoxystrobin and fenamidone had higher binding affinity than the rest of fungicides, which

also showed strong affinity toward F129L cytochrome b. Coumoxystrobin, fluoxastrobin and orysastrobin did not bind to F129L cytochrome b indicating that these three QoIs may not be effective against this mutation. Azoxystrobin, the identified resistant fungicide, did not bind to the G143A mutated cytochrome b. The low-risk fungicides, folpet and ferbam, did not bind to cytochrome b. Thiram, captan and zineb only showed weak binding affinities indicating that these low-risk fungicides may not be effective against inhibiting F129L mutated cytochrome b.

a)

Level								Mean
Azoxystrobin	A							0.000000
Coumoxystrobin	A							0.000000
Enoxastrobin	A							0.000000
Fluoxastrobin	A							0.000000
Folpet	A							0.000000
Mancozeb	A							0.000000
Orysastrobin	A							0.000000
Picoxystrobin	A							0.000000
Pyraclostrobin	A							0.000000
Pyraoxystrobin	A							0.000000
Triclopyricarb	A							0.000000
Ferbam	A							-0.548516
Fenaminstrobin	A	B						-2.322297
Zineb	A	B						-2.413280
Metominostrobin		B	C					-3.576347
Thiram		B	C					-3.699497
Captan		B	C	D				-3.704573
Metyltetraprole		B	C	D	E			-4.142343
Dimoxystrobin		B	C	D	E			-4.468513
Fenamidone			C	D	E	F		-5.784293
Flufenoxystrobin			C	D	E	F		-6.108357
Ametoctradin			C	D	E	F		-6.155867
Famoxadone				D	E	F		-6.697047
Pyrametostrobin					E	F	G	-7.039287
Ubiquinol						F	G	-7.805133
Mandestrobin						F	G	-7.911273
Pyribencarb							G	-9.760807

b)

Level								Mean
Azoxystrobin	A							0.000000
Coumoxystrobin	A							0.000000
Enoxastrobin	A							0.000000
Fluoxastrobin	A							0.000000
Folpet	A							0.000000
Mancozeb	A							0.000000
Orysastrobin	A							0.000000
Picoxystrobin	A							0.000000
Pyrametostrobin	A							0.000000
Triclopyricarb	A							0.000000
Fenaminstrobin	A	B						-0.698797
Ferbam	A	B	C					-1.122497
Flufenoxystrobin	A	B	C					-1.201850
Dimoxystrobin	A	B	C	D				-1.650087
Zineb	A	B	C	D	E			-2.287473
Ubiquinol	A	B	C	D	E			-2.407950
Pyraclostrobin		B	C	D	E	F		-3.116827
Metyltetraprole			C	D	E	F	G	-3.304817
Captan				D	E	F	G	H	-3.898560
Famoxadone				D	E	F	G	H	-4.020590
Metominostrobin				D	E	F	G	H	-4.032077
Pyraoxystrobin				D	E	F	G	H	-4.120707
Pyribencarb					E	F	G	H	-4.670590
Thiram					E	F	G	H	-4.749297
Fenamidone						F	G	H	-5.058327
Ametoctradin							G	H	-5.767163
Mandestrobin								H	-5.912817

Figure 13: The performance of select QoI fungicides on F129L and G143A-F129L mutated cytochrome b of *Botrytis cinerea* in specific grid box.

The QoIs fenamidone, mandestrobin, ametoctradin, pyribencarb and thiram showed strong binding affinity toward the G143A-F129L double mutated cytochrome b of *Botrytis cinerea*. The G143A-F129L double mutation may not be usual since ubiquinol did not show any strong affinity to the double mutated cytochrome b. Pyraoxystrobin, metominostrobin, famoxadone, captan, metylteraprole, pyraclostrobin and zineb showed higher binding affinity

than the rest of the fungicides with the double-mutated cytochrome b, but they may not be as effective as the top binding fungicides, i.e., fenamidone, ametoctradin, pyribencarb and thiram. Coumoxystrobin, fluoxastrobin azoxystrobin and orysastrobin did not bind appreciably and may not be appropriate for *Botrytis cinerea* cytochorme b inhibition. Among the low-risk group, folpet and ferbam emerged to be not effective against cytochrome b inhibition.

An analysis of the binding behavior of ametoctradin, pyraoxystrobin, mandestrobin, enoxastrobin and pyribencarb at the vicinity of the G143 and F129 residues of WT cytochrome b of *Botrytis cinerea* indicated that they all bound close to the two residues (Figure 14). For the G143A mutation, picoxystrobin, metominostrobin, pyribencarb, famoxadone and mandestrobin bound to the same site as WT cytochrome b. This position was also the binding site for ubiquinol on both WT and G143A cytochrome b, indicating that this site is crucial when deciding effective QoIs targeting *Botrytis cinerea* cytochrome b inhibition.

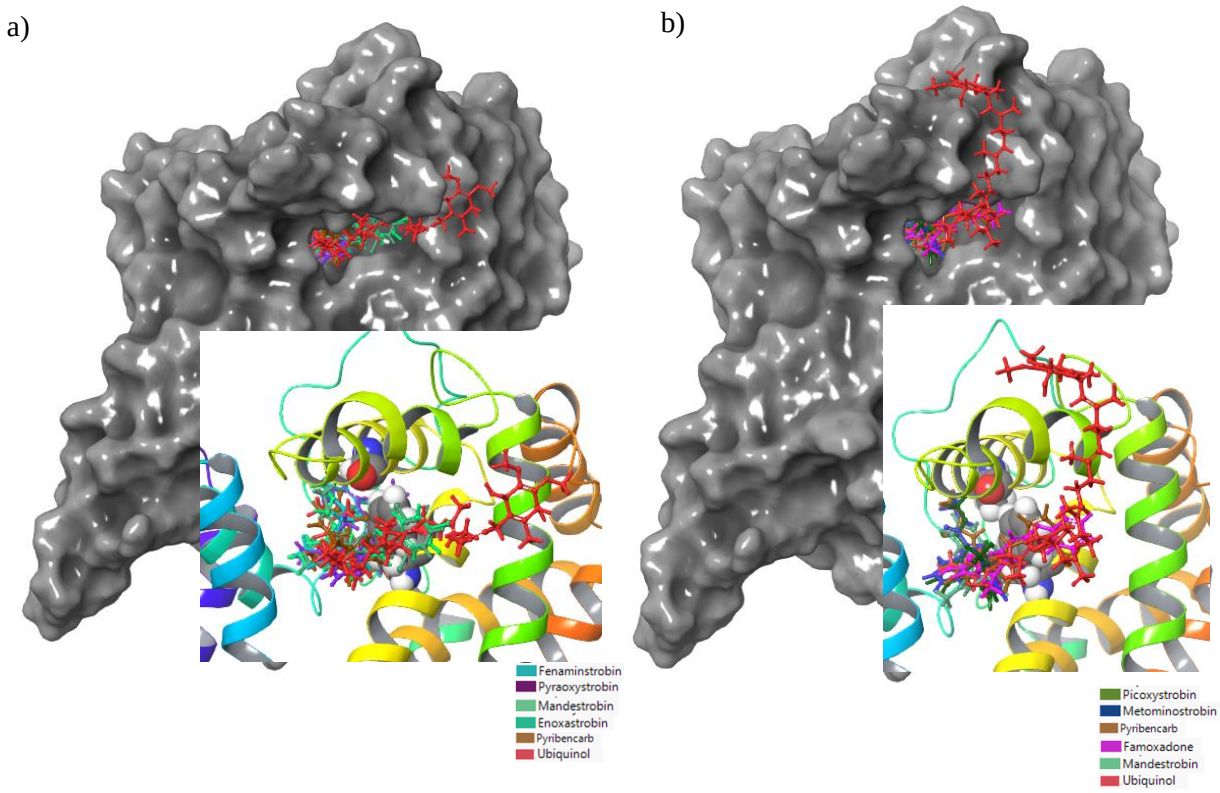

Figure 14: a) Fenamidtrobin, Pyraoxystrobin, Mandestrobin, Enoxastrobin, Pyribencarb and Ubiquinol with WT cytochrome b and b) Picoxystrobin, Metominostrobin, Pyribencarb, Famoxadone, Mandestrobin and Ubiquinol with G143A cytochrome b of *Botrytis cinerea*.

Analysis of interactions (Figure 15) of cytochrome b of WT *Botrytis cinerea* with ubiquinol and pyraoxystrobin indicated that hydrophobic bonding was the primary interaction that occurred. There was also a hydrogen bonding with PHE164 and ARG178 for ubiquinol and GLU273 for pyraoxystrobin. For the G143A mutated cytochrome b, hydrophobic bonding still played a major role in pyribencarb. The interaction with the residue F129 was hydrophobic regardless of the ligand. However, the interaction of ligands with the residue G143 was not apparent in WT cytochrome b; however, pyribencarb showed hydrophobic bonding once the G143A mutation occurred.

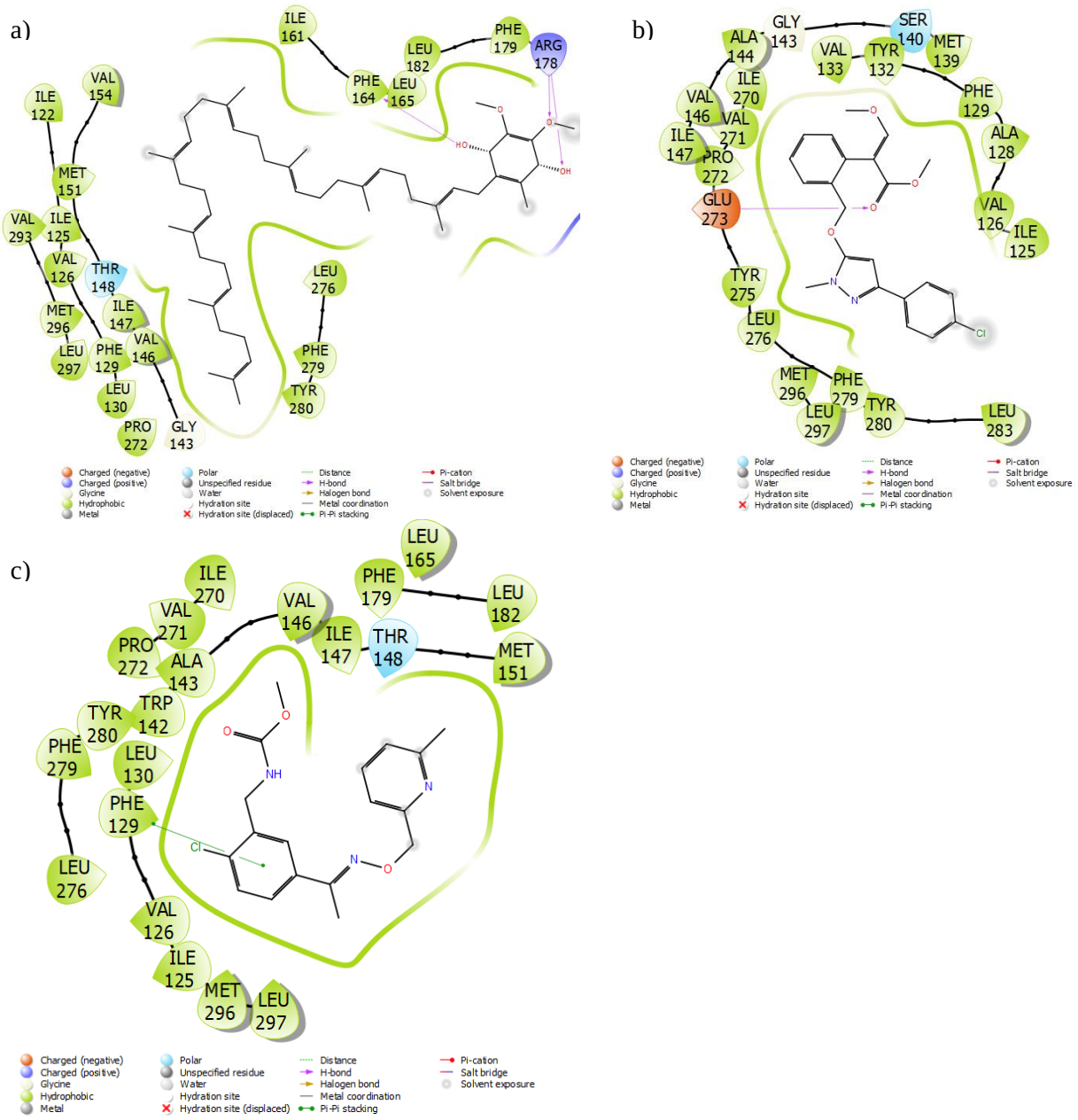

Figure 15: a) Ubiquinol and b) Pyraoxystrobin with WT cytochrome b and c) Pyribencarb with *Botrytis cinerea* cytochrome b with G143A mutation.

3.5 AutoQSAR model evaluation

3.5.1 Application of AutoQSR to predict fungicides for *Botrytis cinerea*

3.5.1.1 Training data set without validation sets

An initial training set was developed using 16 QoI and 18 non-QoI fungicides. The top five QSAR models and their performance parameters generated for *Botrytis cinerea* are depicted in Figure 16, and were pls_19, kpls_radial_19, kpls_dendritic_19, kpls_desc_19 and kpls_linear_19. Based on the scoring functions, the best model was pls_19 that was generated by partial least square regression (PLS), using the 19^{th} spilt of the learning set into a test and training set (34 ligands) without validation set. This model had a standard deviation (S.D) of 2.1184, R^2 of 0.6378, root-mean-square error (RMSE) of 2.1419, Q^2 of 0.6172 and a ranking score of 0.5892. Binding affinity, Y(Obs), and predicted affinity, Y(Pred), from the QSAR model of all selected ligands is shown in Figure 17, with 75% of ligands belonging to the training set and 25% ligands in the test set for *Botrytis cinerea*. The five scatter plots in Figure 18 were generated based on Y(Obs) and Y(Pred). The results indicate that about 50% of training sets were close to the regression line.

Model Report

Model Code	Score	S.D.	R^2	RMSE	Q^2	Q^2 MW (Null Hypothesis)
pls_19	0.5892	2.1184	0.6378	2.1419	0.6172	-0.0635
kpls_radial_19	0.5595	1.8525	0.7110	2.1152	0.6267	-0.0635
kpls_dendritic_19	0.5593	1.6052	0.7830	2.0310	0.6558	-0.0635
kpls_desc_19	0.5544	1.9419	0.6956	2.1414	0.6174	-0.0635
kpls_linear_19	0.5219	1.6506	0.7706	2.1168	0.6261	-0.0635
kpls_radial_39	0.4979	1.9519	0.6875	2.2512	0.5641	-1.2909
kpls_dendritic_34	0.4899	1.7542	0.7610	2.1877	0.5655	-0.5910
kpls_linear_34	0.4792	1.7329	0.7668	2.2016	0.5600	-0.5910
kpls_radial_16	0.4760	1.9404	0.7073	2.2709	0.5352	-1.2336
kpls_dendritic_44	0.4308	1.4941	0.8236	2.2315	0.5745	0.1264

Figure 16: Top 10-ranked QSAR models without a validation set for fungicides used in *Botrytis cinerea*.

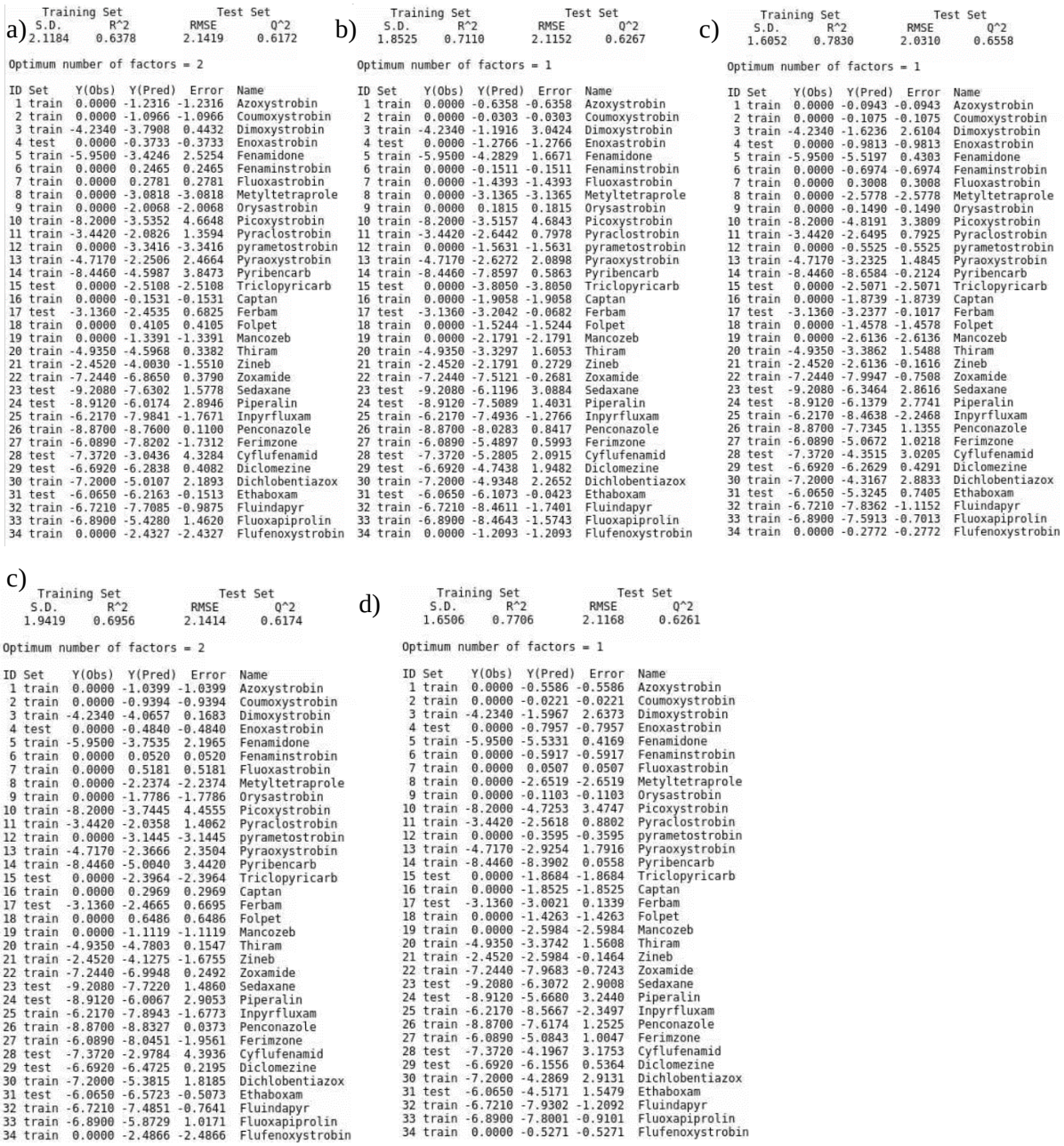

Figure 17: Model reports for a) pls_19, b) kpls_radial_19, c) kpls_dendritic_19, d) kpls_desc_19 and e) kpls_linear_19 models.

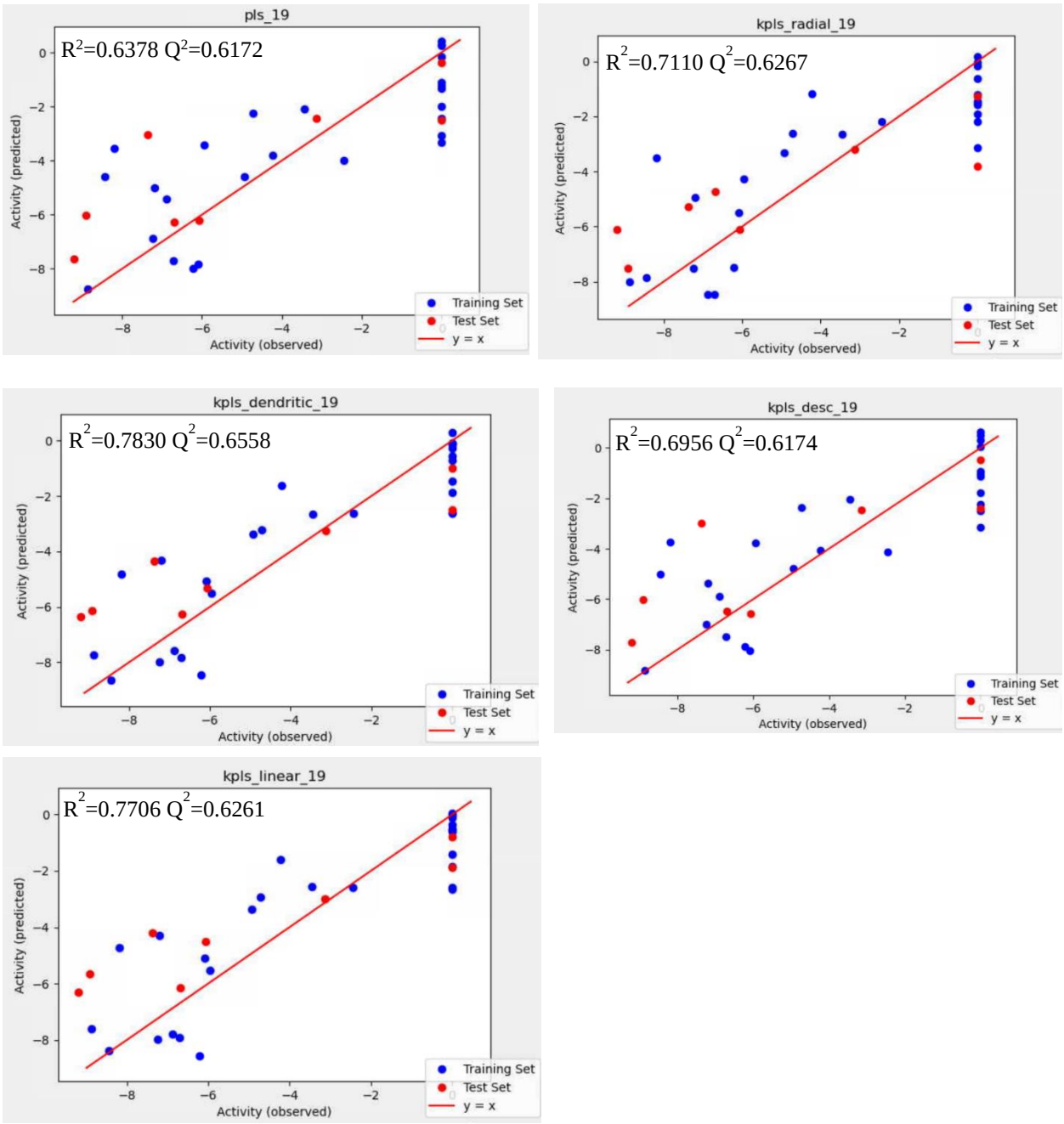

Figure 18: Scatter plot about performance for a) pls_19, b) kpls_radial_19, c) kpls_dendritic_19, d) kpls_desc_19 and (e) kpls_linear_19 models.

In order to evaluate if the predictions could be improved, it was decided to refine the models by systematically removing outliers that were chemically distinct from the ones that

function as QoIs and/or when the difference between actual and predicted affinities were larger than 3 kCal/mol.

3.5.1.1.1 Iteration #1

The new external validation set that includes 19 ligands was used to estimate the prediction accuracy of the QSAR model made by the top five numeric models listed in Figure 16 (Table 4). The R^2 value of the best-fit line was 0.06, meaning the QSAR model was not able to predict with an acceptable level of accuracy for the given validation set. Also, some ligands in Figure 19 fell outside the applicability domain of the QSAR model, which would decrease the prediction accuracy of the QSAR model. Visual inspection for Figure 19 showed that metominostrobin, azaconazole, dithianon and picarbutrazox were outliers, indicating these ligands were possibly unsuitable to be included in the validation set to the built model. Both azaconazole and picarbutrazox had multiple heterocyclic nitrogen atoms (Figure 20). Dithianon was the only ligand that contained heterocyclic dual sulfur atoms among 19 ligands. Metominostrobin, azaconazole, dithianon and picarbutrazox had an oxygen-containing aromatic ring, and there were at least two oxygen atoms in each ligand. The structural reasons mentioned above might be possible reasons that caused these four ligands to be improper to be included in the validation set. To improve the prediction accuracy of QSAR model, these ligands would be considered to be removed in the next iteration.

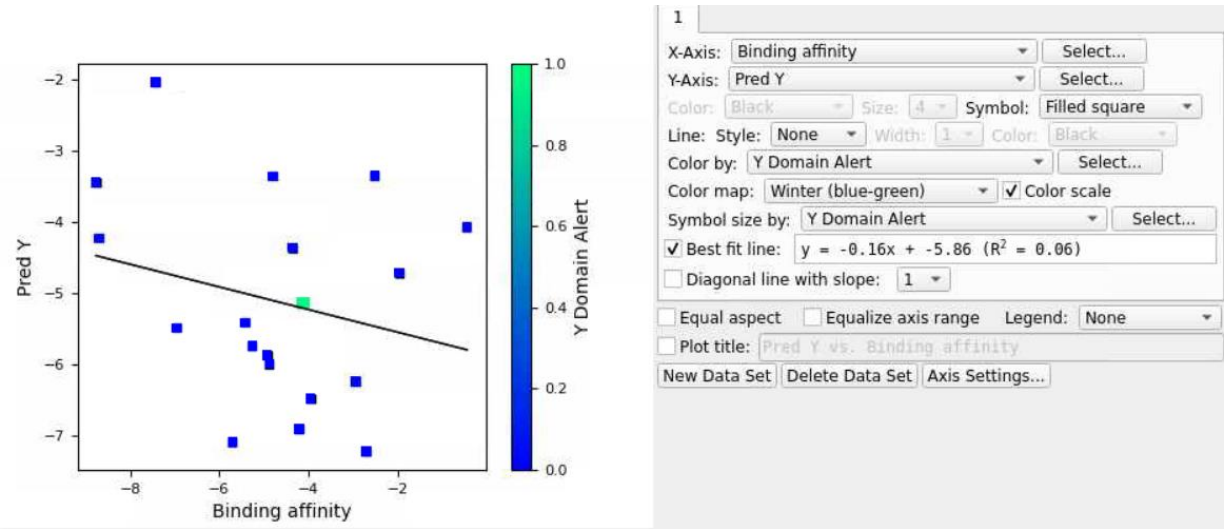

Figure 19: Scatter plot of external validation set for all top five models in Figure 16.

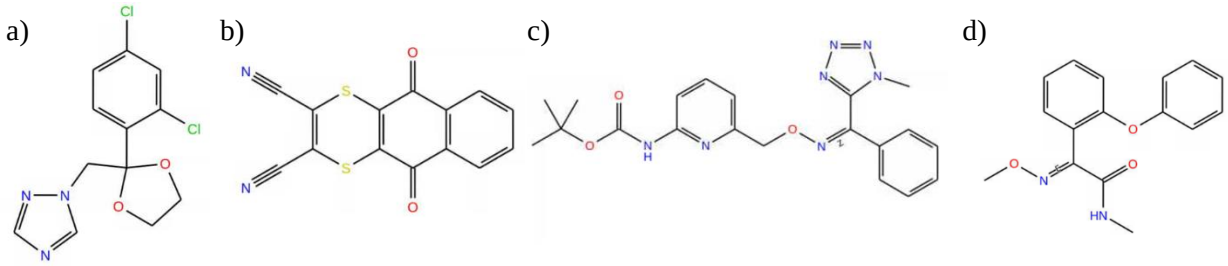

Figure 20: Four compounds a) Azaconazole, b) Dithianon, c) Picarbutrazox and d) Metominostrobin that were outliers in Figure 19.

Table 4: Calculated binding affinity (via docking simulations) and predicted binding affinity between 19 selected ligands and G143A mutated cytochrome b of *Botrytis cinerea* by using QSAR model without validation set.

Fungicide	Calculated Binding Affinity	Predicted Binding Affinity
Furametpyr	-2.705	-7.218
Azaconazole	-5.702	-7.084
Penthiopyrad	-4.203	-6.899
Oxathiapiprolin	-3.960	-6.481
Triazoxide	-2.937	-6.233
Fenpropidin	-4.878	-5.989
Fenoxanil	-4.928	-5.862
Isoflucypram	-5.261	-5.737
Ametoctradin	-6.954	-5.485
Flusulfamide	-5.418	-5.410
Polyoxin	-4.119	-5.132
Diethofencarb	-1.966	-4.710
Tebufloquin	-4.352	-4.359
Mandestrobin	-8.690	-4.224
Picarbutrazox	-0.453	-4.068
Famoxadone	-8.765	-3.443
Iprodione	-4.797	-3.353
Dithianon	-2.515	-3.347
Metominostrobin	-7.417	-2.032

3.5.1.1.2 Iteration #2

After removing metominostrobin, azaconazole, dithianon and picarbutrazox, 15 ligands were next considered in the validation set (Table 5). The R^2 value of the best-fit line increased from 0.06 to 0.26, indicating the four outliers might be potential factors that affected the prediction accuracy of the QSAR model. Both furametpyr and iprodione had chlorine in their chemical structure, which was similar to azaconazole that was removed in first iteration (Figure 22). Furametpyr, iprodione and penthiopyrad had heterocyclic dual nitrogen atoms. Diethofencarb had a similar structure to metominostrobin that was removed in the first iteration. Based on the visual inspection of Figure 21 and similar chemical structures, furametpyr, iprodione, penthiopyrad and diethofencarb were considered as potential outliers.

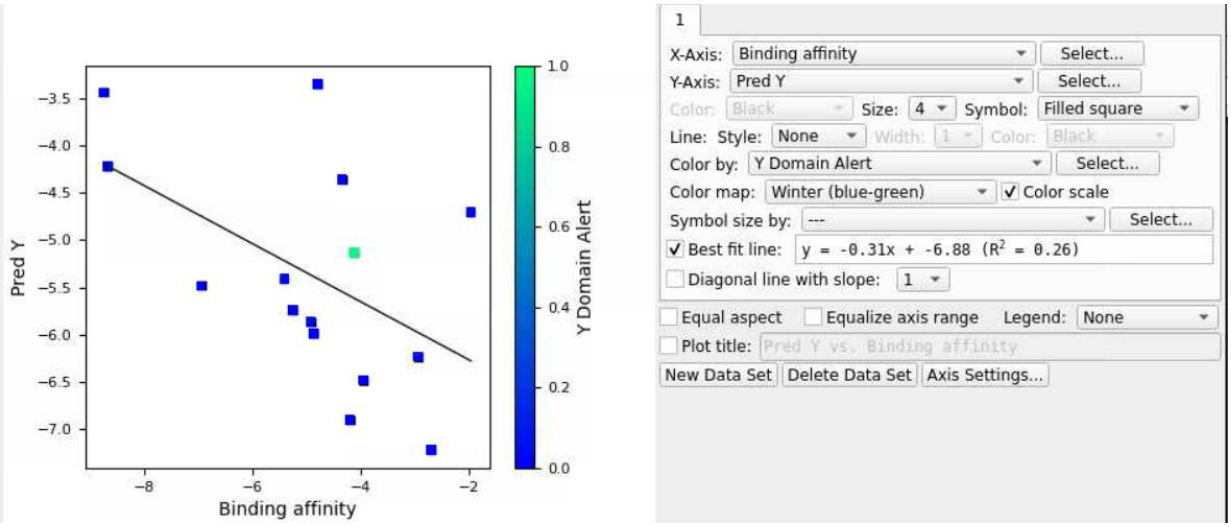

Figure 21: Scatter plot of external validation set after removing four outliers in Figure 19.

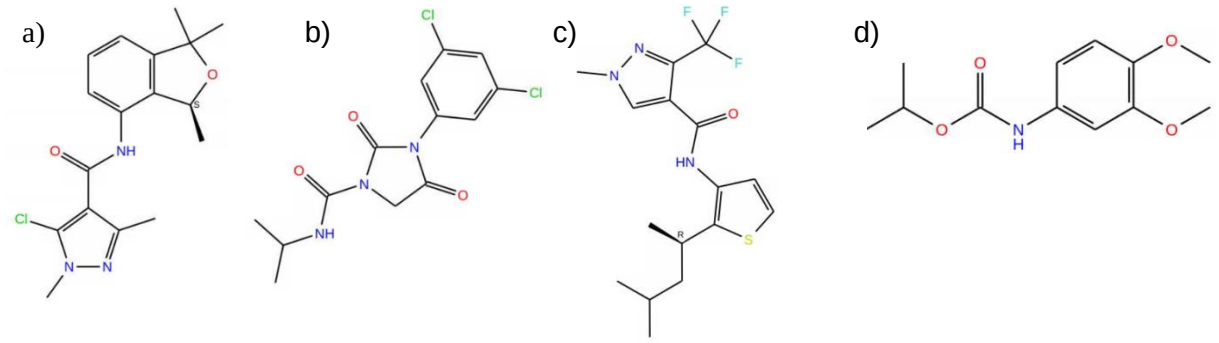

Figure 22: Four compounds a) Furametpyr, b) Iprodione, c) Penthiopyrad and d) Diethofencarb that were outliers in Figure 21.

Table 5: Calculated binding affinity (via docking simulations) and predicted binding affinity between 15 selected ligands and G143A mutated cytochrome b of *Botrytis cinerea* by using QSAR model without validation set.

Fungicide	**Calculated Binding Affinity**	**Predicted Binding Affinity**
Furametpyr	-2.705	-7.218
Penthiopyrad	-4.203	-6.899
Oxathiapiprolin	-3.960	-6.481
Triazoxide	-2.937	-6.233
Fenpropidin	-4.878	-5.989
Fenoxanil	-4.928	-5.862
Isoflucypram	-5.261	-5.737
Ametoctradin	-6.954	-5.485
Flusulfamide	-5.418	-5.410
Polyoxin	-4.119	-5.132
Diethofencarb	-1.966	-4.710
Tebufloquin	-4.352	-4.359
Mandestrobin	-8.690	-4.224
Famoxadone	-8.765	-3.443
Iprodione	-4.797	-3.353

3.5.1.1.3 Iteration #3

After removing the eight outliers (metominostrobin, azaconazole, dithianon, picarbutrazox, furametpyr, iprodione, penthiopyrad and diethofencarb) in the next iteration, the R^2 value in Figure 23 of the best-fit line increased from 0.26 to 0.53. The compounds in Table 6 as external validation set were more acceptable than the data set in Table 5, meaning that they would be expected to generate better predictions. The top predictions that would withstand G143A mutated cytochrome b of *Botrytis cinerea* were fenpropidin (an amine), fenoxail (a melanin biosynthesis inhibitor dehydrates), isoflucypram (a succinate dehydrogenase inhibitor) and ametoctradin (a QoI). Although oxathiapiprolin and triazoxide had high predicted binding affinity, their original affinity was low, so they may not be acceptable. Chlorine and multiple heterocyclic nitrogen might be considered as similarities in outliers' structure.

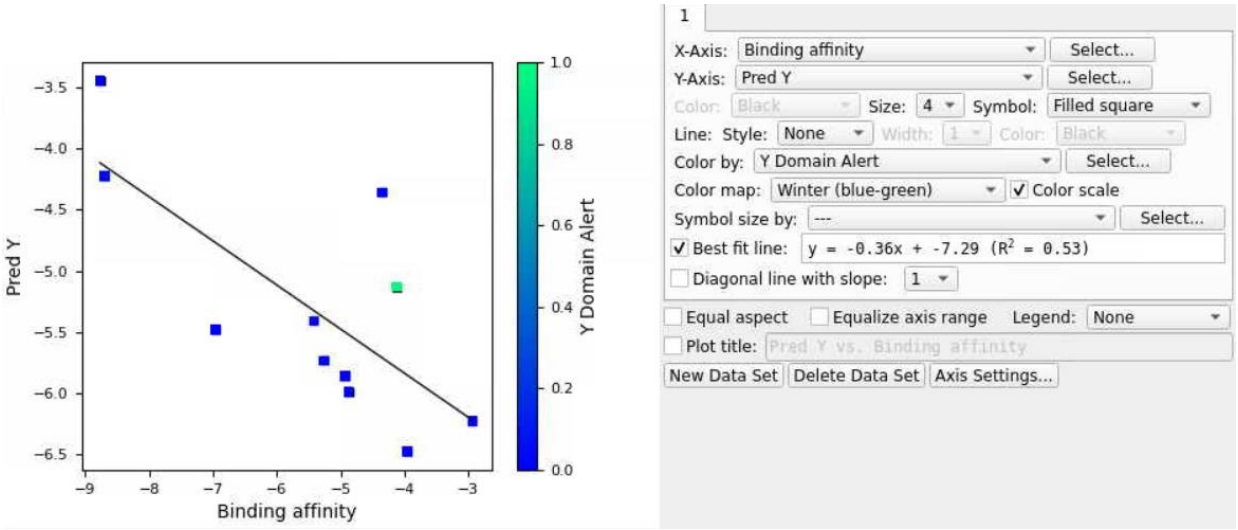

Figure 23: Scatter plot of external validation set after removing four outliers in Figure 21.

Table 6: Calculated binding affinity (via docking simulations) and predicted binding affinity between 11 selected ligands and G143A mutated cytochrome b of *Botrytis cinerea* by using QSAR model without validation set.

Fungicide	**Calculated Binding Affinity**	**Predicted Binding Affinity**
Oxathiapiprolin	-3.960	-6.481
Triazoxide	-2.937	-6.233
Fenpropidin	-4.878	-5.989
Fenoxanil	-4.928	-5.862
Isoflucypram	-5.261	-5.737
Ametoctradin	-6.954	-5.485
Flusulfamide	-5.418	-5.410
Polyoxin	-4.119	-5.132
Tebufloquin	-4.352	-4.359
Mandestrobin	-8.690	-4.224
Famoxadone	-8.765	-3.443

3.5.1.2 Training data set with validation sets

In this case, two QoI fungicides, picoxystrobin and pyribencarb, were assigned as a validation set for the QSAR models. This resulted in 32 ligands in the training set for the QSAR model (Figure 25). The ranking score for the top five QSAR models with a validation set (Figure 24) were higher than the model without the validation set, meaning that test set predictions of model with validation set might be more accurate. Top QSAR models shown for *Botrytis cinerea* in Figure 24 were kpls_molprint2D_39, kpls_radial_8, kpls_linear_30, kpls_dendritic_30 and kpls_dendritic_39. The best model was kpls_molprint2D_39 that was generated by kernel partial least square regression (KPLS) with molprint2D fingerprint, using the 39th spilt of the learning set into a test and training set (32 ligands) with the validation set (2 ligands). This model had a S.D of 1.8732, R^2 of 0.7081, RMSE of 1.8919, Q^2 of 0.6860 and ranking score of 0.6582. From the plots in Figure 26, training sets were closer to the regression line (Figure 18) indicating the better prediction ability of the model.

Model Report

Model Code	Score	S.D.	R^2	RMSE	Q^2	Q^2 MW (Null Hypothesis)
kpls_molprint2D_39	0.6582	1.8732	0.7081	1.8919	0.6860	0.1725
kpls_radial_8	0.6570	1.8034	0.7316	1.8652	0.6865	-0.5827
kpls_linear_30	0.6218	1.9272	0.7152	1.9482	0.5546	-1.5647
kpls_dendritic_30	0.6068	1.8913	0.7258	1.9626	0.5480	-1.5647
kpls_dendritic_39	0.5888	1.4775	0.8184	1.8814	0.6894	0.1725
kpls_linear_39	0.5818	1.4847	0.8167	1.8971	0.6842	0.1725
kpls_linear_40	0.5717	1.6210	0.7815	1.9602	0.6613	0.1650
kpls_radial_39	0.5714	1.6681	0.7686	1.9765	0.6573	0.1725
kpls_radial_30	0.5322	1.9012	0.7229	2.0992	0.4829	-1.5647
kpls_molprint2D_40	0.5297	1.9253	0.6918	2.1363	0.5977	0.1650

Figure 24: Top 10-ranked QSAR model reports with validation sets for fungicides used in *Botrytis cinerea*.

a)

Training Set		Test Set	
S.D.	R^2	RMSE	Q^2
1.8732	0.7081	1.8919	0.6860

Optimum number of factors = 1

ID	Set	Y(Obs)	Y(Pred)	Error	Name
1	train	0.0000	-0.3674	-0.3674	Azoxystrobin
2	train	0.0000	0.2836	0.2836	Coumoxystrobin
3	train	-4.2340	-1.7477	2.4863	Dimoxystrobin
4	test	0.0000	-1.8764	-1.8764	Enoxastrobin
5	train	-5.9500	-4.9577	0.9923	Fenamidone
6	train	0.0000	-2.1022	-2.1022	Fenaminstrobin
7	train	0.0000	-1.4236	-1.4236	Fluoxastrobin
8	train	0.0000	-0.6732	-0.6732	Metyltetraprole
9	test	0.0000	-2.5727	-2.5727	Orysastrobin
10	train	-3.4420	-1.5155	1.9265	Pyraclostrobin
11	train	0.0000	1.3704	1.3704	pyrametostrobin
12	train	-4.7170	-0.9159	3.8011	Pyraoxystrobin
13	train	0.0000	-1.0953	-1.0953	Triclopyricarb
14	train	0.0000	-2.9122	-2.9122	Captan
15	test	-3.1360	-4.4439	-1.3079	Ferbam
16	train	0.0000	-2.3433	-2.3433	Folpet
17	train	0.0000	-3.7729	-3.7729	Mancozeb
18	test	-4.9350	-4.4439	0.4911	Thiram
19	train	-2.4520	-3.7729	-1.3209	Zineb
20	train	-7.2440	-8.3919	-1.1479	Zoxamide
21	test	-9.2080	-5.4768	3.7312	Sedaxane
22	train	-8.9120	-7.2108	1.7012	Piperalin
23	train	-6.2170	-5.4768	0.7402	Inpyrfluxam
24	train	-8.8700	-8.3718	0.4982	Penconazole
25	train	-6.0890	-5.8389	0.2501	Ferimzone
26	train	-7.3720	-6.2429	1.1291	Cyflufenamid
27	test	-6.6920	-5.3921	1.2999	Diclomezine
28	train	-7.2000	-5.1205	2.0795	Dichlobentiazox
29	train	-6.0650	-5.3898	0.6752	Ethaboxam
30	test	-6.7210	-6.5737	0.1473	Fluindapyr
31	train	-6.8900	-7.6645	-0.7745	Fluoxapiprolin
32	test	0.0000	-0.9534	-0.9534	Flufenoxystrobin

b)

Training Set		Test Set	
S.D.	R^2	RMSE	Q^2
1.8034	0.7316	1.8652	0.6865

Optimum number of factors = 1

ID	Set	Y(Obs)	Y(Pred)	Error	Name
1	train	0.0000	-0.3619	-0.3619	Azoxystrobin
2	train	0.0000	0.1319	0.1319	Coumoxystrobin
3	train	-4.2340	-1.1572	3.0768	Dimoxystrobin
4	train	0.0000	0.4464	0.4464	Enoxastrobin
5	test	-5.9500	-3.6137	2.3363	Fenamidone
6	test	0.0000	-0.4535	-0.4535	Fenaminstrobin
7	train	0.0000	-2.1305	-2.1305	Fluoxastrobin
8	train	0.0000	-2.9093	-2.9093	Metyltetraprole
9	train	0.0000	0.4589	0.4589	Orysastrobin
10	test	-3.4420	-1.4727	1.9693	Pyraclostrobin
11	train	0.0000	-1.6323	-1.6323	pyrametostrobin
12	train	-4.7170	-1.8294	2.8876	Pyraoxystrobin
13	test	0.0000	-2.5428	-2.5428	Triclopyricarb
14	train	0.0000	-2.2462	-2.2462	Captan
15	train	-3.1360	-3.0359	0.1001	Ferbam
16	train	0.0000	-1.9878	-1.9878	Folpet
17	train	0.0000	-2.2509	-2.2509	Mancozeb
18	train	-4.9350	-3.2755	1.6595	Thiram
19	train	-2.4520	-2.2509	0.2011	Zineb
20	train	-7.2440	-7.2460	-0.0020	Zoxamide
21	train	-9.2080	-7.9810	1.2270	Sedaxane
22	test	-8.9120	-6.2117	2.7003	Piperalin
23	train	-6.2170	-7.6173	-1.4003	Inpyrfluxam
24	train	-8.8700	-8.4120	0.4580	Penconazole
25	train	-6.0890	-3.8953	2.1937	Ferimzone
26	train	-7.3720	-6.5400	0.8320	Cyflufenamid
27	train	-6.6920	-6.5711	0.1209	Diclomezine
28	train	-7.2000	-4.3108	2.8892	Dichlobentiazox
29	test	-6.0650	-4.8418	1.2232	Ethaboxam
30	train	-6.7210	-8.4829	-1.7619	Fluindapyr
31	test	-6.8900	-6.2315	0.6585	Fluoxapiprolin
32	test	0.0000	-1.6132	-1.6132	Flufenoxystrobin

c)

Training Set		Test Set	
S.D.	R^2	RMSE	Q^2
1.9272	0.7152	1.9482	0.5546

Optimum number of factors = 1

ID	Set	Y(Obs)	Y(Pred)	Error	Name
1	train	0.0000	-0.8721	-0.8721	Azoxystrobin
2	train	0.0000	0.1781	0.1781	Coumoxystrobin
3	train	-4.2340	-0.9975	3.2365	Dimoxystrobin
4	test	0.0000	-0.8473	-0.8473	Enoxastrobin
5	test	-5.9500	-3.8890	2.0610	Fenamidone
6	train	0.0000	-0.4923	-0.4923	Fenaminstrobin
7	train	0.0000	-0.6838	-0.6838	Fluoxastrobin
8	train	0.0000	-1.8774	-1.8774	Metyltetraprole
9	train	0.0000	-0.5887	-0.5887	Orysastrobin
10	test	-3.4420	-1.4680	1.9740	Pyraclostrobin
11	train	0.0000	-1.0506	-1.0506	pyrametostrobin
12	train	-4.7170	-1.7187	2.9983	Pyraoxystrobin
13	test	0.0000	-1.5683	-1.5683	Triclopyricarb
14	train	0.0000	-3.6663	-3.6663	Captan
15	test	-3.1360	-3.8378	-0.7018	Ferbam
16	test	0.0000	-3.4565	-3.4565	Folpet
17	train	0.0000	-3.6698	-3.6698	Mancozeb
18	train	-4.9350	-3.8476	1.0874	Thiram
19	train	-2.4520	-3.6698	-1.2178	Zineb
20	test	-7.2440	-5.4511	1.7929	Zoxamide
21	train	-9.2080	-9.0403	0.1677	Sedaxane
22	train	-8.9120	-7.2627	1.6493	Piperalin
23	train	-6.2170	-7.9913	-1.7743	Inpyrfluxam
24	train	-8.8700	-8.1030	0.7670	Penconazole
25	train	-6.0890	-4.0332	2.0558	Ferimzone
26	train	-7.3720	-6.5853	0.7867	Cyflufenamid
27	train	-6.6920	-5.4836	1.2084	Diclomezine
28	train	-7.2000	-3.9691	3.2309	Dichlobentiazox
29	train	-6.0650	-5.8516	0.2134	Ethaboxam
30	train	-6.7210	-8.4304	-1.7094	Fluindapyr
31	test	-6.8900	-5.0497	1.8403	Fluoxapiprolin
32	train	0.0000	0.0230	0.0230	Flufenoxystrobin

d)

Training Set		Test Set	
S.D.	R^2	RMSE	Q^2
1.8913	0.7258	1.9626	0.5480

Optimum number of factors = 1

ID	Set	Y(Obs)	Y(Pred)	Error	Name
1	train	0.0000	-0.5673	-0.5673	Azoxystrobin
2	train	0.0000	0.2340	0.2340	Coumoxystrobin
3	train	-4.2340	-1.1062	3.1278	Dimoxystrobin
4	test	0.0000	-0.7538	-0.7538	Enoxastrobin
5	test	-5.9500	-3.9903	1.9597	Fenamidone
6	train	0.0000	-0.5506	-0.5506	Fenaminstrobin
7	train	0.0000	-0.5588	-0.5588	Fluoxastrobin
8	train	0.0000	-1.7685	-1.7685	Metyltetraprole
9	train	0.0000	-0.6863	-0.6863	Orysastrobin
10	test	-3.4420	-1.4775	1.9645	Pyraclostrobin
11	train	0.0000	-1.1330	-1.1330	pyrametostrobin
12	train	-4.7170	-1.9138	2.8032	Pyraoxystrobin
13	test	0.0000	-1.7893	-1.7893	Triclopyricarb
14	train	0.0000	-3.6356	-3.6356	Captan
15	test	-3.1360	-3.8285	-0.6925	Ferbam
16	test	0.0000	-3.4606	-3.4606	Folpet
17	train	0.0000	-3.6513	-3.6513	Mancozeb
18	train	-4.9350	-3.8358	1.0992	Thiram
19	train	-2.4520	-3.6513	-1.1993	Zineb
20	test	-7.2440	-5.4857	1.7583	Zoxamide
21	train	-9.2080	-9.0287	0.1793	Sedaxane
22	train	-8.9120	-7.2815	1.6305	Piperalin
23	train	-6.2170	-8.0864	-1.8694	Inpyrfluxam
24	train	-8.8700	-8.0876	0.7824	Penconazole
25	train	-6.0890	-4.0518	2.0372	Ferimzone
26	train	-7.3720	-6.6783	0.6937	Cyflufenamid
27	train	-6.6920	-5.5091	1.1829	Diclomezine
28	train	-7.2000	-3.9972	3.2028	Dichlobentiazox
29	train	-6.0650	-5.8889	0.1761	Ethaboxam
30	train	-6.7210	-8.4055	-1.6845	Fluindapyr
31	test	-6.8900	-4.9407	1.9493	Fluoxapiprolin
32	train	0.0000	0.1555	0.1555	Flufenoxystrobin

e)

Training Set		Test Set	
S.D.	R^2	RMSE	Q^2
1.4775	0.8184	1.8814	0.6894

Optimum number of factors = 1

ID	Set	Y(Obs)	Y(Pred)	Error	Name
1	train	0.0000	0.1536	0.1536	Azoxystrobin
2	train	0.0000	-0.5037	-0.5037	Coumoxystrobin
3	train	-4.2340	-2.1713	2.0627	Dimoxystrobin
4	test	0.0000	-1.3947	-1.3947	Enoxastrobin
5	train	-5.9500	-4.5512	1.3988	Fenamidone
6	train	0.0000	-1.4053	-1.4053	Fenaminstrobin
7	train	0.0000	-0.6754	-0.6754	Fluoxastrobin
8	train	0.0000	-1.3153	-1.3153	Metyltetraprole
9	test	0.0000	-1.6255	-1.6255	Orysastrobin
10	train	-3.4420	-0.7807	2.6613	Pyraclostrobin
11	train	0.0000	-0.1521	-0.1521	pyrametostrobin
12	train	-4.7170	-2.3859	2.3311	Pyraoxystrobin
13	train	0.0000	-0.5293	-0.5293	Triclopyricarb
14	train	0.0000	-2.0738	-2.0738	Captan
15	test	-3.1360	-2.3349	0.8011	Ferbam
16	train	0.0000	-1.5521	-1.5521	Folpet
17	train	0.0000	-2.3314	-2.3314	Mancozeb
18	test	-4.9350	-2.2346	2.7004	Thiram
19	train	-2.4520	-2.3314	0.1206	Zineb
20	train	-7.2440	-7.7730	-0.5290	Zoxamide
21	test	-9.2080	-6.0367	3.1713	Sedaxane
22	train	-8.9120	-9.3382	-0.4262	Piperalin
23	train	-6.2170	-7.1219	-0.9049	Inpyrfluxam
24	train	-8.8700	-9.3681	-0.4981	Penconazole
25	train	-6.0890	-4.2110	1.8780	Ferimzone
26	train	-7.3720	-6.9636	0.4084	Cyflufenamid
27	test	-6.6920	-5.5961	1.0959	Diclomezine
28	train	-7.2000	-4.6213	2.5787	Dichlobentiazox
29	train	-6.0650	-6.0380	0.0270	Ethaboxam
30	test	-6.7210	-7.0542	-0.3332	Fluindapyr
31	train	-6.8900	-7.6135	-0.7235	Fluoxapiprolin
32	test	0.0000	-2.1040	-2.1040	Flufenoxystrobin

Figure 25: Model reports for a) kpls_molprint2D_39, b) kpls_radial_8, c) kpls_linear_30, d) kpls_dendritic_30 and e) kpls_dendtitic_39 models.

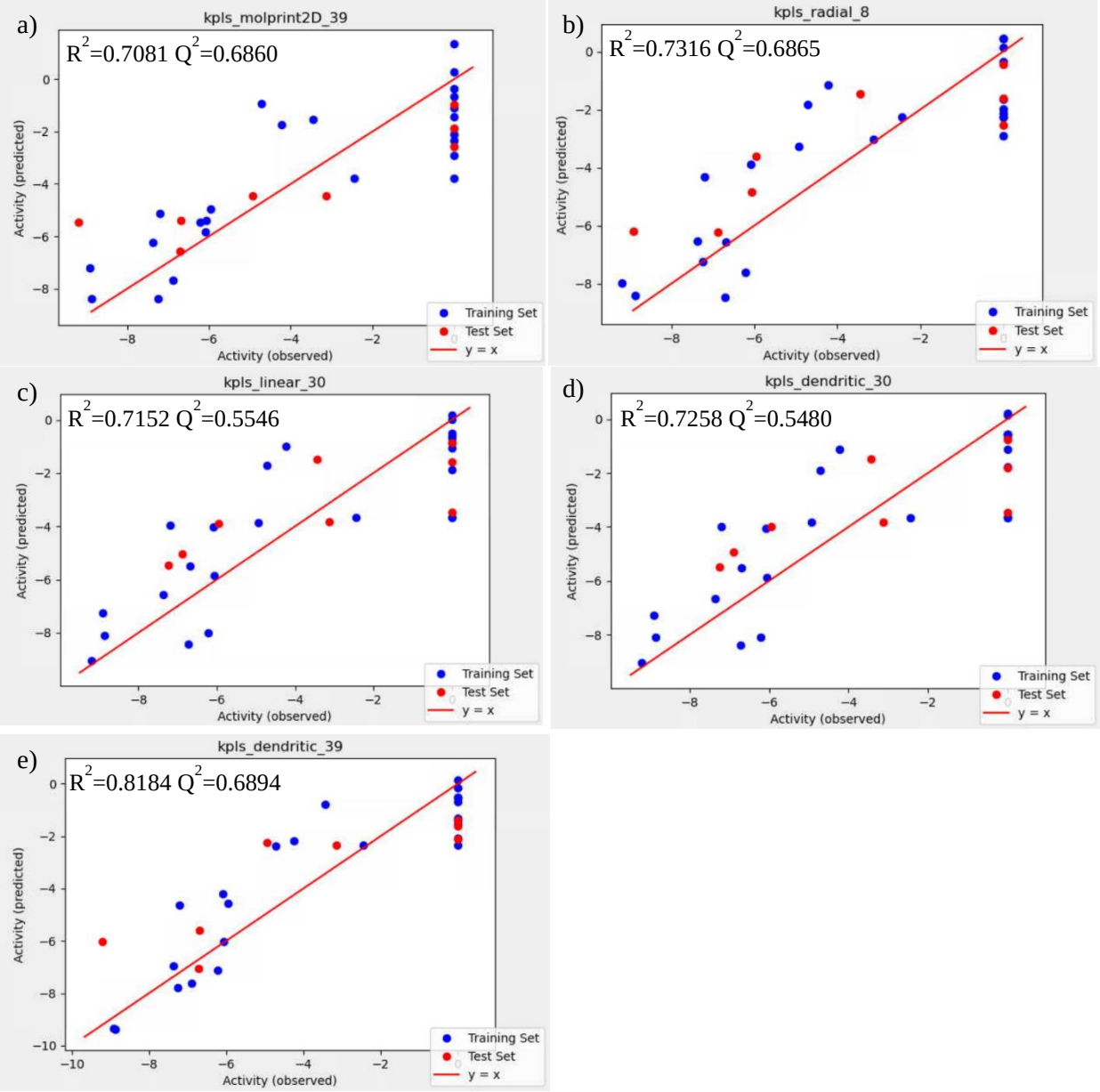

Figure 26: Scatter plot about performance for a) kpls_molprint2D_39, b) kpls_radial_8, c) kpls_linear_30, d) kpls_dendritic_30 and e) kpls_dendritic_39 models.

Similar to the procedure that was adopted in the previous run, several iterations were done while removing chemically distinct outliers.

3.5.1.2.1 Iteration #1

In Table 7, the external validation set had the same 19 ligands to estimate the prediction accuracy of the QSAR model. The R^2 value of the best fit line was 0.05, meaning the QSAR model did not perform well for the given validation set. Visual inspection in Figure 27 showed penthiopyrad, isoflucypram, picarbutrazox and metominostrobin fell outside the applicability domain of the QSAR model, which would decrease the prediction accuracy of the model. Also, penthiopyrad and isoflucypram had fluorine in their chemical structure (Figure 28). Penthiopyrad, isoflucypram and picarbutrazox contained multiple heterocyclic nitrogen atoms. Penthiopyrad, isoflucypram and metominostrobin had nitrogen-hydrogen structures. To improve the prediction accuracy of QSAR model, these ligands were removed in the next iteration.

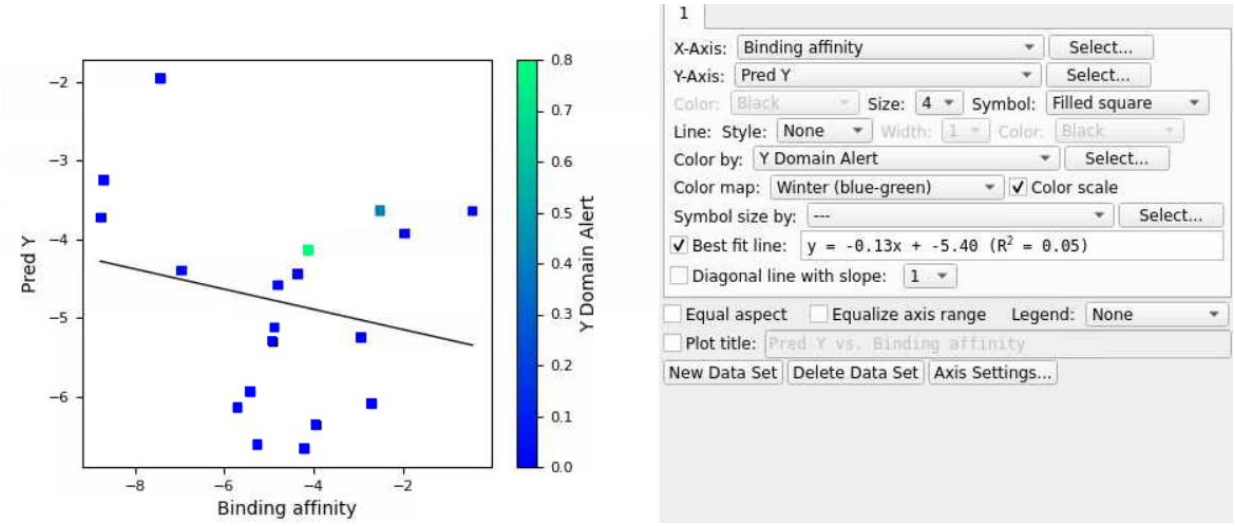

Figure 27: Scatter plot of external validation set for all top five models in Figure 24.

Table 7. Calculated binding affinity (via docking simulations) and predicted binding affinity between 19 selected ligands and G143A mutated cytochrome b of *Botrytis cinerea* by using QSAR model with validation set.

Fungicide	Calculated Binding Affinity	Predicted Binding Affinity
Penthiopyrad	-4.203	-6.652
Isoflucypram	-5.261	-6.601
Oxathiapiprolin	-3.960	-6.351
Azaconazole	-5.702	-6.137
Furametpyr	-2.705	-6.077
Flusulfamide	-5.418	-5.391
Fenoxanil	-4.928	-5.288
Triazoxide	-2.937	-5.241
Fenpropidin	-4.878	-5.115
Iprodione	-4.797	-4.581
Tebufloquin	-4.352	-4.436
Ametoctradin	-6.954	-4.396
Polyoxin	-4.119	-4.141
Diethofencarb	-1.966	-3.925
Famoxadone	-8.765	-3.726
Picarbutrazox	-0.453	-3.643
Dithianon	-2.515	-3.639
Mandestrobin	-8.690	-3.244
Metominostrobin	-7.417	-1.958

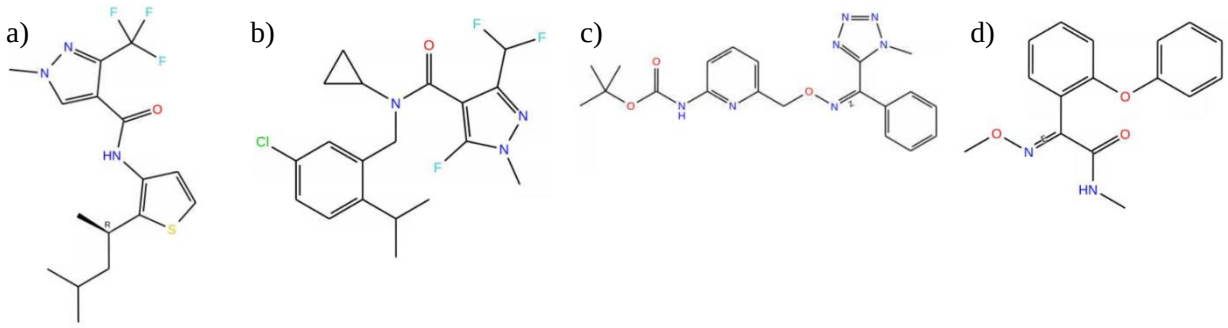

Figure 28: Four compounds a) Penthiopyrad, b) Isoflucypram, c) Picarbutrazox and d) Metominostrobin that were outliers in Figure 27.

3.5.1.2.2 Iteration #2

After removing penthiopyrad, isoflucypram, picarbutrazox and metominostrobin, the R^2 value of the best fit line slightly increased (Table 8). Visual inspection of Figure 29 suggested the presence of several outliers (oxathiapiprolin, azaconazole, flusulfamide, diethofencarb and dithianon) that would be needed to be removed to improve the QSAR model. Oxathiapiprolin and flusulfamide had fluorine in their chemical structure (Figure 30). Azaconazole and flusulfamide had chlorine in their chemical structure. Diethofencarb had similar structure to metominostrobin. Only dithianon contained heterocyclic dual sulfur atoms.

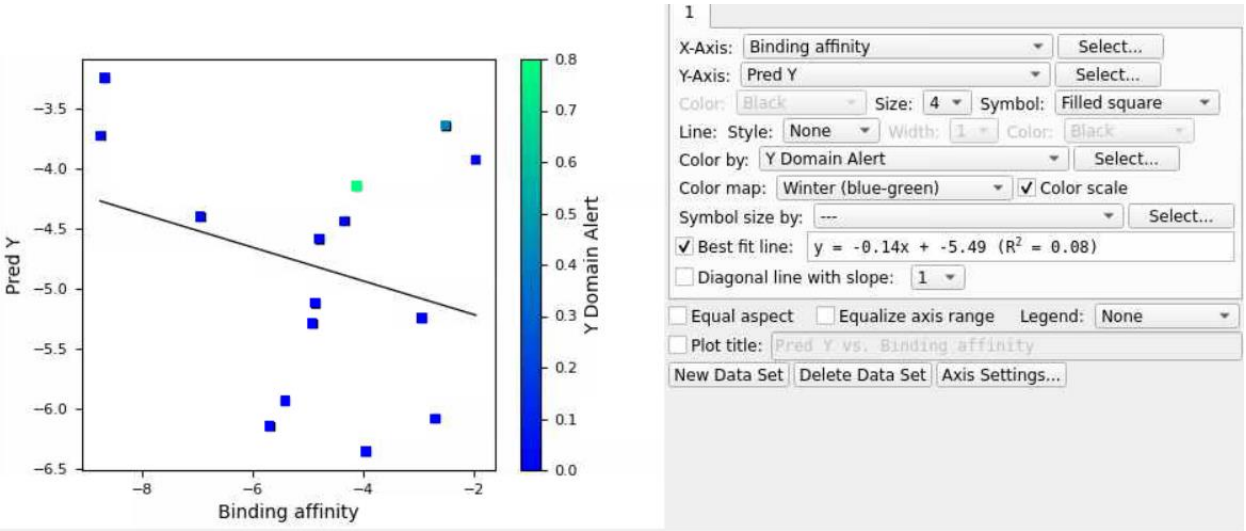

Figure 29: Scatter plot of external validation set after removing four outliers in Figure 27.

Table 8. Calculated binding affinity (via docking simulations) and predicted binding affinity between 15 selected ligands and G143A mutated cytochrome b of *Botrytis cinerea* by using QSAR model with validation set

Fungicide	Calculated Binding Affinity	Predicted Binding Affinity
Oxathiapiprolin	-3.960	-6.351
Azaconazole	-5.702	-6.137
Furametpyr	-2.705	-6.077
Flusulfamide	-5.418	-5.391
Fenoxanil	-4.928	-5.288
Triazoxide	-2.937	-5.241
Fenpropidin	-4.878	-5.115
Iprodione	-4.797	-4.581
Tebufloquin	-4.352	-4.436
Ametoctradin	-6.954	-4.396
Polyoxin	-4.119	-4.141
Diethofencarb	-1.966	-3.925
Famoxadone	-8.765	-3.726
Dithianon	-2.515	-3.639
Mandestrobin	-8.690	-3.244

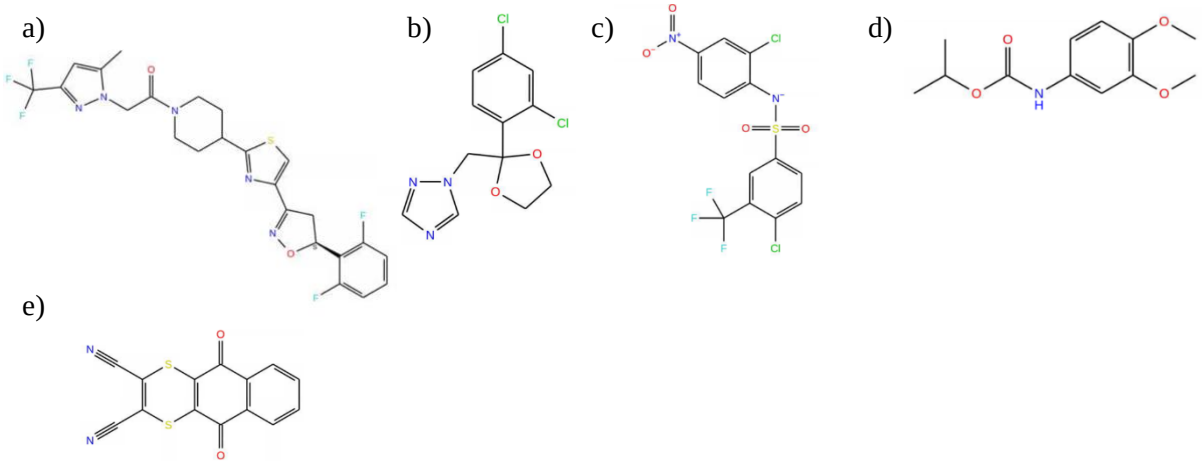

Figure 30: Four compounds a) Oxathiapiprolin, b) Azaconazole, c) Flusulfamide, d) Diethofencarb and d) Dithianon that were considered outliers in Figure 29.

3.5.1.2.3 Iteration #3

To further improve the QSAR model, outliers including oxathiapiprolin, azaconazole, flusulfamide, diethofencarb and dithianon were removed (Table 9). The R^2 value of the best fit line significantly increased from 0.08 to 0.67, indicating those ligands had structural properties that were not predictable using the models (Figure 31). The top predictions that would withstand G143A mutated cytochrome b of *Botrytis cinerea* were fenoxanil (a melanin biosynthesis inhibitor dehydrates), fenpropidin (an amine), iprodione (a dicarboximde) and tebufloquin (a 4-quinolyl-acetate), and Ametoctradin (a QoI). Furametpyr and triazoxide had high predicted affinity but the difference between their original affinity and predicted affinity was higher than the other four ligands. It should be noted that the model was not able to make accurate predictions when ligands had chlorine, fluorine and hetrocyclic nitrogen atom in the chemical structure.

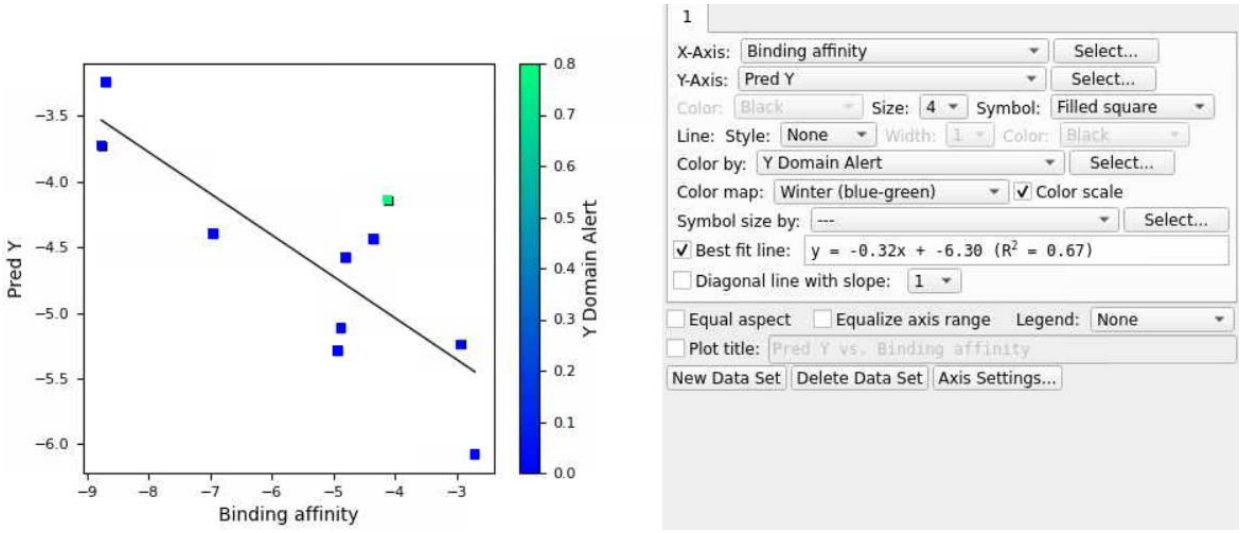

Figure 31: Scatter plot of external validation set after removing five outliers in Figure 29.

Table 9: Calculated binding affinity (via docking simulations) and predicted binding affinity between 10 selected ligands and G143A mutated cytochrome b of *Botrytis cinerea* by using QSAR model with validation set.

Fungicide	**Calculated Binding Affinity**	**Predicted Binding Affinity**
Furametpyr	-2.705	-6.077
Fenoxanil	-4.928	-5.288
Triazoxide	-2.937	-5.241
Fenpropidin	-4.878	-5.115
Iprodione	-4.797	-4.581
Tebufloquin	-4.352	-4.436
Ametoctradin	-6.954	-4.396
Polyoxin	-4.119	-4.141
Famoxadone	-8.765	-3.726
Mandestrobin	-8.690	-3.244

3.5.2 Application of AutoQSR to predict fungicides for *Plasmopara viticola*

3.5.2.1 Training data set without validation sets

Here, an initial training set was developed using 16 QoI and 20 non-QoI fungicides. The top five QSAR models for *Plasmopara viticola* are kpls_desc_2, kpls_radial_24, kpls_linear_22, kpls_radial_22 and pls_2 (Figure 32). The best model was kpls_desc_2, generated by kernel partial least square regression (KPLS) with desc fingerprint, using the 12nd spilt of the learning set into a test and training set (36 ligands) without validation set. This model had a S.D of 1.7498, R^2 of 0.7032, RMSE of 1.615, Q^2 of 0.7350 and ranking score of 0.7116. In Figure 33, 75% ligands occupied the training set and 25% ligands the test set. The scatter plots in Figure 34 indicate that the first four models' training sets correlated closely with the test sets.

Model Report

Model Code	Score	S.D.	R^2	RMSE	Q^2	Q^2 MW (Null Hypothesis)
kpls_desc_2	0.7116	1.7498	0.7032	1.5615	0.7350	0.0226
kpls_radial_24	0.6806	1.5607	0.7489	1.6354	0.7269	0.1147
kpls_linear_22	0.6640	1.4173	0.7931	1.6099	0.7343	0.1112
kpls_radial_22	0.6579	1.5606	0.7491	1.6732	0.7130	0.1112
pls_2	0.6420	1.9451	0.6333	1.7702	0.6594	0.0226
kpls_radial_45	0.6271	1.6222	0.7302	1.7455	0.6800	0.1223
kpls_dendritic_2	0.5756	1.5463	0.7586	1.7997	0.6480	0.0226
kpls_dendritic_22	0.5505	1.4107	0.7950	1.8023	0.6671	0.1112
kpls_linear_47	0.5471	1.4681	0.7821	1.8221	0.6422	0.0948
kpls_radial_47	0.5454	1.6214	0.7342	1.8747	0.6212	0.0948

Figure 32: Top 10-ranked QSAR model reports without validation set for fungicides used in *Plasmopara viticola*.

a)

Training Set		Test Set	
S.D.	R^2	RMSE	Q^2
1.7498	0.7032	1.5615	0.7350

Optimum number of factors = 2

ID	Set	Y(Obs)	Y(Pred)	Error	Name
1	test	0.0000	-1.0075	-1.0075	Azoxystrobin
2	train	-6.1770	-3.7677	2.4093	Coumoxystrobin
3	train	0.0000	-0.4428	-0.4428	Enoxastrobin
4	train	-6.3730	-5.6874	0.6856	Fenamidone
5	train	-7.4660	-3.0180	4.4480	Fenaminstrobin
6	train	0.0000	0.7834	0.7834	Fluoxastrobin
7	test	0.0000	-2.1171	-2.1171	Metyltetraprole
8	train	0.0000	-1.6239	-1.6239	Orysastrobin
9	train	0.0000	-2.6921	-2.6921	Picoxystrobin
10	train	0.0000	-1.3514	-1.3514	Pyraclostrobin
11	test	0.0000	-2.4727	-2.4727	pyrametostrobin
12	train	0.0000	-1.1520	-1.1520	Pyraoxystrobin
13	test	-5.8440	-4.2186	1.6254	Pyribencarb
14	train	0.0000	-0.3196	-0.3196	Triclopyricarb
15	train	0.0000	-2.2729	-2.2729	Captan
16	test	-3.0380	-1.4674	1.5706	Ferbam
17	train	-5.8910	-4.4961	1.3949	Folpet
18	train	-1.8780	-2.5294	-0.6514	Mancozeb
19	train	-4.2850	-5.0062	-0.7212	Thiram
20	train	-2.4080	-4.0191	-1.6111	Zineb
21	train	-6.5560	-6.1151	0.4409	Zoxamide
22	train	-6.5160	-7.6569	-1.1409	Sedaxane
23	train	-6.8510	-7.0587	-0.2077	Piperalin
24	train	-6.4860	-8.3683	-1.8823	Inpyrfluxam
25	train	-7.2910	-7.3043	-0.0133	Penconazole
26	test	-6.4640	-4.7788	1.6852	Ferimzone
27	train	-7.5040	-6.4937	1.0103	Cyflufenamid
28	test	-6.5290	-5.8898	0.6392	Diclomezine
29	train	-6.4320	-3.6284	2.8036	Dichlobentiazox
30	train	-6.2790	-3.4461	2.8329	Flufenoxystrobin
31	train	-7.2240	-7.1503	0.0737	Azaconazole
32	train	-6.1090	-7.0061	-0.8971	Fenoxanil
33	train	-7.2400	-7.0895	0.1505	Iprodione
34	test	-7.2910	-6.2103	1.0807	Penthiopyrad
35	test	-6.6800	-7.5782	-0.8982	Oxathiapiprolin
36	train	-5.0670	-5.1204	-0.0534	Metominostrobin

b)

Training Set		Test Set	
S.D.	R^2	RMSE	Q^2
1.5607	0.7489	1.6354	0.7269

Optimum number of factors = 1

ID	Set	Y(Obs)	Y(Pred)	Error	Name
1	train	0.0000	-0.5844	-0.5844	Azoxystrobin
2	train	-6.1770	-3.4788	2.6982	Coumoxystrobin
3	test	0.0000	-2.8770	-2.8770	Enoxastrobin
4	train	-6.3730	-5.7930	0.5800	Fenamidone
5	train	-7.4660	-4.4231	3.0429	Fenaminstrobin
6	train	0.0000	-0.6105	-0.6105	Fluoxastrobin
7	train	0.0000	-2.2474	-2.2474	Metyltetraprole
8	train	0.0000	-1.7294	-1.7294	Orysastrobin
9	test	0.0000	-2.2333	-2.2333	Picoxystrobin
10	test	0.0000	-0.7546	-0.7546	Pyraclostrobin
11	train	0.0000	0.5119	0.5119	pyrametostrobin
12	train	0.0000	0.1642	0.1642	Pyraoxystrobin
13	train	-5.8440	-4.8203	1.0237	Pyribencarb
14	train	0.0000	-1.0233	-1.0233	Triclopyricarb
15	train	0.0000	-3.6030	-3.6030	Captan
16	test	-3.0380	-3.7681	-0.7301	Ferbam
17	test	-5.8910	-4.3530	1.5380	Folpet
18	train	-1.8780	-2.6717	-0.7937	Mancozeb
19	train	-4.2850	-3.6894	0.5956	Thiram
20	train	-2.4080	-2.6717	-0.2637	Zineb
21	test	-6.5560	-6.0276	0.5284	Zoxamide
22	train	-6.5160	-5.9017	0.6143	Sedaxane
23	train	-6.8510	-7.9132	-1.0622	Piperalin
24	train	-6.4860	-7.1236	-0.6376	Inpyrfluxam
25	train	-7.2910	-8.1414	-0.8504	Penconazole
26	test	-6.4640	-4.2112	2.2528	Ferimzone
27	test	-7.5040	-6.3544	1.1496	Cyflufenamid
28	train	-6.5290	-5.8069	0.7221	Diclomezine
29	train	-6.4320	-4.6564	1.7756	Dichlobentiazox
30	train	-6.2790	-4.2969	1.9821	Flufenoxystrobin
31	train	-7.2240	-7.1865	0.0375	Azaconazole
32	train	-6.1090	-7.5367	-1.4277	Fenoxanil
33	train	-7.2400	-6.3321	0.9079	Iprodione
34	test	-7.2910	-6.4770	0.8140	Penthiopyrad
35	train	-6.6800	-8.2834	-1.6034	Oxathiapiprolin
36	train	-5.0670	-3.2863	1.7807	Metominostrobin

c)

Training Set		Test Set	
S.D.	R^2	RMSE	Q^2
1.4173	0.7931	1.6099	0.7343

Optimum number of factors = 1

ID	Set	Y(Obs)	Y(Pred)	Error	Name
1	train	0.0000	-0.7339	-0.7339	Azoxystrobin
2	train	-6.1770	-4.4838	1.6932	Coumoxystrobin
3	test	0.0000	-2.1268	-2.1268	Enoxastrobin
4	test	-6.3730	-4.1793	2.1937	Fenamidone
5	train	-7.4660	-4.8284	2.6376	Fenaminstrobin
6	train	0.0000	-1.2089	-1.2089	Fluoxastrobin
7	train	0.0000	-0.4627	-0.4627	Metyltetraprole
8	train	0.0000	-2.2218	-2.2218	Orysastrobin
9	test	0.0000	-1.8150	-1.8150	Picoxystrobin
10	train	0.0000	1.1313	1.1313	Pyraclostrobin
11	test	0.0000	-1.5249	-1.5249	pyrametostrobin
12	train	0.0000	-0.0475	-0.0475	Pyraoxystrobin
13	train	-5.8440	-5.2417	0.6023	Pyribencarb
14	train	0.0000	-0.7802	-0.7802	Triclopyricarb
15	train	0.0000	-2.9325	-2.9325	Captan
16	train	-3.0380	-2.8959	0.1421	Ferbam
17	train	-5.8910	-4.2676	1.6234	Folpet
18	train	-1.8780	-2.8687	-0.9907	Mancozeb
19	train	-4.2850	-3.1050	1.1800	Thiram
20	train	-2.4080	-2.8687	-0.4607	Zineb
21	train	-6.5560	-8.3395	-1.7835	Zoxamide
22	train	-6.5160	-6.3522	0.1638	Sedaxane
23	train	-6.8510	-7.6051	-0.7541	Piperalin
24	train	-6.4860	-7.7373	-1.2513	Inpyrfluxam
25	train	-7.2910	-8.1507	-0.8597	Penconazole
26	train	-6.4640	-5.1089	1.3551	Ferimzone
27	test	-7.5040	-5.8253	1.6787	Cyflufenamid
28	test	-6.5290	-6.0916	0.4374	Diclomezine
29	train	-6.4320	-4.5006	1.9314	Dichlobentiazox
30	train	-6.2790	-4.6304	1.6486	Flufenoxystrobin
31	train	-7.2240	-7.6823	-0.4583	Azaconazole
32	test	-6.1090	-5.8568	0.2522	Fenoxanil
33	train	-7.2400	-5.7677	1.4723	Iprodione
34	test	-7.2910	-6.3812	0.9098	Penthiopyrad
35	train	-6.6800	-7.3150	-0.6350	Oxathiapiprolin
36	test	-5.0670	-2.9524	2.1146	Metominostrobin

d)

Training Set		Test Set	
S.D.	R^2	RMSE	Q^2
1.5606	0.7491	1.6732	0.7130

Optimum number of factors = 1

ID	Set	Y(Obs)	Y(Pred)	Error	Name
1	train	0.0000	-0.8496	-0.8496	Azoxystrobin
2	train	-6.1770	-3.5091	2.6679	Coumoxystrobin
3	test	0.0000	-2.1704	-2.1704	Enoxastrobin
4	test	-6.3730	-4.6175	1.7555	Fenamidone
5	train	-7.4660	-4.5114	2.9546	Fenaminstrobin
6	train	0.0000	-1.0117	-1.0117	Fluoxastrobin
7	train	0.0000	-1.1525	-1.1525	Metyltetraprole
8	train	0.0000	-1.8835	-1.8835	Orysastrobin
9	test	0.0000	-2.4794	-2.4794	Picoxystrobin
10	train	0.0000	0.9881	0.9881	Pyraclostrobin
11	test	0.0000	-0.8767	-0.8767	pyrametostrobin
12	train	0.0000	-0.5614	-0.5614	Pyraoxystrobin
13	train	-5.8440	-5.7118	0.1322	Pyribencarb
14	train	0.0000	-0.9616	-0.9616	Triclopyricarb
15	train	0.0000	-3.5025	-3.5025	Captan
16	train	-3.0380	-3.1369	-0.0989	Ferbam
17	train	-5.8910	-4.5472	1.3438	Folpet
18	train	-1.8780	-2.5501	-0.6721	Mancozeb
19	train	-4.2850	-3.4991	0.7859	Thiram
20	train	-2.4080	-2.5501	-0.1421	Zineb
21	train	-6.5560	-7.6263	-1.0703	Zoxamide
22	train	-6.5160	-5.9241	0.5919	Sedaxane
23	train	-6.8510	-8.4378	-1.5868	Piperalin
24	train	-6.4860	-7.2996	-0.8136	Inpyrfluxam
25	train	-7.2910	-7.6751	-0.3841	Penconazole
26	train	-6.4640	-5.3358	1.1282	Ferimzone
27	test	-7.5040	-6.8313	0.6727	Cyflufenamid
28	test	-6.5290	-5.2323	1.2967	Diclomezine
29	train	-6.4320	-4.7903	1.6417	Dichlobentiazox
30	train	-6.2790	-3.7493	2.5297	Flufenoxystrobin
31	train	-7.2240	-6.4769	0.7471	Azaconazole
32	test	-6.1090	-6.1862	-0.0772	Fenoxanil
33	train	-7.2400	-6.0813	1.1587	Iprodione
34	test	-7.2910	-6.6695	0.6215	Penthiopyrad
35	train	-6.6800	-8.6592	-1.9792	Oxathiapiprolin
36	test	-5.0670	-2.2455	2.8215	Metominostrobin

e)

Training Set		Test Set	
S.D.	R^2	RMSE	Q^2
1.9451	0.6333	1.7702	0.6594

Optimum number of factors = 2

ID	Set	Y(Obs)	Y(Pred)	Error	Name
1	test	0.0000	-1.1991	-1.1991	Azoxystrobin
2	train	-6.1770	-3.5475	2.6295	Coumoxystrobin
3	train	0.0000	-0.3819	-0.3819	Enoxastrobin
4	train	-6.3730	-5.5131	0.8599	Fenamidone
5	train	-7.4660	-2.5173	4.9487	Fenaminstrobin
6	train	0.0000	0.5590	0.5590	Fluoxastrobin
7	test	0.0000	-2.3849	-2.3849	Metyltetraprole
8	train	0.0000	-1.7280	-1.7280	Orysastrobin
9	train	0.0000	-2.9018	-2.9018	Picoxystrobin
10	train	0.0000	-1.7005	-1.7005	Pyraclostrobin
11	test	0.0000	-2.7162	-2.7162	pyrametostrobin
12	train	0.0000	-1.4375	-1.4375	Pyraoxystrobin
13	test	-5.8440	-4.0998	1.7442	Pyribencarb
14	train	0.0000	-0.8362	-0.8362	Triclopyricarb
15	train	0.0000	-3.1193	-3.1193	Captan
16	test	-3.0380	-1.3272	1.7108	Ferbam
17	train	-5.8910	-4.6982	1.1928	Folpet
18	train	-1.8780	-2.4618	-0.5838	Mancozeb
19	train	-4.2850	-4.9067	-0.6217	Thiram
20	train	-2.4080	-4.1496	-1.7416	Zineb
21	train	-6.5560	-5.8842	0.6718	Zoxamide
22	train	-6.5160	-7.7344	-1.2184	Sedaxane
23	train	-6.8510	-6.8590	-0.0080	Piperalin
24	train	-6.4860	-8.5448	-2.0588	Inpyrfluxam
25	train	-7.2910	-7.1589	0.1321	Penconazole
26	test	-6.4640	-4.7508	1.7132	Ferimzone
27	train	-7.5040	-6.0471	1.4569	Cyflufenamid
28	test	-6.5290	-5.9267	0.6023	Diclomezine
29	train	-6.4320	-3.3914	3.0406	Dichlobentiazox
30	train	-6.2790	-3.4886	2.7904	Flufenoxystrobin
31	train	-7.2240	-6.9467	0.2773	Azaconazole
32	train	-6.1090	-6.8805	-0.7715	Fenoxanil
33	train	-7.2400	-6.8021	0.4379	Iprodione
34	test	-7.2910	-6.2663	1.0247	Penthiopyrad
35	test	-6.6800	-8.5191	-1.8391	Oxathiapiprolin
36	train	-5.0670	-4.9548	0.1122	Metominostrobin

Figure 33: Model reports for a) kpls_desc_2, b) kpls_radial_24, c) kpls_linear_22, d) kpls_radial_22 and e) pls_2 models.

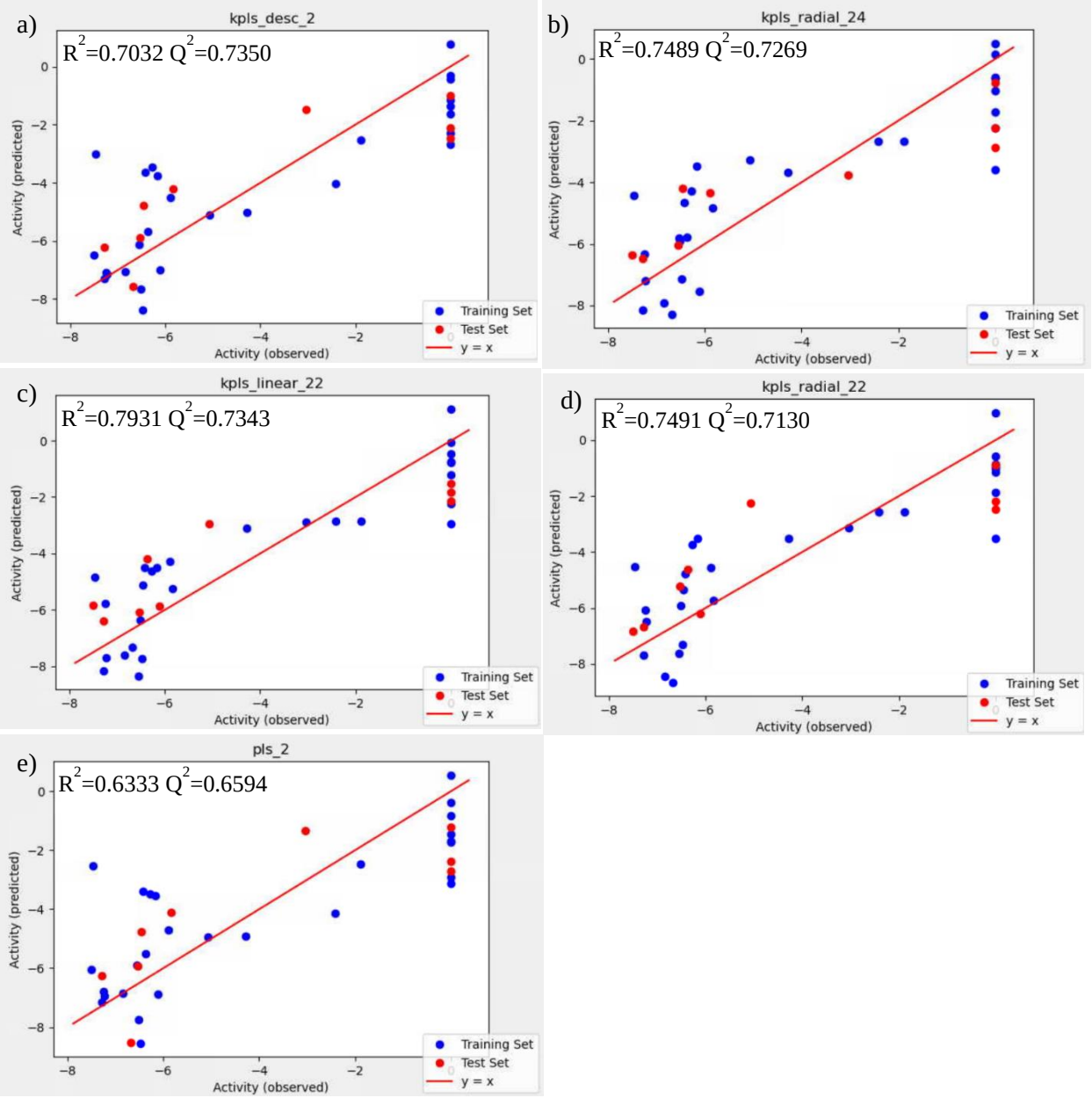

Figure 34: Scatter plot about performance for a) kpls_desc_2, b) kpls_radial_24, c) kpls_linear_22, d) kpls_radial_22 and e) pls_2 models.

Here, in order to evaluate if the predictions could be improved, it was decided to refine the models by systematically removing outliers that were chemically distinct from the ones that function as QoIs and/or when the difference between actual and predicted affinities were larger than 3 kCal/mol as previously done.

3.5.2.1.1 Iteration #1

In this iteration, the external validation set had 17 ligands to estimate the prediction accuracy of the QSAR model (Table 10). The R^2 value of the best-fit line was not impressive (Figure 35). Visual inspection of Figure 34 indicated two apparent ligands, fluindapyr and picarbutrazox, falling outside the applicability domain of the QSAR model. Triazoxide, polyoxin, dithianon and dimoxystrobin also deviated significantly from the regression line. Both fluindapyr and triazoxide had chlorine in their chemical structure (Figure 36). Dithianon was the special ligands that had heterocyclic dual sulfur atoms in aromatic rings. Picarbutrazox and dimoxystrobin had a similar structure. Triazoxide and polyoxin showed oxygen with a negative charge. To improve the prediction accuracy of QSAR model, these ligands would be considered to remove out in the next iteration.

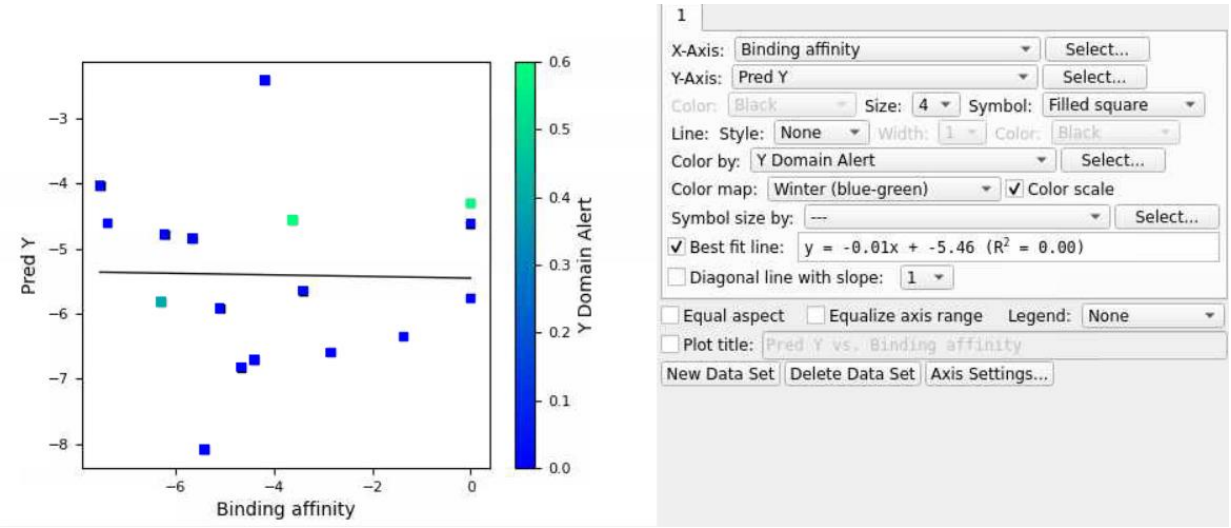

Figure 35: Scatter plot of external validation set for all top five models in Figure 32.

Table 10. Calculated binding affinity (via docking simulations) and predicted binding affinity between 17 selected ligands and G143A mutated cytochrome b of *Plasmopara viticola* by using QSAR model without validation set.

Fungicide	**Calculated Binding Affinity**	**Predicted Binding Affinity**
Fluindapyr	-5.424	-8.091
Furametpyr	-4.667	-6.826
Fenpropidin	-4.410	-6.714
Fluoxapiprolin	-2.857	-6.600
Isoflucypram	-1.367	-6.354
Flusulfamide	-5.110	-5.920
Ametoctradin	-6.299	-5.824
Tebufloquin	0	-5.767
Diethofencarb	-3.406	-5.649
Ethaboxam	-5.662	-4.842
Famoxadone	-6.238	-4.785
Triazoxide	0	-4.617
Mandestrobin	-7.393	-4.611
Polyoxin	-3.621	-4.568
Dithianon	0	-4.306
Dimoxystrobin	-7.548	-4.034
Picarbutrazox	-4.188	-2.413

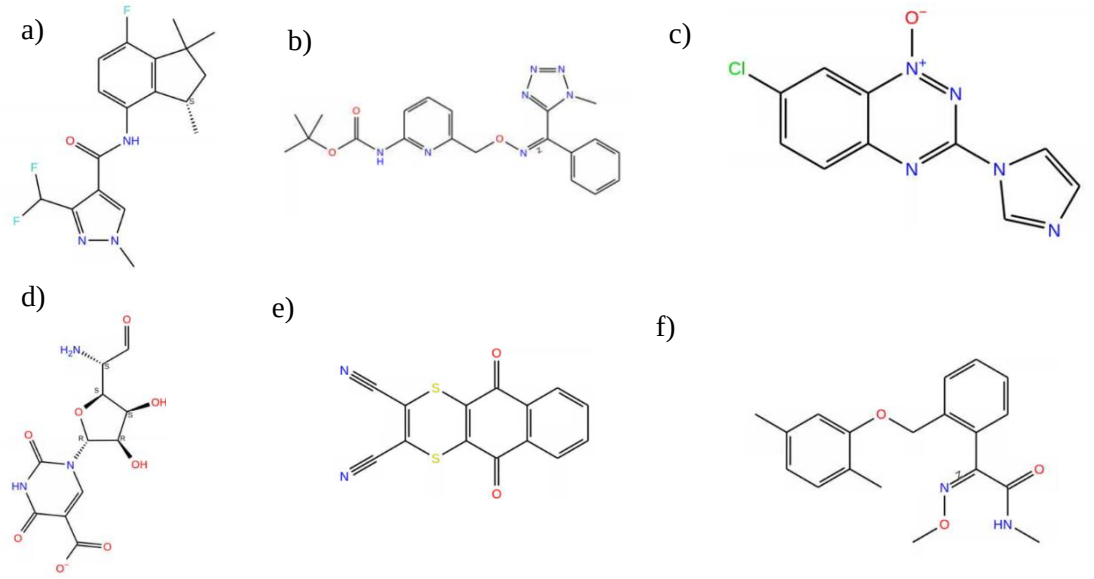

Figure 36: Six compounds a) Fluindapyr, b) Picarbutrazox, c) Triazoxide, d) Polyoxin, e) Dithianon and f) Dimoxystrobin that were outliers in Figure 35.

3.5.2.1.2 Iteration #2

After the first iteration, six ligands were removed and 11 ligands remained in Table 11. Although the R^2 value of the best-fit line increased from 0 to 0.25, there were still some outliers like furametpyr, fenpropidin and tebufloquin shown in Figure 37. Furametpyr had chlorine that was similar to triazoxide in Figure 36. Tebufloquin had fluorine that was similar to fluindapyr. All the three ligands (furametpyr, fenpropidin and tebufloquin) had a similar carbon structure as shown in in Figure 38. To further improve the accuracy, these ligands were removed in the next iteration.

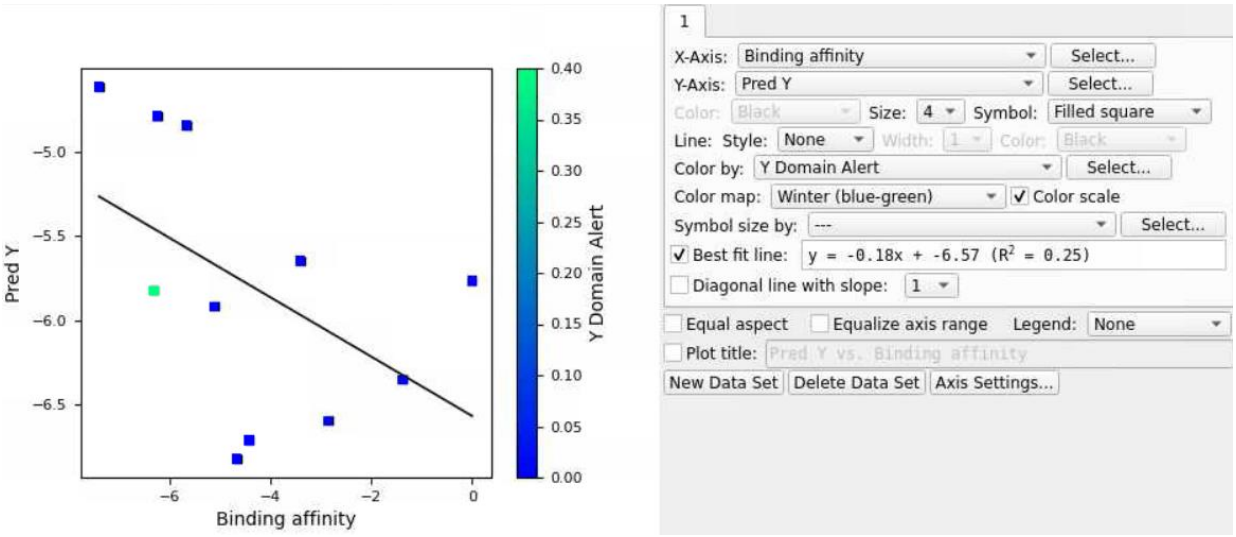

Figure 37: Scatter plot of external validation set for all top five models after removing six outliers in Figure 35.

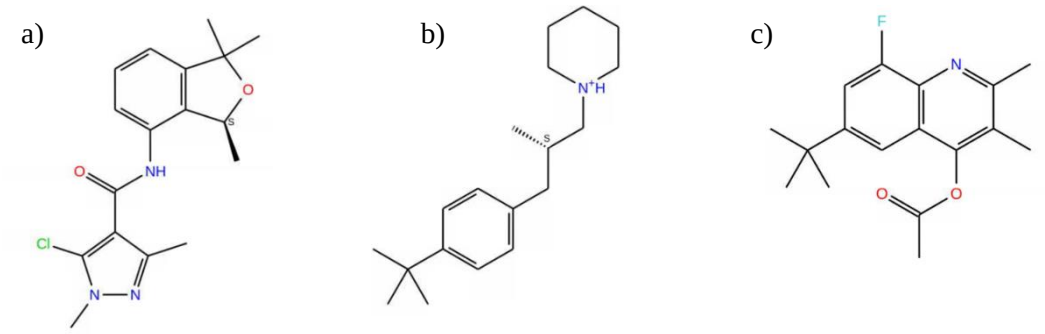

Figure 38: Three compounds a) Furametpyr, b) Fenpropidin and c) Tebufloquin that were outliers in Figure 37.

Table 11. Calculated binding affinity (via docking simulations) and predicted binding affinity between 11 selected ligands and G143A mutated cytochrome b of *Plasmopara viticola* by using QSAR model without validation set.

Fungicide	**Calculated Binding Affinity**	**Predicted Binding Affinity**
Furametpyr	-4.667	-6.826
Fenpropidin	-4.410	-6.714
Fluoxapiprolin	-2.857	-6.600
Isoflucypram	-1.367	-6.354
Flusulfamide	-5.110	-5.920
Ametoctradin	-6.299	-5.824
Tebufloquin	0	-5.767
Diethofencarb	-3.406	-5.649
Ethaboxam	-5.662	-4.842
Famoxadone	-6.238	-4.785
Mandestrobin	-7.393	-4.611

3.5.2.1.3 Iteration #3

After removing the outliers mentioned in second iteration (Table 12), the R^2 value of the best fit line (Figure 39) became 0.63, with an acceptable prediction accuracy. The top predictions that would withstand G143A mutated cytochrome b of *Plasmopara viticola* were flusulfamide (a benzene-sulfonamide), ametoctradin (a QoI), ethaboxam (a thiazole carboxamide) and famoxadone (a QoI). Isoflucypram and diethofencarb showed a high predicted affinity with low original affinity so that they were not appropriate validation set for QSAR prediction model. Outliers for this QSAR model would carry fluorine, chlorine, and oxygen with a charge, and an aromatic ring with sulfur.

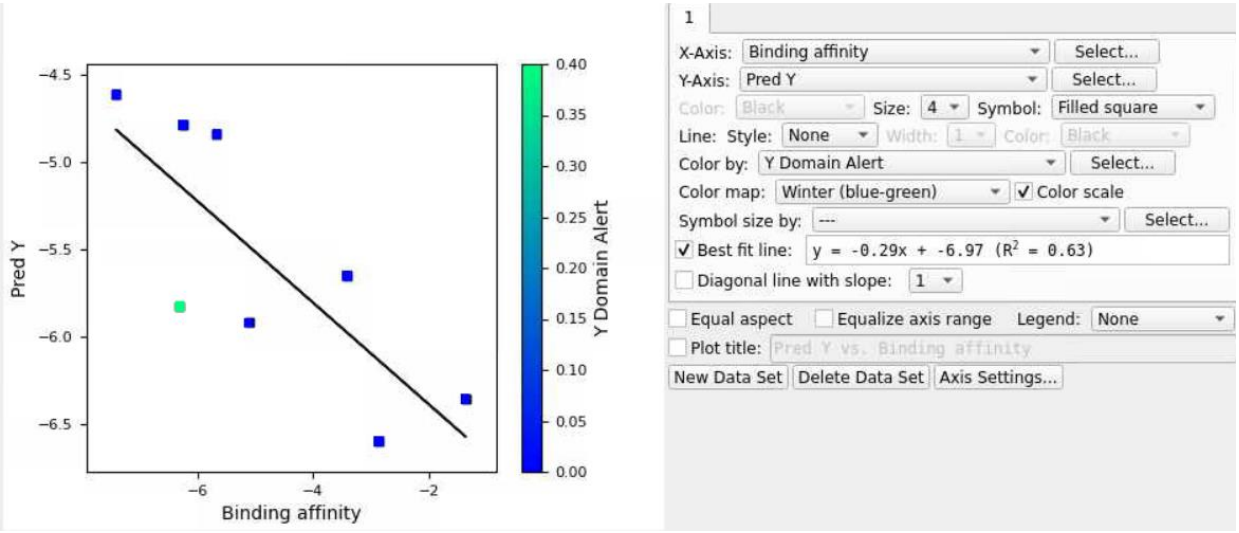

Figure 39: Scatter plot of external validation set for all top five models after removing three outliers in Figure 37.

Table 12. Calculated binding affinity (via docking simulations) and predicted binding affinity between eight selected ligands and G143A mutated cytochrome b of *Plasmopara viticola* by using QSAR model without validation set.

Fungicide	Calculated Binding Affinity	Predicted Binding Affinity
Fluoxapiprolin	-2.857	-6.600
Isoflucypram	-1.367	-6.354
Flusulfamide	-5.110	-5.920
Ametoctradin	-6.299	-5.824
Diethofencarb	-3.406	-5.649
Ethaboxam	-5.662	-4.842
Famoxadone	-6.238	-4.785
Mandestrobin	-7.393	-4.611

3.5.2.2 Training data set with validation sets

In this case, two QoI fungicides, fenaminstrobin and fenamidone, were assigned as the validation set for the QSAR models. Consequently, there were 34 ligands used for the QSAR model (Figure 41). The ranking score for the top five QSAR models with a validation set (Figure 40) were higher than the model without a validation set. The results of QSAR models from both *Botrytis cinerea* and *Plasmopara viticola* showed that a validation set may provide more accurate prediction models. Top QSAR models shown for *Plasmopara viticola* in Figure 40 were kpls_linear_39, kpls_desc_31, kpls_dendritic_31, kpls_linear_2 and kpls_linear_31. The best model was kpls_linear_39 that was generated by kernel partial least square regression (KPLS) with linear fingerprint, using the 39^{th} spilt of the learning set into a test and training set (34 ligands) with validation set. This model had a S.D of 1.4315, R^2 of 0.7953, RMSE of 1.4160, Q^2 of 0.7624 and ranking score of 0.7733. From the scatter plots in Figure 42, the pattern of training sets was similar to the plots in Figure 33.

Model Report

Model Code	Score	S.D.	R^2	RMSE	Q^2	Q^2 MW (Null Hypothesis)
kpls_linear_39	0.7733	1.4315	0.7953	1.4160	0.7624	0.1066
kpls_desc_31	0.7705	1.5857	0.7659	1.4005	0.7614	-0.3689
kpls_dendritic_39	0.7704	1.3903	0.8069	1.4045	0.7662	0.1066
kpls_linear_2	0.7680	1.3868	0.8058	1.4107	0.7885	0.1942
kpls_linear_31	0.7632	1.5812	0.7571	1.4079	0.7589	-0.3689
kpls_dendritic_31	0.7622	1.5533	0.7656	1.4777	0.7344	-0.3689
kpls_radial_31	0.7372	1.6622	0.7316	1.5053	0.7244	-0.3689
pls_31	0.7325	1.7211	0.7242	1.4936	0.7286	-0.3689
kpls_desc_2	0.6927	1.7091	0.7173	1.6569	0.7083	0.1942
pls_2	0.6753	1.8580	0.6658	1.6730	0.7025	0.1942

Figure 40: Top 10-ranked QSAR model reports with validation set for for fungicides used in *Plasmopara viticola*.

a)

Training Set S.D.	Training Set R^2	Test Set RMSE	Test Set Q^2
1.4315	0.7953	1.4160	0.7624

Optimum number of factors = 1

ID	Set	Y(Obs)	Y(Pred)	Error	Name
1	test	0.0000	-2.4836	-2.4836	Azoxystrobin
2	train	-6.1770	-3.7671	2.4099	Coumoxystrobin
3	train	0.0000	0.0155	0.0155	Enoxastrobin
4	train	0.0000	-1.5633	-1.5633	Fluoxastrobin
5	train	0.0000	-0.4981	-0.4981	Metyltetraprole
6	train	0.0000	-1.1987	-1.1987	Orysastrobin
7	train	0.0000	-0.2746	-0.2746	Picoxystrobin
8	train	0.0000	1.2507	1.2507	Pyraclostrobin
9	test	0.0000	-1.4058	-1.4058	pyrametostrobin
10	train	0.0000	-0.0120	-0.0120	Pyraoxystrobin
11	train	-5.8440	-4.5273	1.3167	Pyribencarb
12	train	0.0000	-0.6917	-0.6917	Triclopyricarb
13	train	0.0000	-3.3722	-3.3722	Captan
14	train	-3.0380	-3.5565	-0.5185	Ferbam
15	train	-5.8910	-4.6459	1.2451	Folpet
16	train	-1.8780	-3.4678	-1.5898	Mancozeb
17	test	-4.2850	-3.6604	0.6246	Thiram
18	train	-2.4080	-3.4678	-1.0598	Zineb
19	train	-6.5560	-7.8529	-1.2969	Zoxamide
20	test	-6.5160	-5.9292	0.5868	Sedaxane
21	train	-6.8510	-7.2809	-0.4299	Piperalin
22	train	-6.4860	-7.7241	-1.2381	Inpyrfluxam
23	test	-7.2910	-6.2129	1.0781	Penconazole
24	train	-6.4640	-5.3040	1.1600	Ferimzone
25	test	-7.5040	-5.1571	2.3469	Cyflufenamid
26	test	-6.5290	-5.8468	0.6822	Diclomezine
27	train	-6.4320	-4.6090	1.8230	Dichlobentiazox
28	train	-6.2790	-4.0203	2.2587	Flufenoxystrobin
29	train	-7.2240	-7.0790	0.1450	Azaconazole
30	test	-6.1090	-5.9480	0.1610	Fenoxanil
31	train	-7.2400	-6.0749	1.1651	Iprodione
32	train	-7.2910	-7.9161	-0.6251	Penthiopyrad
33	train	-6.6800	-6.9772	-0.2972	Oxathiapiprolin
34	train	-5.0670	-3.1909	1.8761	Metominostrobin

b)

Training Set S.D.	Training Set R^2	Test Set RMSE	Test Set Q^2
1.5857	0.7659	1.4005	0.7614

Optimum number of factors = 2

ID	Set	Y(Obs)	Y(Pred)	Error	Name
1	train	0.0000	-0.0223	-0.0223	Azoxystrobin
2	train	-6.1770	-2.8913	3.2857	Coumoxystrobin
3	test	0.0000	0.1754	0.1754	Enoxastrobin
4	train	0.0000	0.7086	0.7086	Fluoxastrobin
5	train	0.0000	0.3846	0.3846	Metyltetraprole
6	train	0.0000	-0.9345	-0.9345	Orysastrobin
7	train	0.0000	-3.2886	-3.2886	Picoxystrobin
8	train	0.0000	-0.9671	-0.9671	Pyraclostrobin
9	train	0.0000	-2.0821	-2.0821	pyrametostrobin
10	train	0.0000	-0.9167	-0.9167	Pyraoxystrobin
11	test	-5.8440	-4.0786	1.7654	Pyribencarb
12	test	0.0000	-2.0481	-2.0481	Triclopyricarb
13	train	0.0000	-1.8613	-1.8613	Captan
14	train	-3.0380	-2.2697	0.7683	Ferbam
15	train	-5.8910	-4.3970	1.4940	Folpet
16	train	-1.8780	-2.6440	-0.7660	Mancozeb
17	train	-4.2850	-4.1806	0.1044	Thiram
18	test	-2.4080	-4.8237	-2.4157	Zineb
19	train	-6.5560	-6.3244	0.2316	Zoxamide
20	train	-6.5160	-8.1444	-1.6284	Sedaxane
21	train	-6.8510	-7.1294	-0.2784	Piperalin
22	train	-6.4860	-8.6045	-2.1185	Inpyrfluxam
23	train	-7.2910	-6.9206	0.3704	Penconazole
24	train	-6.4640	-6.0181	0.4459	Ferimzone
25	train	-7.5040	-7.0410	0.4630	Cyflufenamid
26	test	-6.5290	-6.3066	0.2224	Diclomezine
27	train	-6.4320	-3.8631	2.5689	Dichlobentiazox
28	train	-6.2790	-3.8005	2.4785	Flufenoxystrobin
29	train	-7.2240	-6.7431	0.4809	Azaconazole
30	test	-6.1090	-6.3899	-0.2809	Fenoxanil
31	train	-7.2400	-6.2985	0.9415	Iprodione
32	test	-7.2910	-5.8168	1.4742	Penthiopyrad
33	test	-6.6800	-7.1401	-0.4601	Oxathiapiprolin
34	train	-5.0670	-4.9292	0.1378	Metominostrobin

c)

Training Set S.D.	Training Set R^2	Test Set RMSE	Test Set Q^2
1.3903	0.8069	1.4045	0.7662

Optimum number of factors = 1

ID	Set	Y(Obs)	Y(Pred)	Error	Name
1	test	0.0000	-2.4017	-2.4017	Azoxystrobin
2	train	-6.1770	-3.8256	2.3514	Coumoxystrobin
3	train	0.0000	0.1218	0.1218	Enoxastrobin
4	train	0.0000	-1.6422	-1.6422	Fluoxastrobin
5	train	0.0000	-0.2450	-0.2450	Metyltetraprole
6	train	0.0000	-1.3003	-1.3003	Orysastrobin
7	train	0.0000	-0.2010	-0.2010	Picoxystrobin
8	train	0.0000	1.3493	1.3493	Pyraclostrobin
9	test	0.0000	-1.5057	-1.5057	pyrametostrobin
10	train	0.0000	0.1005	0.1005	Pyraoxystrobin
11	train	-5.8440	-4.6705	1.1735	Pyribencarb
12	train	0.0000	-0.8057	-0.8057	Triclopyricarb
13	train	0.0000	-3.3248	-3.3248	Captan
14	train	-3.0380	-3.5084	-0.4704	Ferbam
15	train	-5.8910	-4.5728	1.3182	Folpet
16	train	-1.8780	-3.4164	-1.5384	Mancozeb
17	test	-4.2850	-3.6047	0.6803	Thiram
18	train	-2.4080	-3.4164	-1.0084	Zineb
19	train	-6.5560	-7.8953	-1.3393	Zoxamide
20	test	-6.5160	-5.6900	0.8260	Sedaxane
21	train	-6.8510	-7.4287	-0.5777	Piperalin
22	train	-6.4860	-7.5701	-1.0841	Inpyrfluxam
23	test	-7.2910	-6.4012	0.8898	Penconazole
24	train	-6.4640	-5.2502	1.2138	Ferimzone
25	test	-7.5040	-5.1255	2.3785	Cyflufenamid
26	test	-6.5290	-6.1485	0.3805	Diclomezine
27	train	-6.4320	-4.6016	1.8304	Dichlobentiazox
28	train	-6.2790	-4.4093	1.8697	Flufenoxystrobin
29	train	-7.2240	-7.2565	-0.0325	Azaconazole
30	test	-6.1090	-6.0332	0.0758	Fenoxanil
31	train	-7.2400	-6.0561	1.1839	Iprodione
32	train	-7.2910	-7.7458	-0.4548	Penthiopyrad
33	train	-6.6800	-6.8544	-0.1744	Oxathiapiprolin
34	train	-5.0670	-3.3804	1.6866	Metominostrobin

d)

Training Set S.D.	Training Set R^2	Test Set RMSE	Test Set Q^2
1.3868	0.8058	1.4107	0.7885

Optimum number of factors = 1

ID	Set	Y(Obs)	Y(Pred)	Error	Name
1	test	0.0000	-2.3820	-2.3820	Azoxystrobin
2	train	-6.1770	-3.6406	2.5364	Coumoxystrobin
3	train	0.0000	0.2951	0.2951	Enoxastrobin
4	train	0.0000	-1.3615	-1.3615	Fluoxastrobin
5	train	0.0000	-1.2162	-1.2162	Metyltetraprole
6	train	0.0000	-0.5476	-0.5476	Orysastrobin
7	train	0.0000	-0.2526	-0.2526	Picoxystrobin
8	test	0.0000	-0.4025	-0.4025	Pyraclostrobin
9	train	0.0000	-0.1326	-0.1326	pyrametostrobin
10	train	0.0000	0.6205	0.6205	Pyraoxystrobin
11	train	-5.8440	-4.7601	1.0839	Pyribencarb
12	test	0.0000	-1.8649	-1.8649	Triclopyricarb
13	train	0.0000	-3.3026	-3.3026	Captan
14	test	-3.0380	-3.8695	-0.8315	Ferbam
15	test	-5.8910	-3.6734	2.2176	Folpet
16	train	-1.8780	-3.6541	-1.7761	Mancozeb
17	train	-4.2850	-3.8044	0.4806	Thiram
18	train	-2.4080	-3.6541	-1.2461	Zineb
19	test	-6.5560	-7.0936	-0.5376	Zoxamide
20	test	-6.5160	-5.6914	0.8246	Sedaxane
21	train	-6.8510	-7.1765	-0.3255	Piperalin
22	train	-6.4860	-7.3919	-0.9059	Inpyrfluxam
23	test	-7.2910	-7.1210	0.1700	Penconazole
24	train	-6.4640	-5.0065	1.4575	Ferimzone
25	train	-7.5040	-7.2713	0.2327	Cyflufenamid
26	train	-6.5290	-6.3230	0.2060	Diclomezine
27	train	-6.4320	-4.3922	2.0398	Dichlobentiazox
28	train	-6.2790	-4.3666	1.9124	Flufenoxystrobin
29	train	-7.2240	-7.6193	-0.3953	Azaconazole
30	train	-6.1090	-7.4680	-1.3590	Fenoxanil
31	train	-7.2400	-6.2636	0.9764	Iprodione
32	train	-7.2910	-7.7966	-0.5056	Penthiopyrad
33	train	-6.6800	-7.2093	-0.5293	Oxathiapiprolin
34	train	-5.0670	-3.0523	2.0147	Metominostrobin

e)

Training Set S.D.	Training Set R^2	Test Set RMSE	Test Set Q^2
1.5812	0.7571	1.4079	0.7589

Optimum number of factors = 1

ID	Set	Y(Obs)	Y(Pred)	Error	Name
1	train	0.0000	-0.7023	-0.7023	Azoxystrobin
2	train	-6.1770	-4.0529	2.1241	Coumoxystrobin
3	test	0.0000	-1.3660	-1.3660	Enoxastrobin
4	train	0.0000	-1.1355	-1.1355	Fluoxastrobin
5	train	0.0000	-0.8193	-0.8193	Metyltetraprole
6	train	0.0000	-1.9540	-1.9540	Orysastrobin
7	train	0.0000	0.0689	0.0689	Picoxystrobin
8	train	0.0000	0.5797	0.5797	Pyraclostrobin
9	train	0.0000	-0.4633	-0.4633	pyrametostrobin
10	train	0.0000	0.3089	0.3089	Pyraoxystrobin
11	test	-5.8440	-3.7030	2.1410	Pyribencarb
12	test	0.0000	-1.7012	-1.7012	Triclopyricarb
13	train	0.0000	-3.9677	-3.9677	Captan
14	train	-3.0380	-3.9369	-0.8989	Ferbam
15	train	-5.8910	-4.5429	1.3481	Folpet
16	train	-1.8780	-4.1376	-2.2596	Mancozeb
17	train	-4.2850	-4.1001	0.1849	Thiram
18	test	-2.4080	-4.1376	-1.7296	Zineb
19	train	-6.5560	-7.6134	-1.0574	Zoxamide
20	train	-6.5160	-6.3305	0.1855	Sedaxane
21	train	-6.8510	-7.2062	-0.3552	Piperalin
22	train	-6.4860	-6.9609	-0.4749	Inpyrfluxam
23	train	-7.2910	-8.1309	-0.8399	Penconazole
24	train	-6.4640	-4.2480	2.2160	Ferimzone
25	train	-7.5040	-7.3227	0.1813	Cyflufenamid
26	test	-6.5290	-5.7559	0.7731	Diclomezine
27	train	-6.4320	-4.0391	2.3929	Dichlobentiazox
28	train	-6.2790	-3.9048	2.3742	Flufenoxystrobin
29	train	-7.2240	-7.6264	-0.4024	Azaconazole
30	test	-6.1090	-6.2949	-0.1859	Fenoxanil
31	train	-7.2400	-6.1569	1.0831	Iprodione
32	test	-7.2910	-6.3324	0.9586	Penthiopyrad
33	test	-6.6800	-5.2757	1.4043	Oxathiapiprolin
34	train	-5.0670	-2.7843	2.2827	Metominostrobin

Figure 41: Model reports for a) kpls_linear_39, b) kpls_desc_31, c) kpls_dendritic_39, d) kpls_linear_2 and e) kpls_linear_31 models.

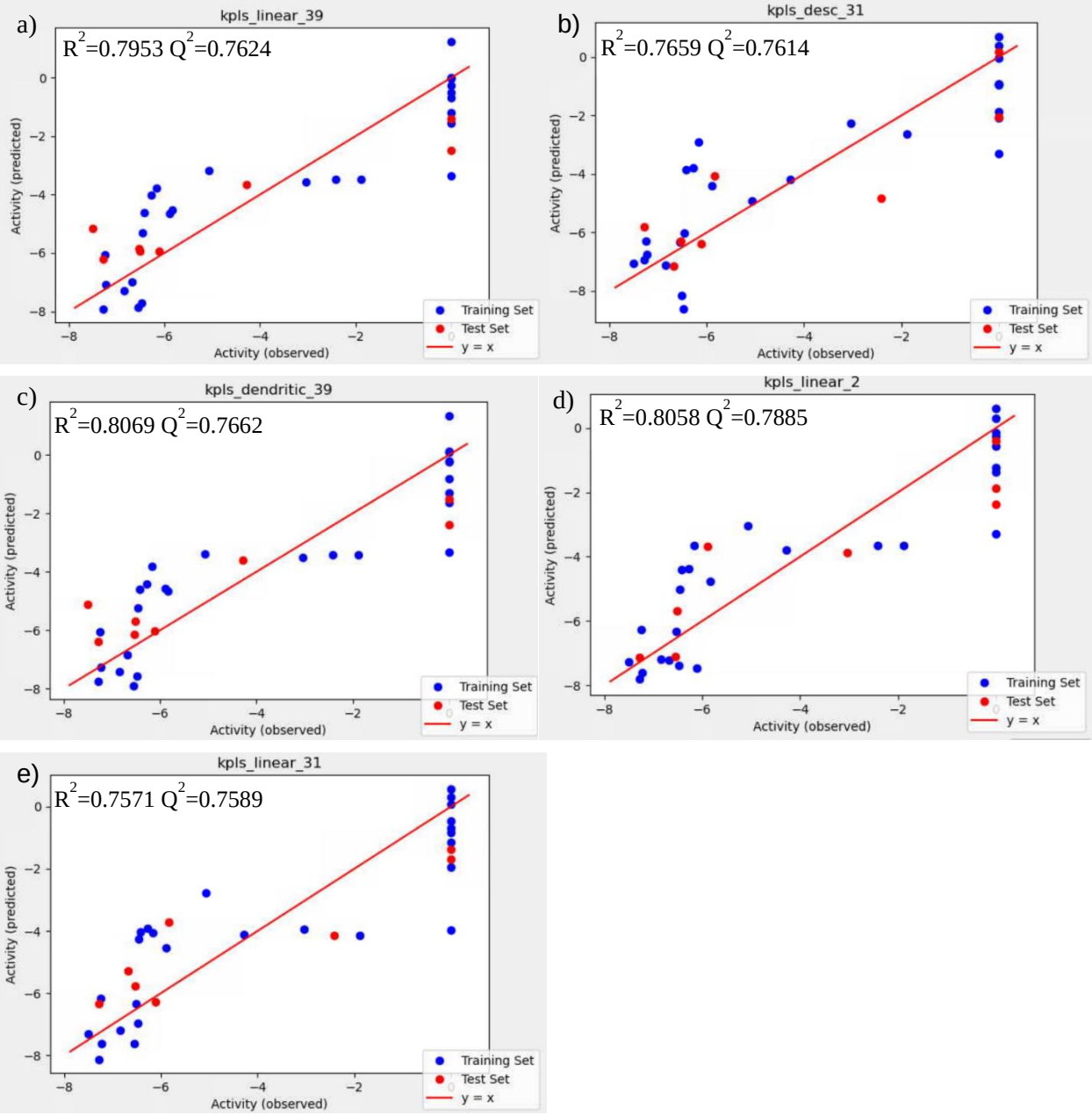

Figure 42: Scatter plot about performance for a) kpls_linear_39, b) kpls_desc_31, c) kpls_dendritic_39, d) kpls_linear_2 and e) kpls_linear_31 models.

3.5.2.2.1 Iteration #1

The predicted binding affinities in Table 13 were slightly lower than those in Table 10. The R^2 value of the best-fit line was 0.03 shown in Figure 43. Visual inspection of Figure 43 showed three apparent ligands (fluindapyr, picarbutrazox and dimoxystrobin) falling outside the

applicability domain of the QSAR model, which affected the prediction accuracy of the QSAR model. Dithianon was another ligand that lay further from the regression line, and it was the only ligand that contained an aromatic ring with sulfur (Figure 44). Fluindapyr and picarbutrazox had similar aromatic rings. To improve the prediction accuracy of QSAR model, these ligands were removed during the next iteration.

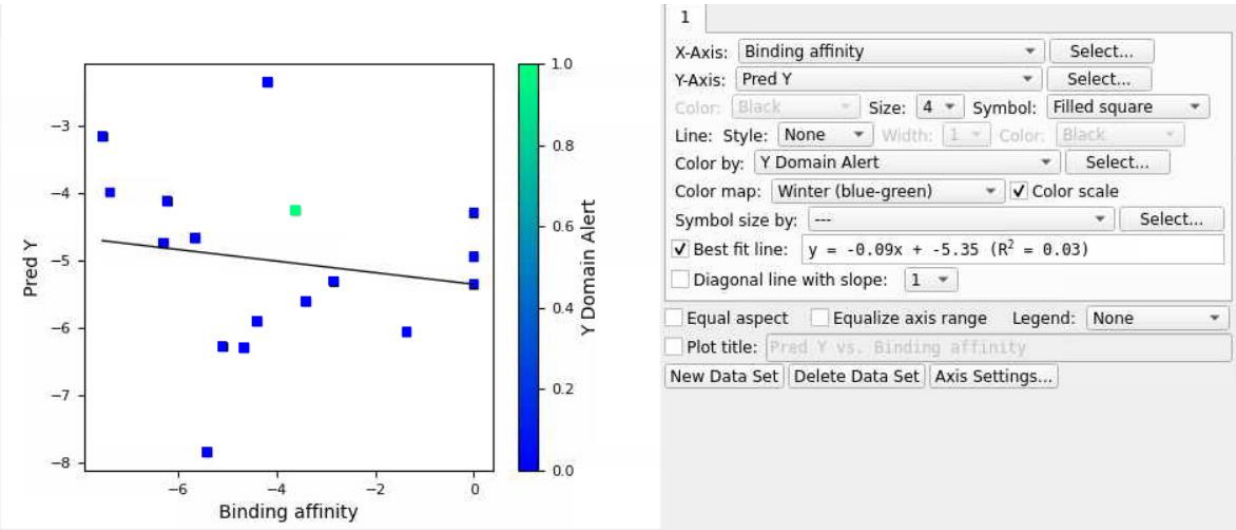

Figure 43: Scatter plot of external validation set for all top five models in Figure 40.

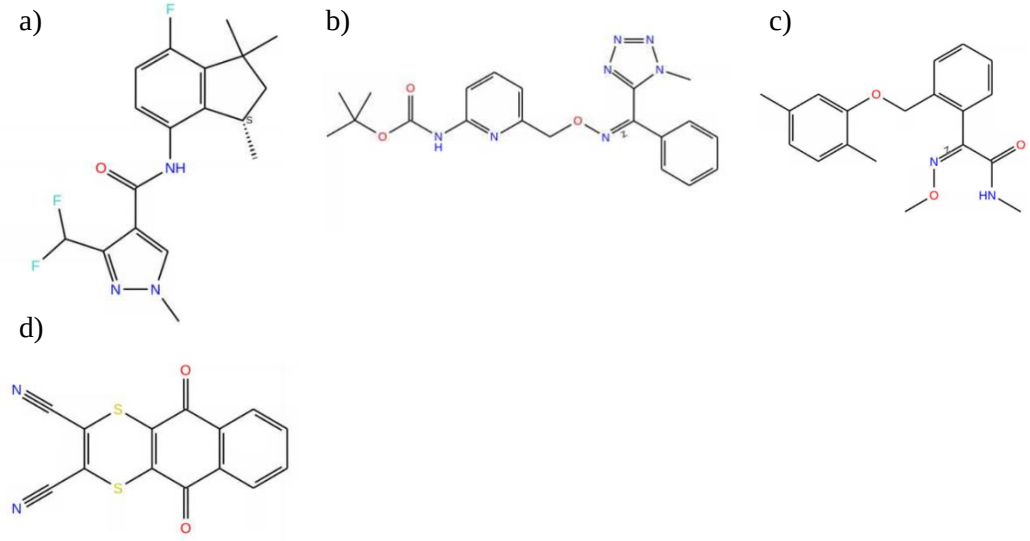

Figure 44: Four compounds a) Fluindapyr, b) Picarbutrazox, c) Dimoxystrobin and d) Dithianon that were outliers in Figure 43.

Table 13: Calculated binding affinity (via docking simulations) and predicted binding affinity between 17 selected ligands and G143A mutated cytochrome b of *Plasmopara viticola* by using QSAR model with validation set.

Fungicide	**Calculated Binding Affinity**	**Predicted Binding Affinity**
Fluindapyr	-5.424	-7.845
Furametpyr	-4.667	-6.300
Flusulfamide	-5.110	-6.275
Isoflucypram	-1.367	-6.054
Fenpropidin	-4.410	-5.903
Diethofencarb	-3.406	-5.608
Tebufloquin	0	-5.436
Fluoxapiprolin	-2.857	-5.307
Triazoxide	0	-4.943
Ametoctradin	-6.299	-4.740
Ethaboxam	-5.662	-4.672
Dithianon	0	-4.287
Polyoxin	-3.621	-4.257
Famoxadone	-6.238	-4.117
Mandestrobin	-7.393	-3.989
Dimoxystrobin	-7.548	-3.157
Picarbutrazox	-4.188	-2.351

3.5.2.2.2 Iteration #2

After the first iteration, four ligands were removed and 13 ligands remained in Table 14. The R^2 value of the best fit line shown on Figure 30 improved from 0.03 to 0.16 in this iteration (Figure 45). Furametpyr, flusulfamide, tebufloquin, triazoxide, polyoxin, famoxadone and mandestrobin were outliers based on visual inspection. Furametpyr, flusulfamide and triazoxide had chlorine. Flusulfamide and tebufloquin had fluorine in their ligands structure (Figure 46). Both triazoxide and polyoxin had oxygen with a charge in their ring structure. Famoxadone and mandestrobin had similar structure to dimoxystrobin. For further improvement on the model, these ligands were removed.

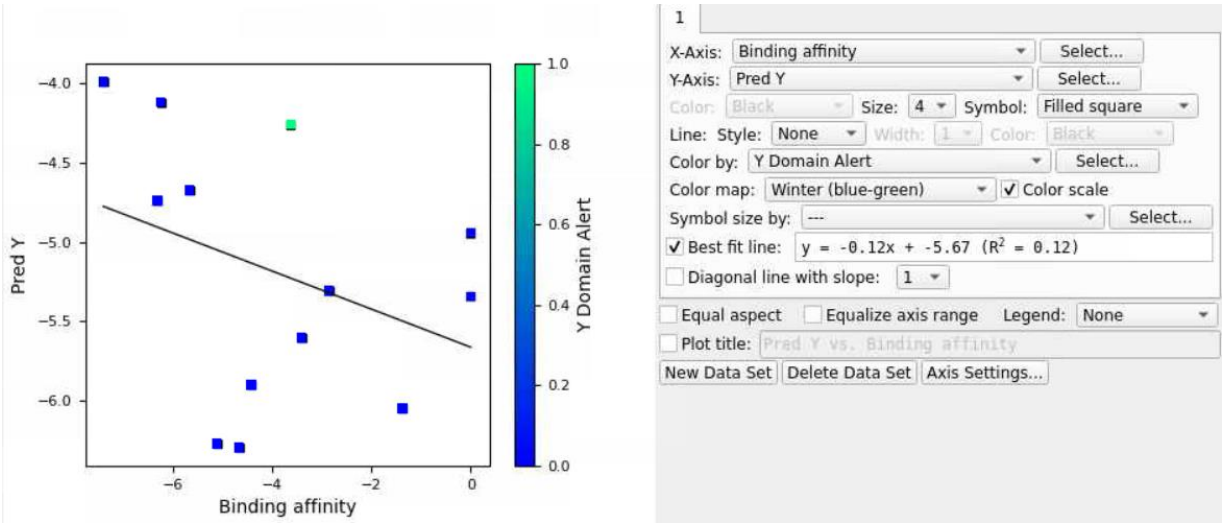

Figure 45: Scatter plot of external validation set after removing four outliers in Figure 43.

Table 14. Calculated binding affinity (via docking simulations) and predicted binding affinity between 13 selected ligands and G143A mutated cytochrome b of *Plasmopara viticola* by using QSAR model with validation set.

Fungicide	Calculated Binding Affinity	Predicted Binding Affinity
Furametpyr	-4.667	-6.300
Flusulfamide	-5.110	-6.275
Isoflucypram	-1.367	-6.054
Fenpropidin	-4.410	-5.903
Diethofencarb	-3.406	-5.608
Tebufloquin	0	-5.436
Fluoxapiprolin	-2.857	-5.307
Triazoxide	0	-4.943
Ametoctradin	-6.299	-4.740
Ethaboxam	-5.662	-4.672
Polyoxin	-3.621	-4.257
Famoxadone	-6.238	-4.117
Mandestrobin	-7.393	-3.989

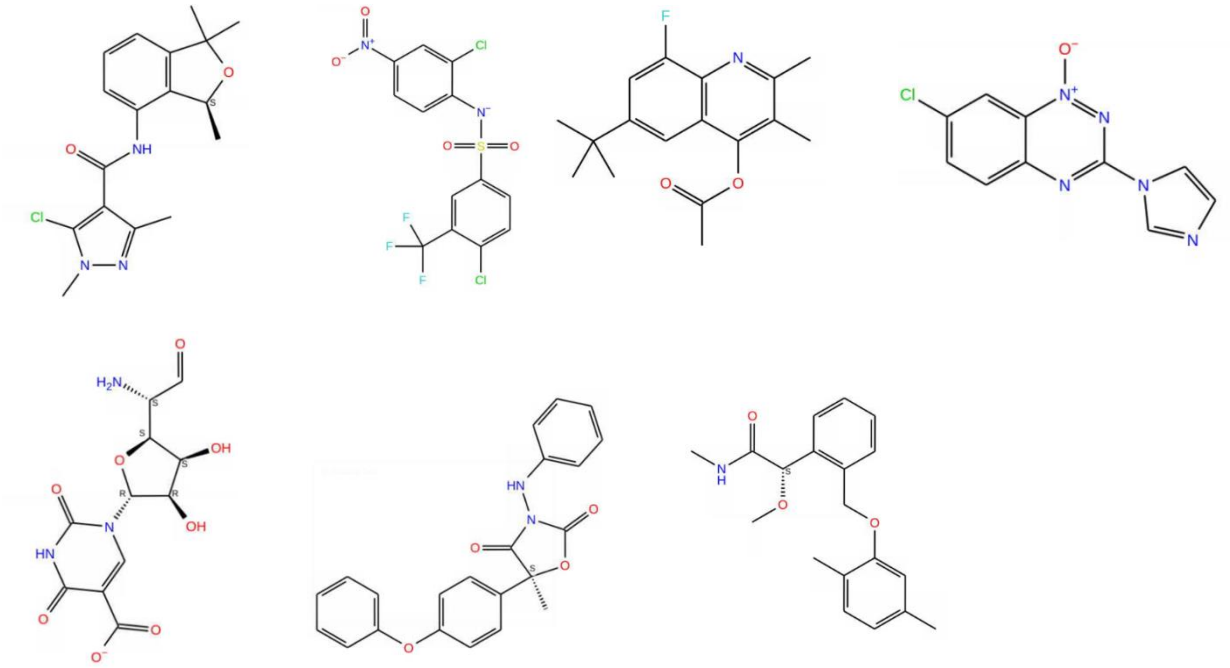

Figure 46: Four compounds a) Furametpyr, b) Flusulfamide, c) Tebufloquin, d) Triazoxide, e) Polyoxin, f) Famoxadone and g) Mandestrobin that were outliers in Figure 45.

3.5.2.2.3 Iteration #3

In this case, the R^2 value of the best-fit line shown on Figure 47 was 0.64, meaning the prediction accuracy of QSAR models was acceptable. The top predictions that would withstand G143A mutated cytochrome b of *Plasmopara viticola* were fenpropidin (an amine), ametoctradin (a QoI) and ethaboxam (a thiazole carboxamide). Isoflucypram, diethofencarb and fluoxapiprolin were not appropriate selection since their predicted affinities were very different from their original affinities (Table 15). Outliers for this QSAR model also contained fluorine and chlorine, which was similar to QSAR model with using a validation set.

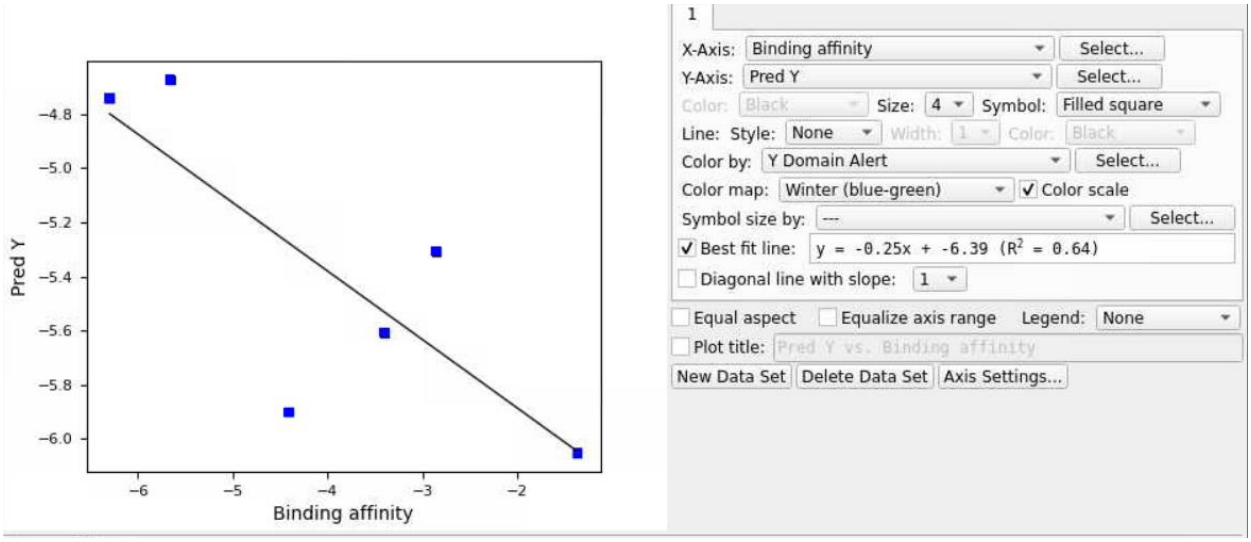

Figure 47: Scatter plot of external validation set after removing seven outliers in Figure 45.

Table 15. Calculated binding affinity (via docking simulations) and predicted binding affinity between six selected ligands and G143A mutated cytochrome b of *Plasmopara viticola* by using QSAR model with validation set.

Fungicide	Calculated Binding Affinity	Predicted Binding Affinity
Isoflucypram	-1.367	-6.054
Fenpropidin	-4.410	-5.903
Diethofencarb	-3.406	-5.608
Fluoxapiprolin	-2.857	-5.307
Ametoctradin	-6.299	-4.740
Ethaboxam	-5.662	-4.672

4. CONCLUSIONS

The primary purpose of this study was to use *in silico* simulations to select the highest affinity QoI fungicides to cytochrome b targets of *Plasmopara viticola* and *Botrytis cinerea*. Based on different in-silico simulation methods that consisted of generalized and site-directed ligand impingement methods, both docking and MD simulations showed ubiquinol to be the highest affinity ligand for cytochrome b, regardless of the sourced organism. Ubiquinol bound to cytochrome b primarily via hydrophobic interactions.

For the case of WT cytochrome b of *Plasmopara viticola*, mandestrobin, fenaminstrobin, dimoxystrobin, fenamidone, famoxadone and ametoctradin bound with highest affinity and thus are considered as effective fungicides. They were also effective agents against G143A and F129L mutated cytochrome b. Ametoctradin and Metominostrobin had a strong affinity to WT, G143A, and G143A-F129L double mutated cytochrome b but did not bind strongly enough to the receptor with F129L mutation. While coumoxystrobin, flufenoxystrobin and pyribencarb showed strong affinity towards F129L mutated cytochrome b, their affinities were poor toward WT and other mutated versions, suggesting their susceptibility toward potential resistance. As a resistant fungicide, azoxystrobin did not bind to WT, G143A, F129L and G143A-F129L mutated cytochrome b as expected. Although folpet, a FRAC code low-risk fungicide, showed reasonable affinity toward G143A and F129L mutated cytochrome b, only thiram had stable and strong affinities toward all four variations of cytochrome b among the selected low-risk fungicides. According to the general analysis, mandestrobin, fenaminstrobin, dimoxystrobin, famoxadone, fenamidone, ametoctradin and thiram emerged as those with the strongest affinity from high-risk and low-risk groups toward *Plasmopara viticola* cytochrome b. Based on MD simulations and MM-GBSA calculations, two high-risk QoI fungicides, famoxadone and fenamidone, showed

strong affinity toward *Plasmopara viticola* cytochrome b with site-directed docking. Mandestrobin and thiram had slightly weaker but still acceptable affinity and stability. These MD results consolidated what was revealed by the docking analysis.

Pyribencarb, mandestrobin, fenamidone, famoxadone and ametoctradin were effective agents against WT, G143A and F129L mutated cytochrome b of *Botrytis cinerea*. Among these fungicides, mandestrobin, fenamidone and ametoctradin showed strong affinity toward cytochrome b with the G143A-F129L double mutation, indicating that they are potential candidates against the four variations of cytochrome b. While pyraoxystrobin and metominostrobin had a strong affinity toward WT cytochrome b, its affinity was poor toward mutated cytochrome b. The low-risk fungicides, folpet and captan had a strong affinity with WT cytochrome b but did not bind to any of the mutated versions of *Botrytis cinerea* cytochrome b. Thiram showed consistent but moderate affinities. Based on the general analysis, mandestrobin, pyribencarb, famoxadone, ametoctradin, fenamidone and thiram emerged as those with the strongest affinity from high-risk and low-risk fungicides toward to all four version of *Botrytis cinerea* cytochrome b.

According to the binding affinity simulation analysis, famoxadone and mandestrobin, emerged as the top binders for both *Plasmopara viticola* and *Botrytis cinerea* cytochrome b regardless of common mutations. Thiram, on the other hand, emerged as a reasonable low-risk fungicide that works on WT and mutated versions of both fungi. However, the affinity analysis clearly indicated the difficulty of making such broad-spectrum recommendations due to the peculiarities of cytochrome b proteins within different organisms.

Based on a QSAR analysis with an extended array of fungicides, fenpropidin (an amine), fenoxail (a melanin biosynthesis inhibitor dehydrates), isoflucypram (a succinate dehydrogenase

inhibitor) and ametoctradin (a QoI) emerged to be effective against G143A mutated cytochrome b of *Botrytis cinerea*. Moreover, fenoxanil, fenpropidin, iprodione (a dicarboximde), tebufloquin (a 4-quinolyl-acetate), and ametoctradin emerged as high-affinity inhibitors in an analysis with a secondary validation set. The QSAR analysis without a validation set revealed flusulfamide (a benzene-sulfonamide), ametoctradin, ethaboxam (a thiazole carboxamide) and famoxadone (a QoI) emerged as effective fungicides against G143A mutated cytochrome b of *Plasmopara viticola*. Also, fenpropidin, ametoctradin and ethaboxam showed strong affinity on the analysis with a secondary validation set. Based on both the docking simulations and QSAR analysis, ametoctradin emerged as a potential high-affinity QoI fungicide against the G143A mutation.

4.1 Suggestion for future studies

The modeling results should be experimentally validated via *in vitro* and/or *in planta* field studies. Free energy perturbation could be used to improve the accuracy of the modeling results and thus should be considered in future studies. The accuracy of the QSAR model needs to be improved using a substantial amount (at least 50 compounds) of experimental (validation) data.

REFERENCES

[1] Agrios, G. N. (2005). *Plant pathology*: Elsevier.

[2] Arnold, K., Bordoli, L., Kopp, J., & Schwede, T. (2006). The SWISS-MODEL workspace: a web-based environment for protein structure homology modelling. *Bioinformatics, 22*(2), 195-201.

[3] Bartlett, D. W., Clough, J. M., Godwin, J. R., Hall, A. A., Hamer, M., & Parr-Dobrzanski, B. (2002). The strobilurin fungicides. *Pest Management Science: formerly Pesticide Science, 58*(7), 649-662.

[4] Caffi, T., Rossi, V., & Carisse, O. (2011). Evaluation of a dynamic model for primary infections caused by Plasmopara viticola on grapevine in Quebec. *Plant health progress, 12*(1), 22.

[5] Chen, W.-J., Delmotte, F., Cervera, S. R., Douence, L., Greif, C., & Corio-Costet, M.-F. (2007). At least two origins of fungicide resistance in grapevine downy mildew populations. *Applied and environmental microbiology, 73*(16), 5162-5172.

[6] Colovos, C., & Yeates, T. O. (1993). Verification of protein structures: patterns of nonbonded atomic interactions. *Protein science, 2*(9), 1511-1519.

[7] Dean, R., Van Kan, J. A., Pretorius, Z. A., Hammond-Kosack, K. E., Di Pietro, A., Spanu, P. D., . . . Ellis, J. (2012). The Top 10 fungal pathogens in molecular plant pathology. *Molecular plant pathology, 13*(4), 414-430.

[8] Elmer, P., & Reglinski, T. (2006). Biosuppression of Botrytis cinerea in grapes. *Plant Pathology, 55*(2), 155-177.

[9] FAO. (2020). FAOSTAT statistical database. Food and Agriculture Organization of the United Nations. Retrieved from https://www.fao.org/faostat/en/#data/QCL.

[10] Fisher, N., Meunier, B., & Biagini, G. A. (2020). The cytochrome bc1 complex as an antipathogenic target. *Febs Letters, 594*(18), 2935-2952.

[11] Foster, A. J. (2018). Identification of fungicide targets in pathogenic fungi. *Physiology and genetics*, 277-296.

[12] Grasso, V., Palermo, S., Sierotzki, H., Garibaldi, A., & Gisi, U. (2006). Cytochrome b gene structure and consequences for resistance to Qo inhibitor fungicides in plant pathogens. *Pest Management Science: formerly Pesticide Science, 62*(6), 465-472.

[13] Hahn, M. (2014). The rising threat of fungicide resistance in plant pathogenic fungi: Botrytis as a case study. *Journal of chemical biology, 7*(4), 133-141.

[14] Hollomon, D. W. (2015). Fungicide resistance: facing the challenge-a review. *Plant protection science, 51*(4), 170-176.

[15] Irwin, J. (2019). *ZINC15. docking. org: Over 1.5 billion compounds you can search and buy; 550 million lead-like you can dock.* Paper presented at the Abstracts of Papers of the American Chemical Society.

[16] Jorgensen, W. L., & Tirado-Rives, J. (1988). The OPLS [optimized potentials for liquid simulations] potential functions for proteins, energy minimizations for crystals of cyclic peptides and crambin. *Journal of the American Chemical Society, 110*(6), 1657-1666.

[17] Kalibaeva, G., Ferrario, M., & Ciccotti, G. (2003). Constant pressure-constant temperature molecular dynamics: a correct constrained NPT ensemble using the molecular virial. *Molecular Physics, 101*(6), 765-778.

[18] Kassemeyer, H.-H. (2017). Fungi of grapes. In *Biology of Microorganisms on Grapes, in Must and in Wine* (pp. 103-132): Springer.

[19] Kim, S., Chen, J., Cheng, T., Gindulyte, A., He, J., He, S., . . . Yu, B. (2021). PubChem in 2021: new data content and improved web interfaces. *Nucleic acids research, 49*(D1), D1388-D1395.

[20] Kramer, Jaclyn, Skyler Simnitt, and Linda Calvin (2021), Fruit and Tree Nuts Outlook: September 2021, FTS-373, U.S. Department of Agriculture, Economic Research Service, September 29, 2021.

[21] Kumar, B. K., Faheem, n., Sekhar, K. V. G. C., Ojha, R., Prajapati, V. K., Pai, A., & Murugesan, S. (2022). Pharmacophore based virtual screening, molecular docking, molecular dynamics and MM-GBSA approach for identification of prospective SARS-CoV-2 inhibitor from natural product databases. *Journal of Biomolecular Structure and Dynamics, 40*(3), 1363-1386.

[22] Laskowski, R. A., Rullmann, J. A. C., MacArthur, M. W., Kaptein, R., & Thornton, J. M. (1996). AQUA and PROCHECK-NMR: programs for checking the quality of protein structures solved by NMR. *Journal of biomolecular NMR, 8*(4), 477-486.

[23] Maldonado, M., Guo, F., & Letts, J. A. (2021). Atomic structures of respiratory complex III2, complex IV, and supercomplex III2-IV from vascular plants. *Elife, 10*.

[24] Mezei, I., Lukić, M., Berbakov, L., Pavković, B., & Radovanović, B. (2022). Grapevine Downy Mildew Warning System Based on NB-IoT and Energy Harvesting Technology. *Electronics, 11*(3), 356.

[25] Mounkoro, P., Michel, T., Benhachemi, R., Surpateanu, G., Iorga, B. I., Fisher, N., & Meunier, B. (2019). Mitochondrial complex III Qi-site inhibitor resistance mutations found in laboratory selected mutants and field isolates. Pest management science, 75(8), 2107-2114.

[26] Mulgaonkar, N., Wang, H., Mallawarachchi, S., Růžek, D., Martina, B., & Fernando, S. (2022). In silico and in vitro evaluation of imatinib as an inhibitor for SARS-CoV-2. *Journal of Biomolecular Structure and Dynamics*, 1-10.

[27] Murray, R. E., Candan, A. P., & Vazquez, D. E. (2019). *Manual de poscosecha de frutas: manejo integrado de patógenos*. Ediciones INTA

[28] Pontius, J., Richelle, J., & Wodak, S. J. (1996). Deviations from standard atomic volumes as a quality measure for protein crystal structures. *Journal of molecular biology, 264*(1), 121-136.

[29] Schrödinger Release 2022-4: AutoQSAR, Schrödinger, LLC, New York, NY, 2021.

[30] Sierotzki, H., Kraus, N., Assemat, P., Stanger, C., Cleere, S., Windass, J., & Gisi, U. (2005). *Evolution of resistance to QoI fungicides in Plasmopara viticola populations in Europe.* Paper presented at the Modern fungicides and antifungal compounds IV: 14th International Reinhardsbrunn Symposium, Friedrichroda, Thuringia, Germany, April 25-29, 2004.

[31] Samuel, S., Papayiannis, L. C., Leroch, M., Veloukas, T., Hahn, M., & Karaoglanidis, G. S. (2011). Evaluation of the incidence of the G143A mutation and cytb intron presence in the cytochrome bc-1 gene conferring QoI resistance in Botrytis cinerea populations from several hosts. Pest management science, 67(8), 1029-1036.

[32] Waterhouse, A., Bertoni, M., Bienert, S., Studer, G., Tauriello, G., Gumienny, R., . . . Bordoli, L. (2018). SWISS-MODEL: homology modelling of protein structures and complexes. *Nucleic acids research, 46*(W1), W296-W303.

[33] Wenz, T., Covian, R., Hellwig, P., MacMillan, F., Meunier, B., Trumpower, B. L., & Hunte, C. (2007). Mutational analysis of cytochrome b at the ubiquinol oxidation site of yeast complex III. *Journal of Biological Chemistry, 282*(6), 3977-3988.

[34] Williams, C. J., Headd, J. J., Moriarty, N. W., Prisant, M. G., Videau, L. L., Deis, L. N., . . . Chen, V. B. (2018). MolProbity: More and better reference data for improved all-atom structure validation. *Protein science, 27*(1), 293-315.

[35] Wong, F. P., & Wilcox, W. F. (2000). Distribution of baseline sensitivities to azoxystrobin among isolates of Plasmopara viticola. Plant disease, 84(3), 275-281.

APPENDIX

Table 16. Glide docking scores for fungicides on the top site of three mutated versions *Plasmopara viticola* Cytochrome b targeting at mutated version of G137 and L123.

Fungicide	**G137A average docking score**	**L123F average docking score**	**Double mutation average docking score**	**Resistance**	**Fungicide Type**
Ubiqunol	-8.6020	-10.2483	-9.6594	HR	NA
Famoxadone	-4.6450	-7.4714	-4.7018	HR	QoI
Fenamidone	-6.1589	-6.4199	-6.5964	HR	QoI
Mandestrobin	-5.8189	-6.9176	-7.6937	HR	QoI
Fenaminstrobin	-7.9325	-5.5149	-3.9721	HR	QoI
Pyribencarb	-3.1905	-5.8536	-5.0871	HR	QoI
Dimoxystrobin	-3.9699	-4.3608	-6.8004	HR	QoI
Metominostrobin	-4.2267	-4.8323	-6.9727	HR	QoI
Pyraclostrobin	-4.5521	-4.6161	-7.0383	HR	QoI
Flufenoxystrobin	-2.2911	-3.0611	-4.0351	HR	QoI
Metyltetraprole	-4.4752	-3.9500	-7.6200	HR	QoI
Ametoctradin	-5.6017	-4.9131	-5.3848	HR/R	QoI
Thiram	-4.4892	-4.5784	-4.5284	LR	DTC
Ferbam	-3.2534	-3.2846	-3.4527	LR	DTC
Mancozeb	-2.4433	-2.4208	-2.6703	LR	DTC
Zineb	-2.8342	-2.5861	-3.0747	LR	DTC
Folpet	-3.9663	-2.5276	-2.7277	LR	PHT
Captan	-4.0550	-4.2980	-4.0246	LR	PHT
Azoxystrobin	-3.4418	-4.9330	-4.5320	HR/R	QoI